

**Development and Application of Liquid Chromatography
Coupled to Isotope Ratio Mass Spectrometry**

Dissertation

zur Erlangung des akademischen Grades eines

Doktors der Naturwissenschaften

– Dr. rer. nat. –

vorgelegt von

Lijun Zhang

geboren in Hunan

Fakultät für Chemie

der

Universität Duisburg-Essen

2013

Die vorliegende Arbeit wurde im Zeitraum von Juli 2009 bis Oktober 2013 im Arbeitskreis von Prof. Dr. Torsten Schmidt im Fachgebiet Instrumentelle Analytische Chemie der Universität Duisburg-Essen durchgeführt.

Tag der Disputation: 19.02.2014

Gutachter: Prof. Dr. Torsten C. Schmidt

Prof. Dr. Oliver J. Schmitz

Vorsitzender: Prof. Dr. Eckart Hasselbrink

Abstract

Stable isotope analysis has found widespread applications in various disciplines such as archaeology, geochemistry, biology, food authenticity, and forensic science. Coupling chromatography to isotope ratio mass spectrometry for compound-specific isotope analysis (CSIA) is a trend, as it provides several advantages over bulk isotope analysis, e.g., relatively simple sample preparation, the ability to measure individual compounds in a complex mixture in one run, and the reduced sample size required for precise isotope analysis. Gas chromatography coupled to isotope ratio mass spectrometry (GC/IRMS) has been well-established for compound-specific isotope analysis of volatile organic compounds within the last two decades. However, an interface combining liquid chromatography with isotope ratio mass spectrometry (LC/IRMS) was not commercially available until 2004. The current design of the interface requires using a carbon-free eluent in chromatographic separation. This requirement limits the application of the most frequently used reversed-phase liquid chromatography in CSIA, because the elution strength of water at room temperature is too low to serve as mobile phase in reversed-phase separations.

In order to increase the elution strength of water, we propose using high temperature water for chromatographic elution. The polarity of water decreases with an increase of temperature, yielding increased elution strength in reversed-phase columns. Therefore, high temperature water can be used as eluent instead of organic solvent for combining reversed-phase liquid chromatography with isotope ratio mass spectrometry (RPLC/IRMS). Additionally, temperature gradients can replace organic solvent gradients to increase chromatographic resolution. This is very important for LC/IRMS analysis, as precise isotope analysis requires baseline separation of analytes.

In this thesis, high-temperature reversed-phase liquid chromatography was coupled to, and for the first time carefully evaluated for, isotope ratio mass spectrometry (HT-RPLC/IRMS). The effect of column bleed on measured isotope ratios was investigated at high temperature in isothermal mode and in temperature gradient mode. Four different revised-phase columns were proven to be compatible with IRMS for compound-specific isotope analysis. The developed method was applied to measure caffeine in different drinks. Naturally occurring and industrially synthesized caffeine was observed to have two distinct $\delta^{13}\text{C}$ -ranges, from -25 to -32‰ and from -33 to -38‰ , respectively. On the basis of two different $\delta^{13}\text{C}$ -ranges, four out of 38 drinks were suspected of being mislabelled due to added but non-labelled synthetic caffeine with $\delta^{13}\text{C}$ -values falling in the range of synthetic caffeine. Furthermore, HTLC/IRMS

was applied to measure non-polar and water-insoluble compounds, here steroids, for the first time. The use of steroid isotope analysis for pharmaceutical product control by HTLC/IRMS was demonstrated. The major advantage is that steroids can be analysed without derivatization. By overcoming current limitations in sample preparation, the method might become applicable for doping control purposes. Another potential application of LC/IRMS in doping control is the isotope analysis of 5-Aminoimidazole-4-carboxamide ribonucleotide (AICAR), a gene doping drug. Here, the first method for compound-specific isotope analysis of AICAR has been presented. The endogenous AICAR in urine and industrially synthesized AICAR were observed to have significantly different isotope signature. It shows that isotope analysis of LC/IRMS could potentially be used for the detection of AICAR abuse. The methodological developments presented in the thesis will lead to new applications of LC/IRMS.

Contents

<i>Abstract</i>	<i>1</i>
<i>Chapter 1 General introduction</i>	<i>7</i>
1.1 Stable isotope analysis	8
1.2 Isotope fractionation	8
1.3 Instrumentation	10
1.3.1 IRMS _____	10
1.3.2 EA/IRMS _____	11
1.3.3 GC/IRMS _____	12
1.3.4 LC/IRMS _____	13
1.4 History of LC/IRMS	14
1.5 Chromatographic method in LC/IRMS	16
1.5.1 Ion interaction _____	16
1.5.2 Mixed-mode columns _____	18
1.5.3 Reversed-phase liquid chromatography _____	20
1.6 Applications of LC/IRMS	21
1.6.1 Archaeology _____	21
1.6.2 Nutrition and physiology _____	22
1.6.3 Soil science and geochemistry _____	23
1.6.4 Food quality control _____	24
1.7 Aim of the PhD work	25
1.8 References	27
<i>Chapter 2 High temperature reversed-phase liquid chromatography coupled to isotope ratio mass spectrometry</i>	<i>35</i>
2.1 Abstract	36
2.2 Introduction	37
2.3 Experimental	38
2.3.1 Chemicals and reagents _____	38
2.3.2 Instrumentation _____	39
2.3.3 Chromatographic conditions _____	39
2.3.4 Isotopic calculation _____	42

2.3.5 EA/IRMS measurement	43
2.4 Results and discussion	43
2.4.1 Effect of column bleed on $\delta^{13}\text{C}$ measurement	43
2.4.2 Effect of temperature on retention of caffeine	48
2.4.3 Detection limit of HT-RPLC/IRMS	49
2.4.4 Temperature-programmed LC/IRMS for CSIA	50
2.5 Conclusion	52
2.6 Acknowledgements	52
2.7 References	53
<i>Chapter 3 Caffeine in your drink: natural or synthetic?</i>	58
3.1 Abstract	59
3.2 Introduction	60
3.3 Experimental section	61
3.3.1 Chemicals	61
3.3.2 Instrumentation for HT-RPLC/IRMS	62
3.3.3 Isotopic calculation	63
3.3.4 EA/IRMS measurement	65
3.4 Results and discussion	65
3.4.1 Baseline separation of caffeine by HT-RPLC/IRMS	65
3.4.2 Precision and accuracy of caffeine $\delta^{13}\text{C}$	67
3.4.3 Distinguishable $\delta^{13}\text{C}$ ranges of natural and synthetic caffeine	69
3.4.4 Authenticity control of caffeine-containing drinks	71
3.5 Conclusions	73
3.6 Acknowledgements	73
3.7 Appendix: Setting a threshold for assigning an unknown caffeine sample to natural or synthetic provenience	74
3.8 References	76
<i>Chapter 4 Derivatization-free carbon isotope ratio analysis of steroids by hyphenation with high temperature liquid chromatography</i>	80
4.1 Abstract	81
4.2 Introduction	82

4.3 Experimental	83
4.3.1 Materials	83
4.3.2 Instrumentation for HTLC/PDA/IRMS	83
4.3.3 EA/IRMS measurement	84
4.4 Results and discussion	87
4.4.1 Chromatographic separation of steroid mixture	87
4.4.2 Method detection limit	88
4.4.3 Testogel sample	90
4.5 Conclusion	91
4.6 Reference	92
<i>Chapter 5 Carbon isotope analysis of AICAR by liquid chromatography coupled to PDA and isotope ratio mass spectrometry</i>	<i>95</i>
5.1 Abstract	96
5.2 Introduction	97
5.3 Materials and Methods	98
5.3.1 Chemicals and reagents	98
5.3.2 Purification of human urine samples	98
5.3.3 Sample preparation for LC/IRMS	100
5.3.4 LC/PDA/IRMS	100
5.3.5 EA/IRMS measurement	101
5.3.6 Data acquisition and handling	101
5.4 Results and discussion	102
5.4.1 Suitable chromatographic column	102
5.4.2 Detection limit for precise and accurate isotope analysis	102
5.4.3 Spiked urine sample	104
5.4.4 Endogenous AICAR in urine	105
5.5 Conclusion	108
5.6 Acknowledgements	109
5.7 References	110
<i>Chapter 6 General conclusions and future work</i>	<i>112</i>
<i>Supplement</i>	<i>114</i>

List of figures.....	115
List of tables	119
List of abbreviations	121
List of publications	123
Oral presentations	124
Poster Presentations	125
Curriculum Vitae.....	126
Erklärung	127
Acknowledgments	128

Chapter 1 General introduction

Compound-specific isotope analysis (CSIA) has become an essential tool in a wide variety of research areas, including geochemistry, paleodiet, nutrition, food authenticity and sport. At present, there are mainly two methodologies for compound-specific isotope analysis: gas chromatography or liquid chromatography coupled with isotope ratio mass spectrometry (GC/IRMS, LC/IRMS). GC/IRMS has been well developed for hydrogen, carbon, nitrogen, and oxygen isotope analysis over the last two decades. In contrast, the interface coupling LC to IRMS became commercially available in 2004 for the first time. It is able to directly measure carbon isotope ratio of non-volatile and thermally unstable compounds, which might be difficult for GC/IRMS analysis. The system of LC/IRMS needs to use carbon-free eluent that hinders the application of reversed-phase liquid chromatography to compound-specific isotope analysis. In the thesis, a new method of high temperature liquid chromatography coupled to isotope ratio mass spectrometry was developed (HTLC/IRMS) for compound-specific isotope analysis. It allows the use of reversed-phase columns for LC/IRMS analysis and brought the capability for compound-specific isotope analysis of non-volatile and non-polar organic compounds. In this general introduction, stable isotope analysis and the related instrumentation are introduced. But the emphasis is put on chromatographic method developments and applications of LC/IRMS.

1.1 Stable isotope analysis

Precise analysis of the variation in stable isotope composition can provide information about the geographic, chemical, and biological origins of substances.^[1] The first evidence for stable isotopes of Neon was found by Thomson in 1913.^[2] Nowadays, there are 61 elements in the periodic table having two or more naturally occurring stable isotopes. Among these elements, isotope analyses of hydrogen, carbon, nitrogen, oxygen, and sulfur have attracted the most attention of isotope scientists as they are the most common elements in organic and biologically relevant compounds. Different isotopes of an element have the same number of protons but different number of neutrons, which occupy the same position in the periodic table. Stable isotope has half-life longer than 10^{10} years and have an atomic number smaller than 83. In contrast, radioactive isotope has an atomic number higher than 83 and has half-life shorter than 10^{10} years except for the radioactive isotope thorium-232.^[3] Isotopes of an element have the same chemical properties in gross but different masses.

1.2 Isotope fractionation

Isotope fractionation, enrichment of one isotope relative to another in a chemical or physical process, occurs because of the different bond energy of each isotope. The heavier isotopes have stronger bonds and slower reaction rates. Isotope fractionation can be classified into thermodynamic and kinetic isotope effects. The thermodynamic isotope effect, also known as equilibrium or exchange effect, describes isotope exchange reactions between two compounds or phases under equilibrium conditions.^[4, 5] Kinetic isotope fractionation occurs in irreversible reactions where different isotopes move or react at different rates. A typical example of kinetic fractionation is the evaporation of seawater to form clouds in which ^{16}O is enriched relative to the heavier oxygen isotopes in comparison with sea water.^[6]

The naturally occurring variance in stable isotope abundance is very small. Stable isotope analysis at natural abundance level needs precision in the order of 10^{-2} - $10^{-4}\%$.^[7, 8] Thus, conventional mass spectrometer types including quadrupole, ion trap and time of flight which have usually precision in the range between 0.05 and 2% at single ion monitoring and full scanning mode, respectively,^[7] are unable to measure isotope ratios of light elements sufficiently precisely. The light isotopes are several orders of magnitude more abundant than the heavy ones for H, C, O, N, and S. In order to achieve precision as high as possible, the measured isotope ratio is the most abundant heavy isotope versus light isotope for stable isotope: $^2\text{H}/^1\text{H}$, $^{13}\text{C}/^{12}\text{C}$, $^{15}\text{N}/^{14}\text{N}$, $^{18}\text{O}/^{16}\text{O}$, and $^{34}\text{S}/^{32}\text{S}$. The isotopic abundances in mole fraction of these ten isotopes are listed in Table 1.1.^[9]

Table 1.1 Isotopic abundances of hydrogen, carbon, nitrogen, oxygen and sulfur^[9]

Element	Stable isotope ratio	Measured gas	Stable isotopes	Isotopic abundance (mole fraction) ^[9]
Hydrogen	² H/ ¹ H	H ₂	¹ H	0.999 885(70)
			² H	0.000 115(70)
Carbon	¹³ C/ ¹² C	CO ₂	¹² C	0.9893(8)
			¹³ C	0.0107(8)
Nitrogen	¹⁵ N/ ¹⁴ N	N ₂	¹⁴ N	0.996 36(20)
			¹⁵ N	0.003 64(20)
Oxygen	¹⁸ O/ ¹⁶ O	CO	¹⁶ O	0.997 57(16)
			¹⁸ O	0.002 05(14)
Sulfur	³⁴ S/ ³² S	SO ₂	³² S	0.9499(26)
			³⁴ S	0.0425(24)

The commonly used expression of stable isotope ratios at natural abundance is the δ -value. This δ -notation was introduced firstly in the late 1940s by McKinney from the Chicago laboratory of Harold Urey.^[10] It is defined as the relative difference, mostly expressed in parts per thousand (‰, per mil), between the isotope ratio of the sample $R(^hE_c/^lE_c)$ and the international reference material $R(^hE_{ref}/^lE_{ref})$. The equation for calculating $\delta^hE_{c,ref}$ is as follows:

$$\delta^hE_{c,ref} = \frac{R(^hE_c/^lE_c) - R(^hE_{ref}/^lE_{ref})}{R(^hE_{ref}/^lE_{ref})} \quad (1.1)$$

For stable carbon isotope analysis, the internationally accepted reference material is Vienna Pee Dee Belemnite (VPDB), a marine carbonate. It has an accepted ¹³C/¹²C ratio of 0.0111802.^[11] The above equation used for stable carbon isotope analysis can be simplified as:

$$\delta^{13}C_{s,VPDB} = \frac{R(^{13}C/^{12}C)_s}{R(^{13}C/^{12}C)_{VPDB}} - 1 \quad (1.2)$$

1.3 Instrumentation

1.3.1 IRMS

Isotope ratio mass spectrometry (IRMS) was designed specifically for precise stable isotope analysis at low enrichment and natural abundance level. It can be used to measure the stable isotope ratio of hydrogen, carbon, oxygen, nitrogen, and sulfur. The sample of interest has to be converted to a simple gas before entering the isotope ratio mass spectrometer: H_2 for hydrogen isotope analysis, CO_2 for carbon isotope analysis, N_2 for nitrogen isotope analysis, CO for oxygen isotope analysis, SO_2 for sulfur isotope analysis (see also Table 1.1). In an IRMS, the introduced gas is ionized in an electron ionization source and separated by a magnetic sector, which is set to single field strength for isotope analysis of one element.^[12] The ions of interest are collected by the dedicated faraday cups. For example, IRMS instruments designed for carbon isotope analysis have three Faraday cups used for detection of m/z 44, 45, and 46. Each cup is connected to a separate amplifier, which has a different gain so that the output signals for different ions at natural abundance have similar intensity. The isotope ratio is calculated based on the peak area of the detected three ions derived from the sample and the lab working reference gas of CO_2 . A scheme of IRMS for stable carbon isotope analysis can be seen in Figure 1.1.

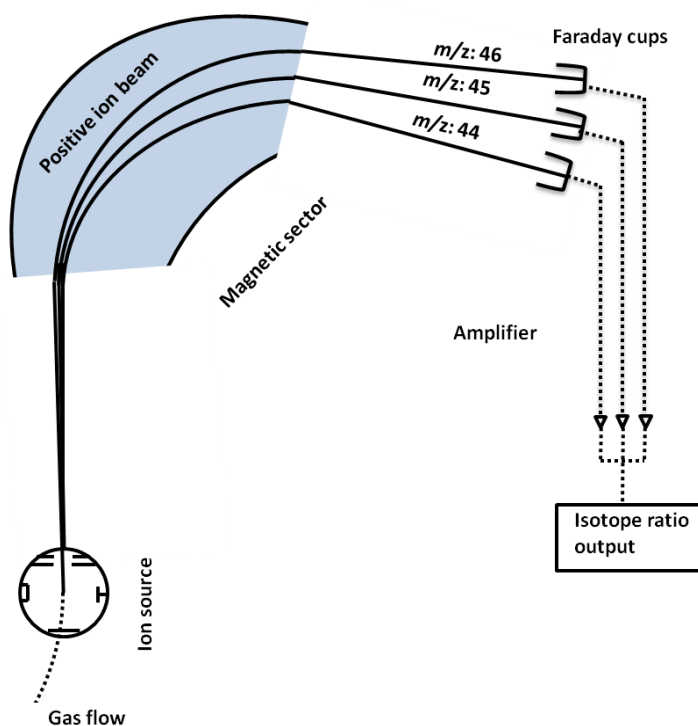


Figure 1.1 Schematic of isotope ratio mass spectrometry for stable carbon isotope analysis.

1.3.2 EA/IRMS

An elemental analyzer hyphenated with an isotope ratio mass spectrometer (EA/IRMS) is mainly used for bulk isotope analysis.^[13] When it is used for measuring the isotope ratio of one compound, the pure compound must be isolated from the matrix prior to EA/IRMS analysis. It can be referred to as off-line compound-specific isotope analysis. In EA/IRMS, the injected sample is first converted to gases (H_2 , CO_2 , CO , N_2 , and SO_2) in a high temperature oven and the formed gases are separated by gas chromatography before entering the IRMS (see the schematic of an EA/IRMS system for carbon and nitrogen isotope analysis in Figure 1.2). The current technology of EA/IRMS allows to measure carbon and nitrogen isotope ratios in a single run within one injection. After introduction, the sample is converted to a mixture of CO_2 , N_2 , and H_2O in a combustion oven at around 1000°C with a pulse of pure oxygen. In a Flash Elemental Analyzer (Thermo Fisher Scientific, Bremen), the oxidation reactor is a quartz tube filled with catalyst of chromium oxide and cobalt oxide mixed with silver.^[14] The filled silver is used to trap sulfur and halogens. The generated gases are carried by a stream of helium into a reduction reactor, where small amounts of nitrogen oxide is reduced to nitrogen and the excess oxygen is removed by the filled copper at around 600°C . In the water trap that follows, moisture is absorbed by the filled absorbent material, $\text{Mg}(\text{ClO}_4)_2$ for example. After that, the mixture of gases goes through a packed gas chromatographic column where the gases are separated. Afterwards, the gases of N_2 and CO_2 are detected by a thermal conductivity detector and introduced into the IRMS system via an open-split interface. For hydrogen and oxygen isotope analysis, the sample is first converted to H_2 and CO at high temperature between ~ 1100 and $\sim 1450^\circ\text{C}$.^[15] The process is known as pyrolysis, high temperature thermal conversion, or high temperature reduction.^[16] The reactor from Thermo Finnigan comprises an outer ceramic tube and an inner glassy carbon tube filled with graphite crucible, glassy carbon particles and silver wool intended to remove halogen atoms.^[17] Besides hydrogen, carbon, and oxygen isotope analysis, sulfur isotope analysis can also be accomplished by EA/IRMS. The bulk material must be first converted to SO_2 to permit analysis by IRMS. The oxidation reactor is typically packed with tungsten oxide and zirconium oxide catalysts, and copper used to remove excess oxygen, which is heated up to 1080°C for combustion.^[18] It has to be noted that there are many variations of EA/IRMS for specific applications of isotope analysis.

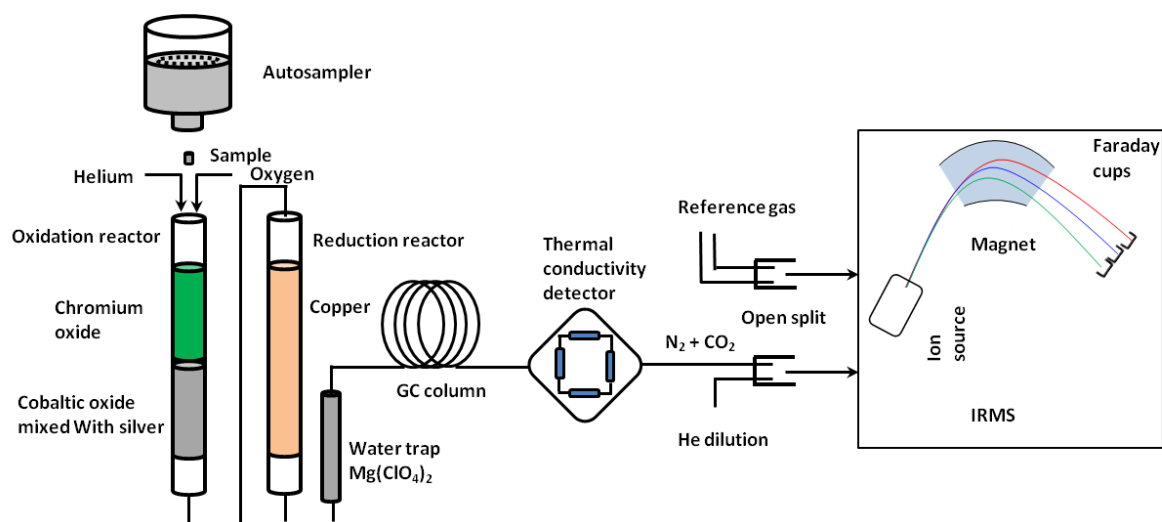


Figure 1.2 Schematic of an EA/IRMS for nitrogen and carbon isotope analysis (Flash Elemental Analyzer coupled with IRMS, Thermo Fisher Scientific, Bremen). It consists of an autosampler, an oxidation reactor, a reduction reactor, a water trap, a gas chromatographic column, a thermal conductivity detector, open split, and an IRMS system.

1.3.3 GC/IRMS

Gas chromatography coupled to isotope ratio mass spectrometry is currently the most frequently used technology for compound-specific isotope analysis (CSIA). It has been widely used in studies of geochemistry, archaeology, environmental chemistry, and food authenticity.^[19, 20] For compound-specific isotope analysis, the advantages of GC/IRMS over EA/IRMS are simpler sample preparation, lower detection limit, and the capacity of analysis of more than one compound in single run. The typical GC/IRMS includes a conventional GC, a chemical reaction interface, and an IRMS. The procedure of GC/IRMS for carbon and nitrogen isotope analysis is simply described as follows and the schematic of GC/IRMS for carbon and nitrogen isotope analysis is presented in Figure 1.3. The sample injection can be done by an autosampler. The analyte of interest is transferred into the gas phase and carried by a stream of helium through a gas chromatographic column where the targeted compounds are separated. There is generally a backflush valve between the outlet of the GC column and the oxidation reactor. It is used to remove the early-eluting solvent from sample that would otherwise exhaust the oxidation capacity of the oxidation reactor.^[21] In the oxidation reactor, the eluted compounds from the chromatographic column are converted to CO_2 , N_2 and H_2O at high temperature with a catalyst. This is followed by a reduction reactor where small amount of nitrogen oxide generated in the oxidation reactor is reduced to N_2 . For the instrument from

Thermo Fisher Scientific, the oxidation reactor consists of a non-porous alumina tube filled with Pt, Cu, and Ni wires and the used temperature is approximately 950°C; the reduction reactor is an alumina tube containing three copper wires and maintained at around 600°C.^[22] Water is then removed by a water permeable Nafion™ membrane, which is purged by a gas stream of helium continuously. The gaseous products are introduced into the ion source of IRMS via an open split. Compound-specific isotope analysis of hydrogen and oxygen can be carried out by GC/IRMS too. After chromatographic separation, the eluted compounds are converted to H₂ and CO by high temperature pyrolysis prior to IRMS analysis.^[23, 24] Sulfur isotope analysis by GC/IRMS has not been reported yet.

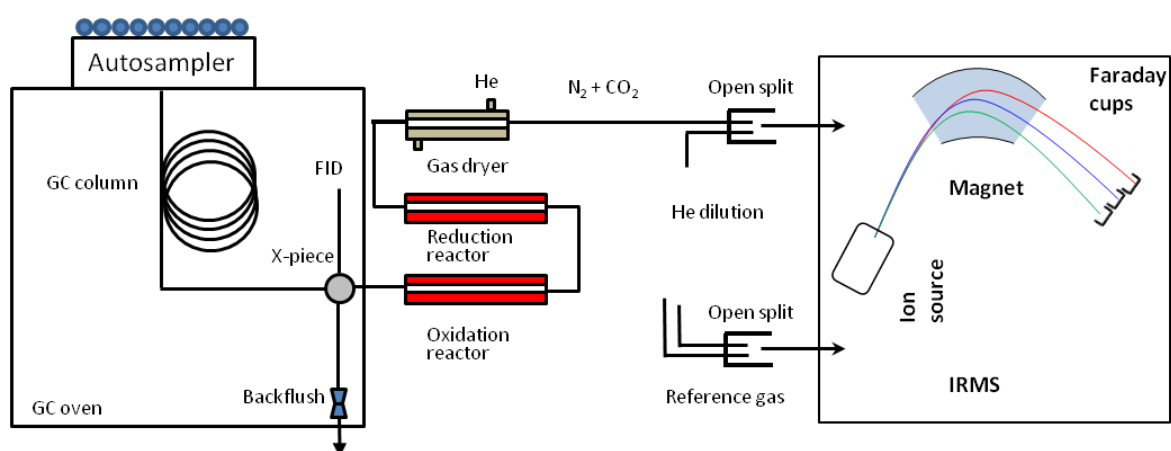


Figure 1.3 Schematic of gas chromatography coupled to isotope ratio mass spectrometry for carbon and nitrogen isotope analysis.

1.3.4 LC/IRMS

Liquid chromatography coupled to isotope ratio mass spectrometry (LC/IRMS) can be used to measure stable carbon isotope ratio of individual compounds that are baseline separated by liquid chromatography. It has been used to measure precisely stable carbon isotope ratios at natural abundance and at low enrichment level (0.005-5%).^[25] This methodology was introduced much later than GC/IRMS. The commercial interface for hyphenating liquid chromatography with IRMS was not available until 2004.^[26] However, it has been attracting increasing interest. It provides an alternative method for isotope analysis of non-volatile and thermally labile compounds that otherwise need derivatization for GC/IRMS analysis. The step of compound derivatization is labour-intensive and might result in isotope error due to a kinetic isotope effect and the added carbon from the derivative.^[27, 28] Based on the current interface design, LC/IRMS has some inherent constraints in terms of compatible mobile phase

composition und flowrate. Nevertheless, LC/IRMS has found application in different fields including food authenticity, archaeology, nutrition and physiology, and geochemistry. The methodological developments of LC/IRMS for extending the application range and improving analytical performance have not yet stopped. The next section contains a brief history of LC/IRMS, chromatographic method development, and advanced applications in LC/IRMS.

1.4 History of LC/IRMS

The realization of hyphenation of liquid chromatography with isotope ratio mass spectrometry is not easy. It is mandatory for gas source IRMS to convert the target compound into a simple and clean gas before it is introduced into the ion source. The injected gas is CO₂ for compound-specific carbon isotope analysis. It is much more straightforward when it comes to coupling GC with IRMS, because the separated compounds are in the gas phase, which can be converted into gases by combustion or pyrolysis. For LC/IRMS, the eluted compounds from a liquid chromatographic column are in liquid phase. The challenge of combining LC with IRMS is to convert the organic compound to CO₂ gas on-line and extract CO₂ gas from the liquid phase into a carrier gas of helium reproducibly and quantitatively, meanwhile preserving the integrity of the chromatographic resolution. It has been proven that baseline separation of CO₂ peaks of individual compounds are the basis for high-precision compound-specific isotope analysis.^[20, 29]

In 1993, Caimi and co-workers described a hyphenation of LC/IRMS. In this system, the effluent containing analytes is deposited on a moving wire, which passes sequentially through a drying oven for solvent removal and a combustion furnace where analytes are converted into CO₂.^[30] The main difficulties of the interface are the isotope fractionation occurring in the drying process and the low recovery of analytes with respect to high-precision isotope analysis.^[25] In 1996, Teffera and co-workers reported an approach of continuous-flow isotope ratio mass spectrometry using a chemical reaction interface. In this system, the LC effluent passes sequentially a desolvation nebulizer, a longitudinal gas diffusion cell, and a momentum separator for desolvation, and the analyte molecules are converted to CO₂ gas using microwave-induced helium plasma and reactant gas of oxygen.^[31, 32] This method has also difficulty in precise isotope analysis due to isotope fractionation in the desolvation process and low sensitivity.^[25] Therefore, neither of these two systems has been put on the market.

The first commercial interface combining LC with IRMS is based on wet chemical oxidation. The idea comes from the well-established methodology of total organic carbon analysis of liquid samples in which organic compounds are oxidized to CO₂ gas in the aqueous phase.^[33]

This first attempt of combining a total organic carbon analyzer with IRMS was done by St-Jean, which was used for bulk isotope analysis of dissolved inorganic and organic carbon.^[34] In this system, persulfate was used for the oxidation of organic compounds in the liquid phase at high temperature of 100°C and the generated CO₂ gas was purged out from the liquid and dried before admitting to IRMS. In 2004, Krummen *et al.* reported firstly an interface combining LC with IRMS based on wet chemical oxidation for compound-specific isotope analysis.^[26] The interface was commercialized under the name of LC-IsoLink by Thermo Finnigan (Bremen, Germany). The interface is composed of an oxidation reactor, a cooler, a separation unit, a gas dryer, and an open split as shown in Figure 1.4. After being injected by an autosampler, the sample goes through a liquid chromatographic column. The organic compounds in the effluent are oxidized continuously into CO₂ gas in the oxidation reactor by sodium or ammonium persulfate under acidic condition and high temperature of 99.9°C. The produced CO₂ gas is extracted into helium by passing a gas permeable membrane which is purged by a counter stream of helium. The CO₂ derived from the analytes are carried by helium passing a gas dryer of a NafionTM tubing and admitted to the ion source of the IRMS via an open split. The system can also be used for bulk isotope analysis when no chromatographic column is installed, which is known as flow injection analysis mode (FIA). In 2010, Morrison *et al.* reported an LC/IRMS system with a second commercially available interface of Liquiface (Isoprime Ltd. Cheadle Hulme, UK). The working principle is also based on wet chemical oxidation.

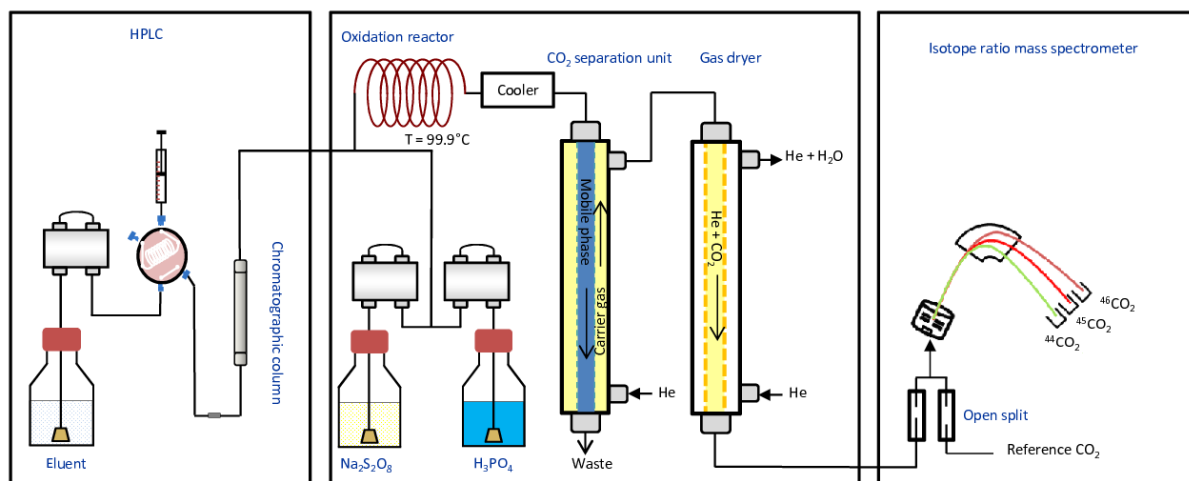


Figure 1.4 The schematic of liquid chromatography coupled to isotope ratio mass spectrometry using an interface of LC-IsoLink for compound-specific isotope analysis. The system can be used for bulk isotope analysis without a column, known as flow injection analysis mode (FIA).

1.5 Chromatographic method in LC/IRMS

Carbon-containing substances cannot be used in the mobile phase for chromatographic separation in LC/IRMS system due to non-selective oxidation and CO_2 gas separation, including organic solvent and carbon-bearing buffers or additives. Therefore, only pure water with phosphate buffer, phosphoric and sulfuric acid, and sodium/potassium hydroxides has been used as eluent. This limitation of carbon-free eluent has hindered the use of reversed-phase columns for compound-specific isotope analysis. Moreover, the configuration of the gas separation unit consisting of three thin membranes requires the flow rate of total effluent not higher than $700 \mu\text{L min}^{-1}$, including the mobile phase of LC, the oxidant and acid reagents.^[26] For meeting this requirement, suitable chromatographic column size must be taken into account. In the previous literature, the used chromatographic methods in LC/IRMS include ion exchange, mixed-mode, and water-compatible reversed-phase columns.^[35]

1.5.1 Ion interaction

The typical separation mechanisms for compound-specific isotope analysis by LC/IRMS are ion interactions including ion attraction and repulsion. The targeted compounds are ionizable organic compounds such as sugars and carbohydrates. Some of them need derivatization for GC/IRMS analysis because of low vapour pressure, for example, sugars. The used columns can be classified into four groups based on the stationary phase: anion exchange, cation exchange, ligand exchange, and ion exclusion column, as summarized in Table 1.2. In several

studies, a Dionex CarboPac PA20 column has been used for compound-specific isotope analysis of water-soluble organic acids and sugars.^[35-41] It is a strong anion exchange column with stationary phase of quaternary ammonium cation. The mobile phase employed for anion exchange elution is an aqueous solution of sodium hydroxide. The used flow rates of eluent are in the range of 250 to 500 $\mu\text{L min}^{-1}$. A major drawback of coupling anion-exchange chromatography to IRMS is the absorption of CO_2 from the atmosphere occurring in the mobile phase of alkaline solution, which can result in high carbon background.^[35] It can also cause unstable background for isotope analysis when gradient is used for separation. In order to obtain low background for carbon isotope analysis, low strength sodium hydroxide has been used for anion-exchange chromatography, from 0.25 to 1 mM. Additionally, Rinne *et al.* used an online carbonate trap column prior to the LC column to minimize the carbon background in IRMS.^[35] Sodium nitrate replacing carbon-bearing acetate to increase ionic strength of mobile phase has been used for analysis of strongly bound acidic carbohydrates, such as muramic acid and uronic acid.^[36, 37] A few studies have investigated the effect of column temperature and concentration of sodium hydroxide on the chromatographic resolution of amino sugars and soluble carbohydrates in a complex matrix including marine, soil and plant extracts for precise carbon isotope analysis.^[36, 37, 40] Another two anion-exchange columns of IonPac AS11 and BioBasic AX have been used for compound-specific isotope analysis of benzene polycarboxylic acids in soil extract and guanosine triphosphate/biphosphate, respectively.^[42, 43]

A type of cation-exchange column of Alltech 700 CH carbohydrate has been coupled to IRMS for isotope analysis of sugars and simple alcohols using high temperature water as mobile phase.^[26, 44] Compound-specific isotope analysis of sugars in honey and simple alcohols in wine has also been accomplished by ligand-exchange column (HyperREZ carbohydrate H^+) coupled to IRMS.^[45-47] The separation mechanism is based on the hydrogen bonding between H^+ counter ion and hydroxyl groups of sugars and alcohols. A few studies have used ion-exclusion chromatography combined with IRMS for sugars and simple carbohydrates isotope analysis.^[48-50] Compared to ion-exchange and ligand-exchange columns that use mainly attractive forces, ion-exclusion columns use mainly repulsive force between an analyte anion and the negatively charged packed gel, which is a sulfonated divinylbenzene-styrene copolymer.

Table 1.2 Chromatographic methods based on ion interaction in LC/IRMS: column, mobile phase composition, and analytes. Anion exchange columns (type 1), cation exchange columns (type 2), ligand exchange columns (type 3), and ion exclusion columns (type 4).

Type	Manufac turer	Column	Size	Mobile phase	Analytes			
1	Dionex	CarboPac PA20	3 × 150 mm, 6.5 μm	52 mM NaOH, flowrate: 250 μL min ⁻¹	Seven monosaccharides ^[35]			
				0.25mM NaOH, flowrate: 500 μL min ⁻¹	Plasma galactose and glucose with labelled ¹³ C ^[39]			
				1 mM NaOH, flowrate: 300 μL min ⁻¹	Plasma glucose with labelled ¹³ C ^[41]			
				1 mM NaOH + 2 mM NaNO ₃ , flowrate: 300 μL min ⁻¹	Seven carbohydrates in marine materials ^[37]			
				1 mM NaOH, flowrate: 300 μL min ⁻¹ , T: 15-55°C	Carbohydrates in conifer needle extract ^[40]			
				2 mM NaOH, flowrate: 400 μL min ⁻¹ , T: 15°C	Glucosamine, galactosamine and mannosamine in soil extract ^[36]			
				2 mM NaOH + 2 mM NaNO ₃ , flowrate: 400 μL min ⁻¹ , T: 35°C	Acid amino acids and muramic acid in soil extract ^[36]			
				100 mM NaOH, flowrate: 250 μL min ⁻¹ , T: 20°C	Sucrose and raffinose from leaves and phloem sap ^[38]			
				IonPac AS11	2 × 250 mm	Gradient elution: A, H ₂ O; B, 100 mM NaOH, flowrate:350 μL min ⁻¹	Benzene polycarboxylic acids in soil extract ^[43]	
						Thermo Fisher	BioBasic AX	NA
2	Alltech	Alltech 700 CH	6.5 × 300 mm, 8 μm	Water, flowrate:300 μL min ⁻¹ , T: 90°C	Sucrose, glucose, and fructose ^[26]			
				Water, flowrate:400 μL min ⁻¹ , T: 80°C	glucose, fructose, glycerol and ethanol ^[44]			
3	Thermo Fisher	HyperREZ Carbohydrate H ⁺	8 × 300 mm	Pure water, flowrate:400 μL min ⁻¹ , T: 25°C	Sucrose, glucose, and fructose in honey extract ^[45]			
				3 mM H ₂ SO ₄ , flowrate:500 μL min ⁻¹ , T: 25°C	Ethanol in wine ^[46]			
				Water, flowrate:400 μL min ⁻¹ , T: 65°C	Glycerol and ethanol in wine ^[47]			
4	Phenom enex	Rezek RCM (Ca ²⁺)	7.8 × 300 mm, 8 μm	Water, flowrate:300 μL min ⁻¹ , T: 55°C	Sugars in honey extract ^[48]			
				Transge nomic	Coregel 87H3	7.8 × 300 mm, 8 μm	8 mM H ₂ SO ₄ , flowrate:500 μL min ⁻¹ , T: 40°C	Hydrosoluble fatty acids ^[49]

1.5.2 Mixed-mode columns

Compound-specific isotope analysis of amino acids has attracted increasing interest as they are basic building blocks of proteins in plants and animals and play an important role in nutrient metabolism.^[51] Liquid chromatography coupled to isotope ratio mass spectrometry is the method of choice for isotope analysis of amino acids, since GC/IRMS requires derivatization of amino acids prior to injection.^[52] The step of derivatization introduces external carbon in the analyte molecules. Thus, it is necessary to correct $\delta^{13}\text{C}$ for obtaining

reliable carbon isotope ratio after measurement, which would be very critical for amino acids at natural abundance.^[40] It is not trivial to achieve baseline separation for precise isotope analysis of amino acids because there are usually a number of different amino acids in complex matrices, for example, plant extract, tissue extract, and human erythrocytes. Godin *et al.* reported a two-dimensional liquid chromatography hyphenated with IRMS for carbon isotope analysis of underivatized amino acids in 2005.^[25] In this work, 11 of the 15 amino acids were baseline resolved using a strong cation-exchange column combined with a reversed-phase C₃₀ column under gradient elution from 5 to 150 mM KH₂PO₄. McCullagh *et al.* presented a mixed-mode column (Primesep A) coupled to IRMS for isotope analysis of 15 underivatized amino acids in 2006.^[53] Primesep A is a reversed-phase column with embedded strong acidic ion-pairing groups providing hydrophobic and cation-exchange interactions for amino acid separation. Using this mixed-mode column combined with gradient elution of aqueous sulfuric acid, baseline separation of 15 free amino acids and precise isotope ratios of individual amino acids were achieved, and the established method was applied to measure amino acids in bone collagen extract.^[53] This method was later extended to compound-specific isotope analysis of amino acids from fish tissues, keratin, casein, hair collagen, human erythrocytes, and plant samples at natural and artificially enriched ¹³C-abundance,^[54-59] which is summarized in Table 1.3. Another mixed-mode column, Primesep 100, was reported for isotope analysis of glutathione and its dimeric form with a tracer of labelled glycine.^[60] McCullagh recently provided an overview of different types of mixed-mode stationary phases including positively and negatively charged and of the ways to improve chromatographic performance by optimizing the parameters, such as, column length, temperature and mobile phase pH.^[29] He also pointed out the challenges of using mixed-mode stationary phase for compound-specific isotope analysis, for example, peak overlay and low throughput.^[29]

Table 1.3 Mixed-mode columns used in LC/IRMS, mobile phase compositions, and analytes. Primesep A (1) and Primesep100 (2)

Type	Size	Mobile phase	Analytes
1	(4.6 × 250 mm, 5 μm)	Gradient elution: A, H ₂ O; B, 0.2% H ₂ SO ₄ , flowrate: 700 μL min ⁻¹	Amino acids from human and faunal bone collagen ^[53] and diets and tissues of fish ^[56]
		Gradient elution: A, H ₂ O; B, 0.1% H ₂ SO ₄ + 10 mm K ₃ PO ₄ ; C, 0.3% H ₂ SO ₄ ; flowrate: 500/600 μL min ⁻¹	Amino acids from keratin , collagen, and casein ^[59]
		Gradient elution: A, H ₂ O; B, 0.1% H ₂ SO ₄ + 10 mm K ₃ PO ₄ ; C, 0.3% H ₂ SO ₄	Amino acids in bone collagen ^[61]
	(2.1 × 250 mm, 5 μm)	Gradient elution: A, H ₂ O; B, 0.03 M H ₂ SO ₄ , flowrate: 260 μL min ⁻¹	Amino acids from hair and bone collagen ^[57]
		Gradient elution: A, H ₂ O; B, 0.03 M H ₂ SO ₄ .	Amino acids in leaves and seeds of plants ^[55]
	(3.2 × 250 mm, 5 μm)	Gradient elution: A, H ₂ O; B, 1 M H ₃ PO ₄ , flowrate:500 μL min ⁻¹	Simultaneous analysis of dimeric glutathione and labelled precursor glycine from human erythrocytes. ^[58]
Gradient elution: A, H ₂ O; B, 0.024 M H ₂ SO ₄ , flowrate:500 μL min ⁻¹		Amino acid from human bone collagen ^[54]	
2	(3.2 × 250 mm, 5 μm)	Gradient elution: A, H ₂ O; B, 1 M H ₃ PO ₄ , flowrate:500 μL min ⁻¹	Glutathione and its dimeric form from human erythrocytes with a tracer of labelled glycine ^[60]

1.5.3 Reversed-phase liquid chromatography

Reversed-phase liquid chromatography was less commonly coupled with isotope ratio mass spectrometry than with conventional mass spectrometry. Only a few water-compatible reversed-phase columns have been used for compound-specific isotope analysis, including C₁₈ and C₁₆ stationary phases, which are listed in Table 1.4.^[26, 62-64] The employed mobile phase is either pure water or phosphate buffer. Due to the low elution strength of aqueous solutions in reversed-phase column, the target analytes are polar organic compounds, such as amino acids, alcohols, and organic acids. A new method of temperature-programmed liquid chromatography coupled to isotope ratio mass spectrometry was reported by Godin *et al.* in 2008.^[65] It has brought more possibilities for coupling reversed-phase columns with IRMS. At high temperature, water behaves more like a weakly polar organic solvent with respect to

elution strength in reversed-phase column, because the relative static permittivity (a relative measure of solvent polarity) and viscosity of water decrease with temperature.^[66] For example, water at 140 °C has a relative static permittivity approximately equivalent to a 50:50 methanol-water mixture (in volume).^[67] Therefore, temperature can replace organic solvent to adjust the elution strength of aqueous mobile phase.

Table 1.4 Reversed-phase columns, mobile phase composition, and analytes in LC/IRMS.

Manufacturer	Column	Size	Mobile phase	Analytes
Merck KGaA	Purospher STAR RP- 18	2 × 55 mm, 3 µm	Water, flowrate:300 µL min ⁻¹ , T: 30°C	Paracetamol and acetylsalicylic acid ^[26]
Waters	Nova-Pak C18	3.9 × 300 mm, 4 µm	10 mM NaH ₂ PO ₄ , flowrate:300 µL min ⁻¹ , T: 30°C	Amino acids ^[26]
Thermo	HyPURITY Aquastar	3 × 250 mm, 5 µm	2 mM KH ₂ PO ₄ , flowate:400 µL min ⁻¹ , T: room temperature	Formic acid, acetic acid, methanol, ethanol ^[64]
Nomura Chemical	Reprosil-Pur C18-AQ	4 × 250 mm, 5 µm	phosphate buffer at pH 2.5, flowrate:500 µL min ⁻¹	Volatile fatty acids from porewater and marine samples ^[62]
Dionex	C16 Acclaim PA2	3 × 150 mm, 3 µm	10 mM phosphate buffer at pH 7, flowrate:500 µL min ⁻¹	Bentazon ^[63]
Thermo	Hypercarb	2.1 × 100 mm, 5 µm	20 mM H ₃ PO ₄ , flowate:220 µL min ⁻¹ , T: 35-110°C 20 mM phosphate buffer at pH 7.2, flowate:500 µL min ⁻¹ , T: 150 and 170°C	Water soluble fatty acids ^[65] Phenolic acids ^[65]

1.6 Applications of LC/IRMS

Since the first commercial interface was introduced in 2004,^[26] LC/IRMS has become a research tool in different areas, such as archaeology, nutrition and physiology, soil science and geochemistry, and food quality control.

1.6.1 Archaeology

The application of stable isotope analysis of amino acids from body tissue to paleodietary reconstruction is an important aspect of archaeology. It provides archaeological science with information of what people ate in the past. Isotope signatures of amino acids preserved in bone collagen and hair can indicate dietary composition. It is based on the principle of ‘you are what you eat’. For example, amino acids derived from marine and terrestrial carbon

sources have a difference in $\delta^{13}\text{C}$ ranging from 3-13‰.^[61] A difference in $\delta^{13}\text{C}$ between glycine and phenylalanine has been used to distinguish terrestrial (average $\Delta\delta^{13}\text{C}_{\text{Gly-Phe}} = 5\text{‰}$) and marine (average $\Delta\delta^{13}\text{C}_{\text{Gly-Phe}} = 12\text{‰}$) protein sources in food.^[68] Compound-specific isotope analysis of amino acid derivatives from archaeological materials has been conducted by GC/IRMS. However, derivatization of the less carbon-contained amino acids can increase the uncertainty of isotope signature. McCullagh *et al.* developed a LC/IRMS method for isotope analysis of 15 amino acids using a mixed-mode analytical column in 2006, which was applied to a number of archaeological bone protein hydrolysates demonstrating its usefulness in palaeodietary reconstruction.^[53] Afterwards, the developed method was extended to measure amino acids in hair from six historical individuals.^[57] It shows that isotope signature of amino acids in hair can provide useful information in addition to collagen amino acids analysis with regard to diet changes and seasonality, since hair is metabolically inert post-keratinisation and grows 1 centimeter per month.^[69] Dunn *et al.* compared the $\delta^{13}\text{C}$ values of collagen amino acids obtained from LC/IRMS and GC/IRMS analysis and pointed out that analytical errors associated with LC/IRMS amino acids analysis are lower than those occurring in GC/IRMS analysis.^[54] Bulk isotope analysis by LC/IRMS without a chromatographic column (FIA mode) has been applied to bulk organic matter in speleothems deposited on cave walls showing potential usefulness in palaeoenvironmental research.^[70]

1.6.2 Nutrition and physiology

There has been a growing interest in applying LC/IRMS to nutrition and physiology studies since the introduction of the commercial interface between LC and IRMS.^[51] First, most biological molecules are non-volatile and polar compounds, such as amino acids and sugars, which are water soluble and could be separated by IRMS-compatible chromatographic methods like ion exchange and mixed-mode columns. This type of compounds need derivatization prior to GC/IRMS analysis, which is more complicated compared with direct LC/IRMS analysis without derivatization. Second, LC/IRMS is able to measure carbon isotope ratios at natural abundance and determine isotopic enrichment using ^{13}C -labelled compounds as tracers. Godin and co-worker measured ^{13}C -enrichment of four labelled amino acids at low level and reported high precision for labelled amino acids. The coefficient of variation is 1% at 0.07 atom percent excess for threonine and alanine, 10% at 0.03 atom percent excess for valine and phenylalanine.^[25] The developed method was applied to a biological sample, a mixture of mucoproteins from a rat colon mucosa, for measuring isotopic enrichment of ^{13}C -threonine. In 2007, Schierbeek *et al.* reported a LC/IRMS method for

measuring the fractional synthesis rate of glutathione in neonatal blood using ^{13}C -glycine as a tracer.^[60] In order to assess the fractional synthesis rate, the isotopic enrichments of the glutathione dimeric form (GSSG) and glutathione's precursor glycine were determined by LC/IRMS and GC/IRMS, respectively. In 2009, the separation method was further optimized for simultaneous analysis of GSSG and glycine by LC/IRMS.^[58] The developed method has been proven useful in a kinetic study of glutathione in neonates providing high precision and sensitivity with small sample volume and low dose tracer administration. Stable isotope analysis of amino acids at natural abundance by LC/IRMS has been used to investigate the effect of dietary non-essential amino acid composition on the $\delta^{13}\text{C}$ values of individual amino acids in fish.^[56] The isotope ratio of amino acids from the diets and tissues of fish were measured by LC/IRMS precisely and accurately. Isotope enrichment analysis with labelled precursors for glucose metabolism had also been conducted by LC/IRMS. Schierbeek *et al.* developed an LC/IRMS method to measure isotope ratio and concentration of plasma glucose at natural abundance and with ^{13}C -labelled glucose.^[41] It shows advantages of little pre-purification, good precision and accuracy, and small sample size (20 μL of plasma). Morrison and co-workers used LC/IRMS to measure concentration and isotope ratio of galactose and glucose in plasma of seven trained cyclists, who had undergone ^{13}C -labelled glucose or galactose before exercise.^[39] This investigation provides an insight into utilization of oral galactose in sustained exercise.

1.6.3 Soil science and geochemistry

Compound-specific isotope analysis of LC/IRMS has found applications in soil microbial research, soil environment, biogeochemistry, and carbon cycling.^[51] Amino sugars, key compounds of microbial cell walls, can be used as biomarkers of microbial residues for investigating soil microbial communities.^[71] Bodé *et al.* reported firstly a LC/IRMS method for amino sugar analysis at natural abundance and low enrichment level in 2009.^[36] In 2013, they applied the developed method to investigate the interaction between bacteria and fungi during plant residue degradation in soil. In this work, LC/IRMS was employed for stable isotope analysis of amino sugar biomarkers, which was produced in the agricultural soil incubated 21 days with ^{13}C -labelled plant residue.^[72] Bai and co-workers have investigated the formation dynamics of amino sugars in two agricultural soils amended with ^{13}C -labelled wheat residues at different quality using stable isotope analysis of formed amino sugars and CO_2 gas.^[71] Tagami *et al.* determined a suitable analysis condition of LC/IRMS for formic acid, acetic acid, methanol and ethanol.^[64] Afterwards, this method was applied to investigate

the behaviour of ^{13}C -labelled acetic acid in the solution of flooded soils.^[73] An LC/IRMS method was developed to measure individual benzene polycarboxylic acids (BPCA) from soil-derived pyrogenic organic matter (PyOM). The future applications of $\delta^{13}\text{C}$ -BPCA measurement by LC/IRMS were discussed, including turnover rates of PyOM in soils and the partitioning of PyOM sources occurring in photosynthetic pathways.^[43] Bulk isotope analysis has been used to measure dissolved organic matter (DOM) in soil water by the use of flow injection analysis mode of LC/IRMS. Scheibe *et al.* assessed the capability of LC/IRMS for determining the carbon and ^{13}C content of DOM in soil water. High conversion efficiency of wet oxidation of the LC-IsoLink interface (99.3%), consistent $\delta^{13}\text{C}$ -values with other methods, low detection limit (10 mg L^{-1}), and high sample throughput were achieved.^[74] Albéric *et al.* have used LC/IRMS in FIA mode for bulk isotope analysis of dissolved organic carbon (DOC) in stream and soil waters from a farmland plot. It shows that mapping the $\delta^{13}\text{C}$ -DOC spatial distribution at the spot scale is possible due to the high sample throughput (10 minutes for triplicate analysis).^[75]

1.6.4 Food quality control

The use of stable isotope analysis in food quality control is a domain where LC/IRMS methods can play an important role. Stable carbon isotope signature can be used to distinguish botanical origins of substances between C_3 and C_4 plants. C_3 plants use the Calvin-Benson cycle to produce 3-phosphoglycerate (containing three carbons) in the process of photosynthesis, while C_4 plants use the Hatch-Slack cycle to produce oxalacetate, a four-carbon molecule. ^{13}C depletion occurs in the process of carbon dioxide fixation, but at different extent between C_3 and C_4 plants. As a result of different ^{13}C depletion, $\delta^{13}\text{C}$ -values of C_3 and C_4 plants vary in different ranges: -25 to -30‰ and -9 to -15‰ , respectively.^[76-78] The third type of photosynthetic pathway is crassulacean acid metabolism (CAM). $\delta^{13}\text{C}$ -values of CAM plants are between -10 to -30‰ . Cabañero *et al.* reported a LC/IRMS method for honey adulteration detection based on the stable carbon isotope analysis of sucrose, glucose, and fructose. It shows that there is a strong correlation between the $\delta^{13}\text{C}$ -values of three sugars in honey: $\Delta\delta^{13}\text{C}_{\text{fructose} - \text{glucose}}, 0 \pm 0.3\text{‰}$; $\Delta\delta^{13}\text{C}_{\text{fructose} - \text{sucrose}}, 1.2 \pm 0.4\text{‰}$; $\Delta\delta^{13}\text{C}_{\text{glucose} - \text{sucrose}}, 1.3 \pm 0.4\text{‰}$. The use of $\Delta\delta^{13}\text{C}$ systematic differences as an authenticity criterion allows the sugar addition (beet sugar, cane sugar, cane syrup, isoglucose syrup and high-fructose corn syrup) to be detected (detection limit from 1-10%). Therefore, the systematic differences of $\Delta\delta^{13}\text{C}_{\text{fructose} - \text{glucose}}$, $\Delta\delta^{13}\text{C}_{\text{fructose} - \text{sucrose}}$, and $\Delta\delta^{13}\text{C}_{\text{glucose} - \text{sucrose}}$, can be used as an authenticity criterion for the detection of honey adulteration.^[45] Elflein *et al.* used two

methods of EA/IRMS of protein and bulk honey isotope analysis and LC/IRMS of fructose, glucose, and disaccharide for honey adulteration detection. Based on 451 authentic honey results, the following limits of $\Delta\delta^{13}\text{C}$ were proposed: $\Delta\delta^{13}\text{C}$ between all measured $\delta^{13}\text{C}$ -values, $\pm 2.1\text{‰}$; $\Delta\delta^{13}\text{C}_{\text{fructose} - \text{glucose}}$, 1.0‰ ; $\Delta\delta^{13}\text{C}_{\text{protein} - \text{honey}}$, $\geq -1.0\text{‰}$.^[48]

Another important application of LC/IRMS in food quality control is the detection of wine adulteration. Grape is a typical C_3 plant. Cabañero *et al.* proposed using GC/IRMS and LC/IRMS for the measurement of ethanol $\delta^{13}\text{C}$ in wine and compared the measured $\delta^{13}\text{C}$ -values with those measured by the official method of EA/IRMS. There were no significant differences between $\delta^{13}\text{C}$ -values measured by these three methods. $\delta^{13}\text{C}$ -values of ethanol in 23 wine samples ranged from -23.49 to -28.30‰ .^[45] In 2008, they reported a new procedure for simultaneous determination of wine glycerol and ethanol using LC/IRMS.^[47] Guyon and co-workers developed an LC/IRMS method for determination of wine glucose, fructose, glycerol, and ethanol isotope ratios. Based on the results of 20 authentic wines, it was concluded that the ratios of $\delta^{13}\text{C}$ -values of these four compounds in non-adulterated wines are constant: $\delta^{13}\text{C}_{\text{glucose/fructose}}$, $1.00 \pm 0.04\text{‰}$; $\delta^{13}\text{C}_{\text{glycerol/ethanol}}$, $1.02 \pm 0.08\text{‰}$.^[44] Jochmann and co-workers used flow injection analysis-isotope ratio mass spectrometry (FIA/IRMS) for bulk isotope analysis of alcoholic beverages. The FIA/IRMS method showed a few advantages over EA/IRMS analysis for bulk isotope analysis of aqueous samples including simple sample preparation, high throughput, and small sample size. The developed method was applied to 81 alcoholic beverages. The study demonstrated that FIA/IRMS can be used as a prescreening method for authenticity control of alcoholic beverage.^[79]

1.7 Aim of the PhD work

The review of previously reported literature on LC/IRMS shows that the detected compounds of LC/IRMS are mainly polar organic molecules and the commonly used separation mechanism is based on ion interactions. However, the most frequently used method in routine separations, reversed-phase LC, was rarely used for compound-specific isotope analysis of LC/IRMS. The reason is that LC/IRMS system needs carbon-free mobile phase. At room temperature, water is a too weak eluent in reversed-phase column. At high temperature, however, water becomes less polar and behaves more like a medium polar eluent such as methanol/water and acetonitrile/water mixtures. It has been proven that temperature gradients can replace organic solvent gradients to improve chromatographic resolution.^[80-82] This is particularly useful for LC/IRMS analysis because precise and accurate compound-specific isotope analysis requires baseline separation of analytes. The use of high temperature makes

reversed-phase columns compatible in LC/IRMS analysis. Although Godin *et al.* already reported the first method of high temperature liquid chromatography coupled to isotope ratio mass spectrometry in 2008, ^[65] this hyphenation still needs further development.

Based on the previous state of the art and described knowledge gaps and problems, the aims of this PhD work were as follows:

- 1) evaluate suitable reversed-phase columns for HTLC/IRMS, including the effect of column bleed on isotope ratio at high temperature in isothermal and temperature-gradient modes; the effect of column temperature on retention, and baseline separation of a mixture of caffeine derivatives and a mixture of phenols (chapter 2).
- 2) apply the developed method (HTLC/IRMS) to measure natural caffeine from different sources including coffee beans, tea leaves, guaraná powder, and maté leaves, and synthetic caffeine, and discriminate the sources of caffeine in 38 drinks as to natural or synthetic based on carbon isotope analysis (chapter 3).
- 3) develop a new approach of temperature-programmed liquid chromatography coupled to isotope ratio mass spectrometry to measure isotope ratios of steroids, typical non-polar organic compounds, and demonstrate the application to a pharmaceutical product (chapter 4).
- 4) develop a new method of LC/IRMS for compound-specific isotope ratio of AICAR, a gene doping drug, and measure isotope ratio of endogenous AICAR in urine and synthetic AICAR for investigating the possibility of the detection of AICAR abuse in sports (chapter 5).

1.8 References

- [1] Z. Muccio, G. P. Jackson. Isotope ratio mass spectrometry. *Analyst* **2009**, *134*, 213.
- [2] J. J. Thomson, *Vol. A 89*, Proceedings of the Royal Society, **1913**, pp. 1.
- [3] J. R. De Laeter, J. K. Böhlke, P. De Bièvre, H. Hidaka, H. S. Peiser, K. J. R. Rosman, P. D. P. Taylor. Atomic weights of the elements: Review 2000 (IUPAC Technical Report). *Pure Appl. Chem.* **2003**, *75*, 683.
- [4] E. A. Schauble. Applying stable isotope fractionation theory to new systems. *Rev. Mineral. Geochem.* **2004**, *55*, 65.
- [5] E. D. Young, A. Galy, H. Nagahara. Kinetic and equilibrium mass-dependent isotope fractionation laws in nature and their geochemical and cosmochemical significance. *Geochim. Cosmochim. Acta* **2002**, *66*, 1095.
- [6] R. M. Lloyd. Oxygen isotope enrichment of sea water by evaporation. *Geochim. Cosmochim. Acta* **1966**, *30*, 801.
- [7] J. T. Brenna, T. N. Corso, H. J. Tobias, R. J. Caimi. High-precision continuous-flow isotope ratio mass spectrometry. *Mass Spectrom. Rev.* **1997**, *16*, 227.
- [8] J. P. Godin, L. B. Fay, G. Hopfgartner. Liquid chromatography combined with mass spectrometry for $\delta^{13}\text{C}$ isotopic analysis in life science research. *Mass Spectrom. Rev.* **2007**, *26*, 751.
- [9] M. Berglund, M. E. Wieser. Isotopic compositions of the elements 2009 (IUPAC technical report). *Pure Appl. Chem.* **2011**, *83*, 397.
- [10] C. R. McKinney, J. M. McCrea, S. Epstein, H. A. Allen, H. C. Urey. Improvements in mass spectrometers for the measurement of small differences in isotope abundance ratios. *Rev. Sci. Instrum.* **1950**, *21*, 724.
- [11] R. A. Werner, W. A. Brand. Referencing strategies and techniques in stable isotope ratio analysis. *Rapid Commun. Mass Spectrom.* **2001**, *15*, 501.
- [12] J. Yinon, *Advances in forensic applications of mass spectrometry*, CRC, Boca Raton, Fla. ; London, **2004**.
- [13] M. A. Jochmann, T. C. Schmidt, *Compound-specific stable isotope analysis*, The Royal Society of Chemistry **2012**.
- [14] O. Kracht, A. Hilker, in *Application Note: 30177*, Thermo Fisher Scientific Inc. , Bremen **2009**.
- [15] S. Benson, C. Lennard, P. Maynard, C. Roux. Forensic applications of isotope ratio mass spectrometry-A review. *Forensic Sci. Int.* **2006**, *157*, 1.

-
- [16] A. Schimmelmann, A. L. Sessions, M. Mastalerz. Hydrogen isotopic (D/H) composition of organic matter during diagenesis and thermal maturation. *Annu. Rev. Earth Planet. Sci.* **2006**, *34*, 501.
- [17] ThermoFinnigan, *High Temperature Conversion Elemental Analyzer Operating Manual, Ident. No. 112 76 01 Issue 11/2001*.
- [18] N. V. Grassineau, D. P. Matthey, D. Lowry. Sulfur isotope analysis of sulfide and sulfate minerals by continuous flow-isotope ratio mass spectrometry. *Anal. Chem.* **2001**, *73*, 220.
- [19] T. C. Schmidt, L. Zwank, M. Elsner, M. Berg, R. U. Meckenstock, S. B. Haderlein. Compound-specific stable isotope analysis of organic contaminants in natural environments: A critical review of the state of the art, prospects, and future challenges. *Anal. Bioanal. Chem.* **2004**, *378*, 283.
- [20] W. Meier-Augenstein. Applied gas chromatography coupled to isotope ratio mass spectrometry. *J. Chromatogr. A* **1999**, *842*, 351.
- [21] U. Flenker, M. Hebestreit, T. Piper, F. Hülsemann, W. Schänzer. Improved performance and maintenance in gas chromatography/isotope ratio mass spectrometry by precolumn solvent removal. *Anal. Chem.* **2007**, *79*, 4162.
- [22] W. A. Brand, in *Finnigan MAT GmbH Patent application*, GB-2270911-A, (UK), **1993**.
- [23] A. L. Sessions. Isotope-ratio detection for gas chromatography. *J. Sep. Sci.* **2006**, *29*, 1946.
- [24] W. A. Brand, A. R. Tegtmeier, A. Hilkert. Compound-specific isotope analysis: extending toward ^{15}N ^{14}N and ^{18}O ^{16}O . *Org. Geochem.* **1994**, *21*, 585.
- [25] J. P. Godin, J. Hau, L. B. Fay, G. Hopfgartner. Isotope ratio monitoring of small molecules and macromolecules by liquid chromatography coupled to isotope ratio mass spectrometry. *Rapid Commun. Mass Spectrom.* **2005**, *19*, 2689.
- [26] M. Krummen, A. W. Hilkert, D. Juchelka, A. Duhr, H. J. Schlüter, R. Pesch. A new concept for isotope ratio monitoring liquid chromatography/mass spectrometry. *Rapid Commun. Mass Spectrom.* **2004**, *18*, 2260.
- [27] G. Rieley. Derivatization of organic compounds prior to gas chromatographic-combustion-isotope ratio mass spectrometric analysis: Identification of isotope fractionation processes. *The Analyst* **1994**, *119*, 915.

- [28] S. Gross, B. Glaser. Minimization of carbon addition during derivatization of monosaccharides for compound-specific $\delta^{13}\text{C}$ analysis in environmental research. *Rapid Commun. Mass Spectrom.* **2004**, *18*, 2753.
- [29] J. S. O. McCullagh. Mixed-mode chromatography/isotope ratio mass spectrometry. *Rapid Commun. Mass Spectrom.* **2010**, *24*, 483.
- [30] R. J. Caimi, J. T. Brenna. High-precision liquid chromatography-combustion isotope ratio mass spectrometry. *Anal. Chem.* **1993**, *65*, 3497.
- [31] M. McLean, M. L. Vestal, Y. Teffera, F. P. Abramson. Element- and isotope-specific detection for high-performance liquid chromatography using chemical reaction interface mass spectrometry. *J. Chromatogr. A* **1996**, *732*, 189.
- [32] Y. Teffera, J. J. Kusmierz, F. P. Abramson. Continuous-flow isotope ratio mass spectrometry using the chemical reaction interface with either gas or liquid chromatographic introduction. *Anal. Chem.* **1996**, *68*, 1888.
- [33] I. Bisutti, I. Hilke, M. Raessler. Determination of total organic carbon-An overview of current methods. *TrAC-Trends in Analytical Chemistry* **2004**, *23*, 716.
- [34] G. St-Jean. Automated quantitative and isotopic (^{13}C) analysis of dissolved inorganic carbon and dissolved organic carbon in continuous-flow using a total organic carbon analyser. *Rapid Commun. Mass Spectrom.* **2003**, *17*, 419.
- [35] D. J. Morrison, K. Taylor, T. Preston. Strong anion-exchange liquid chromatography coupled with isotope ratio mass spectrometry using a Liquiface interface. *Rapid Commun. Mass Spectrom.* **2010**, *24*, 1755.
- [36] S. Bodé, K. Denef, P. Boeckx. Development and evaluation of a high-performance liquid chromatography/isotope ratio mass spectrometry methodology for $\delta^{13}\text{C}$ analyses of amino sugars in soil. *Rapid Commun. Mass Spectrom.* **2009**, *23*, 2519.
- [37] H. T. S. Boschker, T. C. W. Moerdijk-Poortvliet, P. Van Breugel, M. Houtekamer, J. J. Middelburg. A versatile method for stable carbon isotope analysis of carbohydrates by high-performance liquid chromatography/isotope ratio mass spectrometry. *Rapid Commun. Mass Spectrom.* **2008**, *22*, 3902.
- [38] A. Merchant, B. Wild, A. Richter, S. Bellot, M. A. Adams, E. Dreyer. Compound-specific differences in ^{13}C of soluble carbohydrates in leaves and phloem of 6-month-old *Eucalyptus globulus* (Labill). *Plant, Cell Environ.* **2011**, *34*, 1599.
- [39] D. J. Morrison, J. P. O'Hara, R. F. King, T. Preston. Quantitation of plasma ^{13}C -galactose and ^{13}C -glucose during exercise by liquid chromatography/isotope ratio mass spectrometry. *Rapid Commun. Mass Spectrom.* **2011**, *25*, 2484.

-
- [40] K. T. Rinne, M. Saurer, K. Streit, R. T. W. Siegwolf. Evaluation of a liquid chromatography method for compound-specific $\delta^{13}\text{C}$ analysis of plant carbohydrates in alkaline media. *Rapid Commun. Mass Spectrom.* **2012**, 26, 2173.
- [41] H. Schierbeek, T. C. W. Moerdijk-Poortvliet, C. H. P. van Den Akker, F. W. J. te Braake, H. T. S. Boschker, J. B. van Goudoever. Analysis of [U- $\delta^{13}\text{C}_6$]glucose in human plasma using liquid chromatography/isotope ratio mass spectrometry compared with two other mass spectrometry techniques. *Rapid Commun. Mass Spectrom.* **2009**, 23, 3824.
- [42] X. Du, K. Ferguson, R. Gregory, S. R. Sprang. A method to determine ^{18}O kinetic isotope effects in the hydrolysis of nucleotide triphosphates. *Anal. Biochem.* **2008**, 372, 213.
- [43] C. Yarnes, F. Santos, N. Singh, S. Abiven, M. W. I. Schmidt, J. A. Bird. Stable isotopic analysis of pyrogenic organic matter in soils by liquid chromatography-isotope-ratio mass spectrometry of benzene polycarboxylic acids. *Rapid Commun. Mass Spectrom.* **2011**, 25, 3723.
- [44] F. Guyon, L. Gaillard, M. H. Salagoity, B. Médina. Intrinsic ratios of glucose, fructose, glycerol and ethanol $^{13}\text{C}/^{12}\text{C}$ isotopic ratio determined by HPLC-co-IRMS: Toward determining constants for wine authentication. *Anal. Bioanal. Chem.* **2011**, 401, 1555.
- [45] A. I. Cabañero, J. L. Recio, M. Rupérez. Liquid chromatography coupled to isotope ratio mass spectrometry: A new perspective on honey adulteration detection. *J. Agric. Food Chem.* **2006**, 54, 9719.
- [46] A. I. Cabañero, J. L. Recio, M. Rupérez. Isotope ratio mass spectrometry coupled to liquid and gas chromatography for wine ethanol characterization. *Rapid Commun. Mass Spectrom.* **2008**, 22, 3111.
- [47] A. I. Cabañero, J. L. Recio, M. Rupérez. Simultaneous stable carbon isotopic analysis of wine glycerol and ethanol by liquid chromatography coupled to isotope ratio mass spectrometry. *J. Agric. Food Chem.* **2010**, 58, 722.
- [48] L. Elflein, K. P. Raezke. Improved detection of honey adulteration by measuring differences between $^{13}\text{C}/^{12}\text{C}$ stable carbon isotope ratios of protein and sugar compounds with a combination of elemental analyzer - Isotope ratio mass spectrometry and liquid chromatography-Isotope ratio mass spectrometry ($\delta^{13}\text{C}$ -EA/LC-IRMS). *Apidologie* **2008**, 39, 574.

- [49] J. P. Godin, D. Breuillé, C. Obled, I. Papet, H. Schierbeek, G. Hopfgartner, L. B. Fay. Liquid and gas chromatography coupled to isotope ratio mass spectrometry for the determination of ^{13}C -valine isotopic ratios in complex biological samples. *J. Mass Spectrom.* **2008**, *43*, 1334.
- [50] H. Penning, R. Conrad. Carbon isotope effects associated with mixed-acid fermentation of saccharides by *Clostridium papyrosolvens*. *Geochim. Cosmochim. Acta* **2006**, *70*, 2283.
- [51] J.-P. Godin, J. S. O. McCullagh. Review: Current applications and challenges for liquid chromatography coupled to isotope ratio mass spectrometry (LC/IRMS). *Rapid Commun. Mass Spectrom.* **2011**, *25*, 3019.
- [52] G. Docherty, V. Jones, R. P. Evershed. Practical and theoretical considerations in the gas chromatography/combustion/isotope ratio mass spectrometry $\delta^{13}\text{C}$ analysis of small polyfunctional compounds. *Rapid Commun. Mass Spectrom.* **2001**, *15*, 730.
- [53] J. S. O. McCullagh, D. Juchelka, R. E. M. Hedges. Analysis of amino acid $\delta^{13}\text{C}$ abundance from human and faunal bone collagen using liquid chromatography/isotope ratio mass spectrometry. *Rapid Commun. Mass Spectrom.* **2006**, *20*, 2761.
- [54] P. J. H. Dunn, N. V. Honch, R. P. Evershed. Comparison of liquid chromatography-isotope ratio mass spectrometry (LC/IRMS) and gas chromatography-combustion-isotope ratio mass spectrometry (GC/C/IRMS) for the determination of collagen amino acid $\delta^{13}\text{C}$ values for palaeodietary and palaeoecological reconstruction. *Rapid Commun. Mass Spectrom.* **2011**, *25*, 2995.
- [55] A. H. Lynch, J. S. O. McCullagh, R. E. M. Hedges. Liquid chromatography/isotope ratio mass spectrometry measurement of $\delta^{13}\text{C}$ of amino acids in plant proteins. *Rapid Commun. Mass Spectrom.* **2011**, *25*, 2981.
- [56] J. McCullagh, J. Gaye-Siessegger, U. Focken. Determination of underivatized amino acid $\delta^{13}\text{C}$ by liquid chromatography/isotope ratio mass spectrometry for nutritional studies: The effect of dietary non-essential amino acid profile on the isotopic signature of individual amino acids in fish. *Rapid Commun. Mass Spectrom.* **2008**, *22*, 1817.
- [57] M. Raghavan, J. S. O. McCullagh, N. Lynnerup, R. E. M. Hedges. Amino acid $\delta^{13}\text{C}$ analysis of hair proteins and bone collagen using liquid chromatography/isotope ratio mass spectrometry: Paleodietary implications from intra-individual comparisons. *Rapid Commun. Mass Spectrom.* **2010**, *24*, 541.
- [58] H. Schierbeek, D. Rook, F. W. J. te Braake, K. Y. Dorst, G. Voortman, J. P. Godin, L. B. Fay, J. B. V. Goudoever. Simultaneous analysis of ^{13}C -glutathione as its dimeric

- form GSSG and its precursor [l - ^{13}C]glycine using liquid chromatography/isotope ratio mass spectrometry. *Rapid Commun. Mass Spectrom.* **2009**, *23*, 2897.
- [59] C. I. Smith, B. T. Fuller, K. Choy, M. P. Richards. A three-phase liquid chromatographic method for $\delta^{13}\text{C}$ analysis of amino acids from biological protein hydrolysates using liquid chromatography-isotope ratio mass spectrometry. *Anal. Biochem.* **2009**, *390*, 165.
- [60] H. Schierbeek, F. te Braake, J. P. Godin, L. B. Fay, J. B. van Goudoever. Novel method for measurement of glutathione kinetics in neonates using liquid chromatography coupled to isotope ratio mass spectrometry. *Rapid Commun. Mass Spectrom.* **2007**, *21*, 2805.
- [61] K. Choy, C. I. Smith, B. T. Fuller, M. P. Richards. Investigation of amino acid $\delta^{13}\text{C}$ signatures in bone collagen to reconstruct human palaeodiets using liquid chromatography-isotope ratio mass spectrometry. *Geochim. Cosmochim. Acta* **2010**, *74*, 6093.
- [62] V. Heuer, M. Elvert, S. Tille, M. Krummen, X. P. Mollar, L. R. Hmelo, K. U. Hinrichs. Online $\delta^{13}\text{C}$ analysis of volatile fatty acids in sediment/porewater systems by liquid chromatography-isotope ratio mass spectrometry. *Limnology and Oceanography: Methods* **2006**, *4*, 346.
- [63] S. Reinnicke, A. Bernstein, M. Elsner. Small and reproducible isotope effects during methylation with trimethylsulfonium hydroxide (TMSH): A convenient derivatization method for isotope analysis of negatively charged molecules. *Anal. Chem.* **2010**, *82*, 2013.
- [64] K. Tagami, S. Uchida. Online stable carbon isotope ratio measurement in formic acid, acetic acid, methanol and ethanol in water by high performance liquid chromatography-isotope ratio mass spectrometry. *Anal. Chim. Acta* **2008**, *614*, 165.
- [65] J. P. Godin, G. Hopfgartner, L. Fay. Temperature-programmed high-performance liquid chromatography coupled to isotope ratio mass spectrometry. *Anal. Chem.* **2008**, *80*, 7144.
- [66] Y. Yang, M. Belghazi, A. Lagadec, D. J. Miller, S. B. Hawthorne. Elution of organic solutes from different polarity sorbents using subcritical water. *J. Chromatogr. A* **1998**, *810*, 149.
- [67] Y. Yang. Subcritical water chromatography: A green approach to high-temperature liquid chromatography. *J. Sep. Sci.* **2007**, *30*, 1131.

-
- [68] L. T. Corr, J. C. Sealy, M. C. Horton, R. P. Evershed. A novel marine dietary indicator utilising compound-specific bone collagen amino acid $\delta^{13}\text{C}$ values of ancient humans. *J. Archaeol. Sci.* **2005**, 32, 321.
- [69] S. A. Macko, M. H. Engel, V. Andrusevich, G. Lubec, T. C. O'Connell, R. E. M. Hedges. Documenting the diet in ancient human populations through stable isotope analysis of hair. *Philosophical Transactions of the Royal Society B: Biological Sciences* **1999**, 354, 65.
- [70] A. J. Blyth, Y. Shutova, C. Smith. $\delta^{13}\text{C}$ analysis of bulk organic matter in speleothems using liquid chromatography-isotope ratio mass spectrometry. *Org. Geochem.* **2013**, 55, 22.
- [71] Z. Bai, S. Bodé, D. Huygens, X. Zhang, P. Boeckx. Kinetics of amino sugar formation from organic residues of different quality. *Soil Biology and Biochemistry* **2013**, 57, 814.
- [72] S. Bodé, R. Fancy, P. Boeckx. Stable isotope probing of amino sugars - A promising tool to assess microbial interactions in soils. *Rapid Commun. Mass Spectrom.* **2013**, 27, 1367.
- [73] K. Tagami, S. Uchida, N. Ishii. Measurement of the fate of acetic acid form carbon in soil solution of flooded soils using high performance liquid chromatography coupled with isotope ratio mass spectrometry. *Geoderma* **2011**, 165, 25.
- [74] A. Scheibe, L. Krantz, G. Gleixner. Simultaneous determination of the quantity and isotopic signature of dissolved organic matter from soil water using high-performance liquid chromatography/isotope ratio mass spectrometry. *Rapid Commun. Mass Spectrom.* **2012**, 26, 173.
- [75] P. Albéric. Liquid chromatography/mass spectrometry stable isotope analysis of dissolved organic carbon in stream and soil waters. *Rapid Commun. Mass Spectrom.* **2011**, 25, 3012.
- [76] M. M. Bender. Variations in the $^{13}\text{C}/^{12}\text{C}$ ratios of plants in relation to the pathway of photosynthetic carbon dioxide fixation. *Phytochemistry* **1971**, 10, 1239.
- [77] M. J. Kohn, T. E. Cerling. Stable isotope compositions of biological apatite. *Rev. Mineral. Geochem.* **2002**, 48.
- [78] H. L. Schmidt. Food quality control and studies on human nutrition by mass spectrometric and nuclear magnetic resonance isotope ratio determination. *Fresenius' Zeitschrift für Analytische Chemie* **1986**, 324, 760.

-
- [79] M. A. Jochmann, D. Steinmann, S. Manuel, T. C. Schmidt. Flow injection analysis-isotope ratio mass spectrometry for bulk carbon stable isotope analysis of alcoholic beverages. *J. Agric. Food Chem.* **2009**, *57*, 10489.
- [80] L. A. Al-Khateeb, R. M. Smith. High-temperature liquid chromatography of steroids on a bonded hybrid column. *Anal. Bioanal. Chem.* **2009**, *394*, 1255.
- [81] R. M. Smith. Superheated water chromatography-A green technology for the future. *J. Chromatogr. A* **2008**, *1184*, 441.
- [82] Y. Yang. Stationary phases for LC separations at elevated temperatures. *LC-GC North America* **2006**, *24*, 53.

Chapter 2 High temperature reversed-phase liquid chromatography coupled to isotope ratio mass spectrometry

Redrafted from Lijun Zhang, Dorothea M. Kujawinski, Maik A. Jochmann,* Torsten C. Schmidt: High temperature reversed-phase liquid chromatography coupled to isotope ratio mass spectrometry, *Rapid Communications in Mass Spectrometry* 2011, 25, 2971-2980

2.1 Abstract

Compound-specific isotope analysis (CSIA) by liquid chromatography coupled to isotope ratio mass spectrometry (LC/IRMS) has until now been based on ion-exchange separation. In this work, high-temperature reversed-phase liquid chromatography was coupled to, and for the first time carefully evaluated for, isotope ratio mass spectrometry (HT-RPLC/IRMS) with four different stationary phases. Under isothermal and temperature gradient conditions, the column bleed of XBridge C₁₈ (up to 180°C), Acquity C₁₈ (up to 200°C), Triart C₁₈ (up to 150°C), and Zirchrom PBD (up to 150°C) had no influence on precision and accuracy of $\delta^{13}\text{C}$ measurements, demonstrating the suitability of these columns for HTLC/IRMS analysis. Increasing temperature during LC/IRMS analysis of caffeine on two C₁₈ columns was observed to result in shortened analysis time and increased peak height. The detection limit of HT-RPLC/IRMS obtained for caffeine was 30 mg L⁻¹ (corresponding to 12.4 nmol carbon on-column). Temperature-programmed LC/IRMS (I) accomplished complete separation of a mixture of caffeine derivatives and a mixture of phenols and (II) did not affect precision and accuracy of $\delta^{13}\text{C}$ measurements compared with flow injection analysis without a column. With temperature-programmed LC/IRMS, some compounds that coelute at room temperature could be baseline resolved and analyzed for their individual $\delta^{13}\text{C}$ values, leading to an important extension of the application range of CSIA.

2.2 Introduction

Compound-specific isotope analysis (CSIA) can be applied to trace the biochemical origin and environmental fate of compounds.^[1-3] This technology can be established by coupling gas chromatography (GC) or liquid chromatography (LC) with isotope ratio mass spectrometry (GC/IRMS, LC/IRMS). Compared with GC/IRMS, LC/IRMS can be used to directly measure the stable carbon isotope ratio of non-volatile organic compounds in aqueous mixtures, which would otherwise need to be derivatized prior to GC/IRMS analysis. Since the interface for on-line coupling of LC to IRMS was commercially introduced in 2004,^[4] applications of LC/IRMS have been successfully developed for the measurements of different highly soluble compounds (e.g. sugars^[4-6], amino acids^[7-11], and small peptides^[12, 13]), typically based on separation of ion exchange mechanism. In contrast, the most widely used technology in the liquid chromatography community, reversed-phase LC, has rarely been coupled to IRMS for compound-specific isotope analysis so far. It is of interest to develop the method of reversed-phase liquid chromatography coupled to isotope ratio mass spectrometry (RPLC/IRMS), because the currently used method of ion-exchange chromatography (IEC) has its own constraints, which include difficult separation of non-ionic compounds and increased background due to there being more dissolved carbonate in mobile phase with higher pH.^[9, 14] In addition, RPLC is potentially superior to IEC for the separation of weakly ionisable compounds or analytes in ion-rich matrix which may affect the separation of the target compound. The main challenge of coupling RPLC to IRMS is the mandatory use of pure water as eluent since any added organic buffer results in increased background for isotope analysis.^[4]

Liquid water at elevated temperature can serve as eluent in RPLC and a high temperature can be used instead of organic solvent to adjust elution strength. This is because water at elevated temperature behaves more like a moderately polar organic solvent in terms of elution strength due to its decreased polarity.^[15-20] The relative static permittivity of water, a rough measure of a solvent's polarity, reduces from 80 to 35 with a temperature rise from 20 to 200°C. For example, the relative static permittivity of water at 140°C is approximately equivalent to that of a methanol-water mixture (50/50 in v/v).^[21] Although a first example of high temperature reversed-phase liquid chromatography coupled to isotope ratio mass spectrometry (HT-RPLC/IRMS) was reported by Godin *et al.* in 2008 using two columns of sulfonated polystyrene divinylbenzene (PS-DVB) and porous graphitic carbon (Hypercarb™) with an air-bath oven,^[22] this method still needs further substantial development. First, a suite of columns suitable for CSIA need to be evaluated for future applications. Chromatographic

columns with hybrid silica and metal oxide base have been reported to be more thermally stable than the normal silica-based columns.^[23, 24] Second, heating the LC column by an air-bath oven will cause thermal mismatch between the mobile phase near the column walls and in the column centre thus resulting in strong peak broadening and even distortion.^[25, 26] In contrast, a specially designed contact heating system for HTLC minimizes thermal mismatch by using two aluminium blocks for mobile phase preheating and column heating.^[27]

In this work, three different columns with C₁₈ bonded hybrid phases and one Zirchrom PBD column were evaluated for HT-RPLC/IRMS analysis with aluminium blocks being used as the heat-transfer media. For HT-RPLC/IRMS development, the main concern is the effect of column bleed on precision and accuracy of $\delta^{13}\text{C}$ measurement.^[22, 28] This effect was investigated at various temperatures in isothermal mode and in temperature gradient mode by the use of CO₂ pulses and multiple injections of ethanol. The multiple injections of ethanol were used to mimic the elution of compounds and to obtain a chromatogram with multiple peaks being eluted successively. The measured $\delta^{13}\text{C}$ -values by HT-RPLC/IRMS were compared with flow injection analysis (FIA) results for the evaluation of the effect of column bleed on $\delta^{13}\text{C}$ accuracy since no column was used in FIA. The effect of temperature on retention time and peak width of caffeine was investigated. The detection limit of the method was tested for caffeine with column temperatures of 120 and 150°C. Two mixtures of caffeine derivatives and phenols, as examples of temperature-programmed LC/IRMS application, were separated on XBridge C₁₈ and Zirchrom PBD columns, respectively, and $\delta^{13}\text{C}$ values of individual components were measured. The hyphenation of HT-RPLC/IRMS is an alternative methodology for compound-specific isotope analysis of non-ionic compounds which exist widely in food, pharmaceutical compounds, and environmental contaminants.

2.3 Experimental

2.3.1 Chemicals and reagents

Phosphoric acid (99%) and sodium peroxodisulfate (99%) were purchased from Fluka (Buchs, Switzerland). Caffeine (99%), 2,6-dimethylphenol (99%), and 2,4,6-trimethylphenol (99%) were purchased from Fluka (Steinheim, Germany). Theophylline monohydrate (99%) and theobromine (99%) were purchased from Alfa Aesar (Karlsruhe, Germany). Phenol (99.5%) and acetanilide (internal laboratory standard for elemental analysis) were purchased from Merck (Darmstadt, Germany). 3-Methylphenol (98%) was purchased from Fluka (Buchs, Switzerland). Ethanol BCR-656 with $\delta^{13}\text{C}$ -value of $-26.91 \pm 0.07\text{‰}$ was purchased from Institute for Reference Materials and Measurements (IRMM, Geel, Belgium), and NBS 22 oil

with $\delta^{13}\text{C}$ -value of $-30.03 \pm 0.04\text{‰}$ and IAEA-CH-6 with $\delta^{13}\text{C}$ -value of $-10.45 \pm 0.03\text{‰}$ were purchased from International Atomic Energy Agency (IAEA, Vienna, Austria). Triple distilled water from a homemade distillation unit was used for solution preparation and mobile phase. The water used as mobile phase and solutions was degassed in an ultrasonic bath (Bandelin Electronic, Berlin, Germany) for 15 minutes under vacuum condition. A membrane pump (Vacuubrand GmbH & Co., Wertheim, Germany) was used to generate the vacuum. After degassing, it was continuously purged with Helium 5.0 (Air Liquide, Oberhausen, Germany).

2.3.2 Instrumentation

The eluent for liquid chromatography was delivered by a Flux HPLC pump 420 (Tegimenta, Rotkreuz, Switzerland) and further degassed by a Gastorr online degasser (Bischoff Analysentechnik and Geräte GmbH, Leonberg, Germany) to remove residual gas. The injection was performed by a CTC Analytics autosampler (Zwingen, Switzerland) and a sample loop of 10 μL was used. An HT-HPLC 200 column oven (Scientific Instruments Manufacturer GmbH, Oberhausen, Germany) was used for mobile phase preheating and column heating with two aluminium blocks. A LC-IsoLink interface (Thermo Fisher Scientific, Bremen, Germany) was connected with the HT-HPLC oven and Delta V Advantage isotope ratio mass spectrometer (Thermo Fisher Scientific, Bremen, Germany). The flow rate of water was 500 $\mu\text{L min}^{-1}$. The flow rate of sodium peroxodisulfate (0.83 mol L^{-1}) and phosphoric acid (1.50 mol L^{-1}) was 50 $\mu\text{L min}^{-1}$. In order to avoid blockage in the system, two on-line filters with a pore size of 0.5 μm (Vici, Schenk, Switzerland) were placed at the inlet and outlet of the column, and one more was used in front of the oxidation reactor of the LC-IsoLink interface. The scheme of the setup is shown in Figure. 2.1. Without a column, this setup can be used for flow injection analysis mode (FIA/IRMS).

2.3.3 Chromatographic conditions

The evaluated columns for HT-RPLC/IRMS analysis and the investigated temperature ranges for each column are listed in Table 2.1.

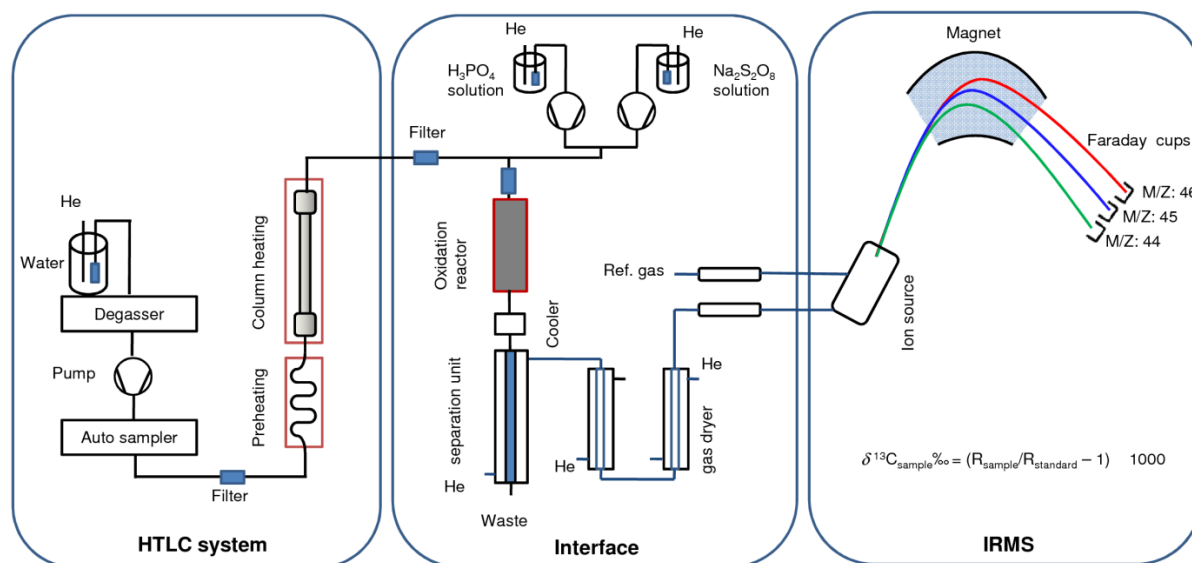


Figure 2.1 The HTLC/IRMS setup.

Table 2.1 Overview of evaluated columns

Manufacturer ^a	Name	Description	Size	Particle size	Temperature range
Waters	XBridge C ₁₈	C ₁₈ bonded ethyl-bridged hybrid phase	50 mm × 3.0 mm	2.5 μm	30-190 ^b
Waters	Acquity UPLC BEH C ₁₈	C ₁₈ bonded ethyl-bridged hybrid phase	50 mm × 2.1 mm	1.7 μm	100-200 ^c
YMC	Triart C ₁₈	C ₁₈ bonded hybrid silica gel	150 mm × 2.0 mm	5 μm	30-150
Zirchrom	Zirchrom PBD	Polybutadiene-coated zirconia	150 mm × 3.0 mm	5 μm	30-150

^aThe address of manufacturer: Waters (Eschborn, Germany); YMC (Dinslaken, Germany); Zirchrom PBD (Anoka, USA).

^bOn XBridge C₁₈ at 190°C, the column bleed affected the precision and accuracy of δ¹³C-values.

^cThe initial temperature on Acquity C₁₈ was 100°C because the back-pressure of the column exceeded the limit pressure of Flux HPLC 420 pump (400 bar), when the used temperature was lower than 100°C with a flow rate of 0.5 mL min⁻¹.

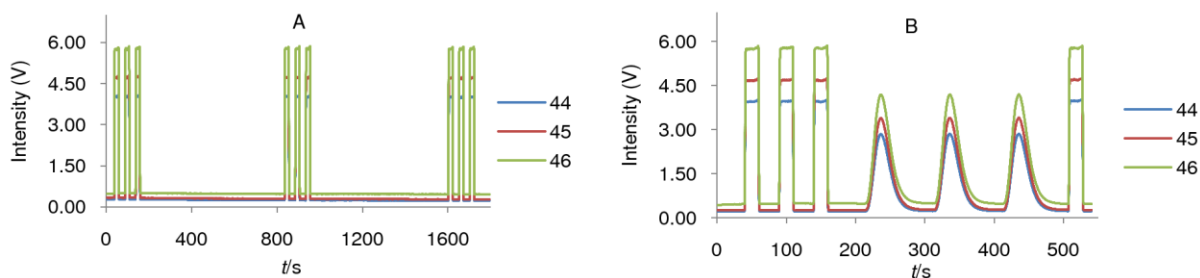


Figure 2.2 HTLC/IRMS chromatograms of CO₂ pulses (A) and multiple injections of 100 mg L⁻¹ ethanol (B) obtained on XBridge C₁₈ column at 100°C. The second reference gas peak was used for calibration of $\delta^{13}\text{C}$ -values.

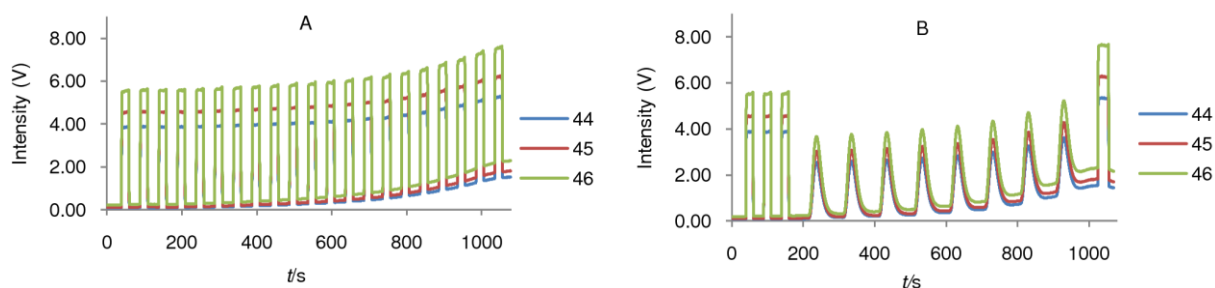


Figure 2.3 Temperature-programmed LC/IRMS chromatograms of successive CO₂ pulses (A) and multiple injections of 100 mg L⁻¹ ethanol (B) obtained on XBridge C₁₈ column. The temperature program was 1 min at 60°C, and then ramped at 20°C min⁻¹ to 120°C where it was held for 1 min, and then at 5 °C min⁻¹ to 180°C where it was held for 1 min.

In isothermal mode, three pulses of CO₂ reference gas with a width of 20 s and a period duration of 50 s were injected in the beginning, in the middle, and at the end of each run over 30 minutes (total of pulses = 9), and ethanol was injected 3 times with an interval of 10 s by using the multiple injection mode with the Isodat 2.5 (Thermo Fisher Scientific, Bremen, Germany) as shown in Figure 2.2.

In temperature gradient mode, pulses of CO₂ reference gas with a width of 20 s and a period duration of 50 s ($n = 21$), and multiple injections of ethanol with an interval of 10 s ($n = 8$) were introduced successively as shown in Figure 2.3. The temperature program on XBridge C₁₈ used to investigate the effect of column bleed on $\delta^{13}\text{C}$ measurements was 1 min at 60°C, and then ramped at 20°C min⁻¹ to 120°C where it was held for 1 min, and then at 5°C min⁻¹ to

180°C where it was held for 1 min. On the Acquity C₁₈ it was 1 min at 100°C, and then ramped to 200°C in 15 min where it was held for 2 min. On the Triart C₁₈ and Zirchrom PBD it was 2 min at 30°C, and then ramped to 150°C in 14 min where it was held for 2 min.

Throughout and after the investigation of the effect of column bleed on $\delta^{13}\text{C}$ measurements, the back-pressure of the four investigated columns did not change notably. XBridge C₁₈ and Acquity C₁₈ were further used to investigate the effect of temperature on retention of caffeine and to measure the method detection limit of HT-RPLC/IRMS. Two columns, XBridge C₁₈ and Zirchrom PBD, were selected for the application of temperature-programmed LC/IRMS because of their different stationary phases. A mixture of caffeine derivatives was used to demonstrate this application on XBridge C₁₈ as caffeine derivatives exist widely in food products. However, these compounds had too short retention time to be separated on Zirchrom PBD at room temperature. Since phenols occur as frequent contaminations in industrial wastewater and they have been studied using a Zirchrom PBD column at high temperature,^[29] a mixture of phenols was used as an example for the separation on Zirchrom PBD column.

2.3.4 Isotopic calculation

All reported isotopic ratios of compounds are expressed as $\delta^{13}\text{C}$ -values relative to an international standard: Vienna Pee Dee Belemnite (VPDB). The $\delta^{13}\text{C}$ -values are defined as:

$$\delta^{13}\text{C}_{s,VPDB} = \frac{R(^{13}\text{C}/^{12}\text{C})_s}{R(^{13}\text{C}/^{12}\text{C})_{VPDB}} - 1 \quad (2.1)$$

In the equation, $R(^{13}\text{C}/^{12}\text{C})_s$ and $R(^{13}\text{C}/^{12}\text{C})_{VPDB}$ (0.0111802) are the $^{13}\text{C}/^{12}\text{C}$ ratio in the sample and in the standard, respectively. At the beginning of each run, three pulses of a laboratory standard gas ($\delta^{13}\text{C} = -37.81\%$) were introduced and the second peak was used for $\delta^{13}\text{C}$ calculation. Another pulse was set at the end of the measurement to control the $\delta^{13}\text{C}$ consistency (see Figure 2.2B). All data acquisition, processing, and evaluation were carried out by Isodat 2.5. Background subtraction was performed automatically by Isodate 2.5, and the background type used for peak integration was ‘individual background’ with start slope and end slope of 0.5 mV s^{-1} except for the chromatograms where the slopes of background increase of some peaks were greater than 2.0 mV s^{-1} . The slope of peak background was calculated by the difference of the backgrounds at the peak start and peak end divided by the peak width. Such a high background change was observed during measurements of the successively multiple injections of ethanol in temperature gradient mode (see Discussion section).

2.3.5 EA/IRMS measurement

The $\delta^{13}\text{C}$ -values of pure compounds were measured with an EA 1110 Elemental Analyzer (CE instrument, Milan, Italy) coupled to MAT 253 IRMS (Thermo Fisher Scientific, Bremen, Germany) with a ConFlo IV interface (Thermo Fisher Scientific, Bremen, Germany). In order to obtain corrected $\delta^{13}\text{C}_{\text{EA/IRMS}}$ value of a compound, the measured $\delta^{13}\text{C}$ -value by EA/IRMS was converted relative to the international standard (VPDB) by using a spreadsheet evaluation as recommended by Werner and Brand.^[30] According to the recommendation, acetanilide used as an internal laboratory standard and blanks of empty capsules were measured along with samples. Isotopic composition of acetanilide was determined and corrected by the use of two-point calibration approach with two certified standard materials of NBS-22 oil (-30.03‰) and IAEA-CH-6 (-10.45‰).^[31]

2.4 Results and discussion

2.4.1 Effect of column bleed on $\delta^{13}\text{C}$ measurement

Hydrolysis of the bonded stationary phase and dissolution of supporting material may occur at elevated temperature, summarized as column bleed.^[32] The column bleed of organic compounds released from the reversed-phase may potentially affect the oxidation of target compounds by consuming the oxidant reagent in the oxidation reactor or reduce the extraction efficiency of CO_2 gas converted from target compounds, resulting in isotope fractionation and unreliable $\delta^{13}\text{C}$ -values. Moreover, carbon background drift, especially in temperature gradient mode, may lead to incorrect peak integration for $\delta^{13}\text{C}$ calculations. In the first report of HTLC/IRMS, the rising and falling background from column bleed significantly affected precision and accuracy of $\delta^{13}\text{C}$ -values when using a HypercarbTM column with temperature ramps up to 110°C .^[22]

In order to validate the HT-RPLC/IRMS method, the effect of column bleed on precision and accuracy of $\delta^{13}\text{C}$ -values was carefully investigated by the use of CO_2 pulses and multiple injections of ethanol at various temperatures in isothermal mode and in temperature gradient mode. Based on a previous report,^[33] the columns with ethyl-bridged hybrid phase are expected to be stable up to 200°C . The Zirchrom PBD was used up to 150°C as recommended by the manufacturer. The YMC Triart C_{18} (Triart C_{18}) with spherical hybrid silica particles was also heated up to 150°C , the highest temperature typically used for high temperature chromatographic column. The reason that we used CO_2 pulses is that having a reliable $\delta^{13}\text{C}$ of CO_2 gas is a primary requirement for all isotope analysis. We used multiple injections of ethanol to mimic the elution of compounds.

Isothermal mode

In isothermal mode, by the use of high temperatures up to 180, 200, 150, and 150°C on XBridge C₁₈, Acquity C₁₈, Triart C₁₈, and Zirchrom PBD, respectively, the column bleed had no significant influence on the precision and accuracy of $\delta^{13}\text{C}$ measurements although the background increased with an increase of column temperature. As shown in Figure 2.4A, all measured $\delta^{13}\text{C}$ -values of CO₂ gas were in the interval of the standard value $\pm 0.5\%$. For multiple injections of ethanol (Figure 2.4B), the $\delta^{13}\text{C}$ -values were consistent with FIA results, lying within the interval of FIA results $\pm 0.5\%$ except for the $\delta^{13}\text{C}$ measured on XBridge C₁₈ at 190°C (the reason is discussed in the next paragraph). The measured $\delta^{13}\text{C}$ -values also showed good precision with $\text{SD} \leq 0.23\%$ in one run ($n = 3$) and within different runs at various temperatures (except for the $\delta^{13}\text{C}$ measured on XBridge C₁₈ at 190°C). The reproducible $\delta^{13}\text{C}$ -values and the insignificant differences, less than 0.5% from FIA results, indicate that the column bleed did not affect the oxidation efficiency of analytes or extraction efficiency of CO₂ gas significantly.

In isothermal mode, the intensity of the background varied according to the stationary phase and temperature. Comparing signal intensity at 150°C, the following sequence was obtained in order of decreasing background: Triart C₁₈ > Acquity C₁₈ > XBridge C₁₈ > Zirchrom PBD. According to a previous report,^[22] nonlinear variation of background affected both precision and accuracy of $\delta^{13}\text{C}$ -values. In this work, the $\delta^{13}\text{C}$ -values were also impacted by a nonlinear variation of background like waves with amplitudes more than 20 mV when using the XBridge C₁₈ column at 190°C. Therefore, the temperature program on XBridge C₁₈ was ramped up to only 180°C. A higher temperature was observed to reduce the back-pressure of the column due to the decreased viscosity of water. For example, the back-pressure of XBridge C₁₈ decreased from 370 to 50 bar by raising temperature from 30 to 180°C. In this work, the decreased back-pressure made the conventional pump and injection valve usable for ultra pressure liquid chromatography column (UPLC). For example, an Acquity C₁₈ column with a particle size of 1.7 μm can be used in this work with a flowrate of 0.5 mL min⁻¹ when the temperature is higher than 100°C.

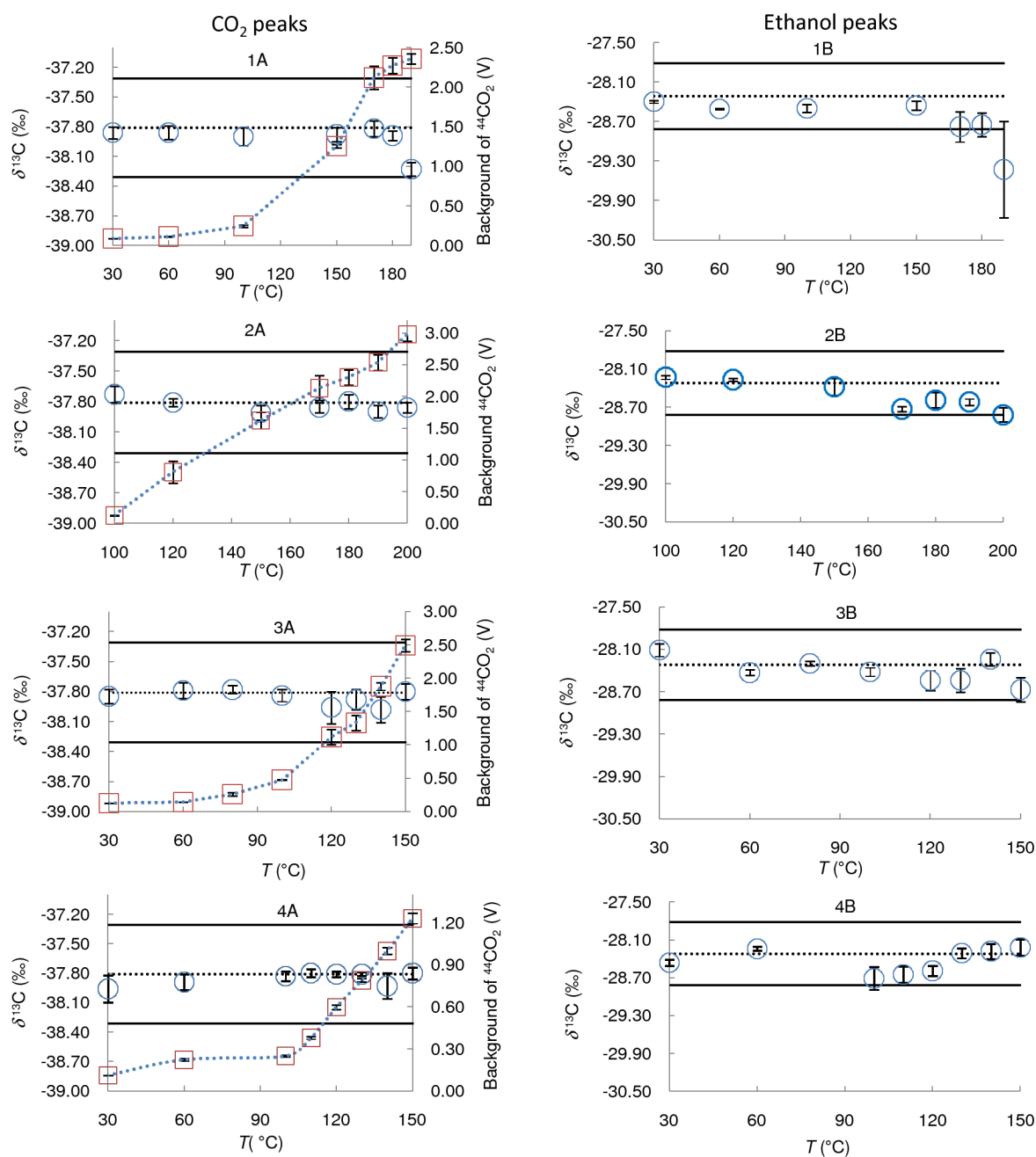


Figure 2.4 (A) $\delta^{13}\text{C}$ of CO₂ gas pulses (circles, left ordinate) and background of ⁴⁴CO₂ (squares, right ordinate) were determined with XBridge C₁₈ (1), Acquity C₁₈ (2), Triart C₁₈ (3), and Zirchrom PBD (4) at various temperatures. Error bars indicate the SD (n = 9). The dotted lines represent the standard value of CO₂ gas (-37.81‰). The horizontal solid lines represent the interval of standard value $\pm 0.5\%$. (B) $\delta^{13}\text{C}$ of multiple injections of 100 mg L⁻¹ ethanol determined with corresponding column at various temperatures. Error bars indicate the SD (n = 3). The dotted lines represent the FIA result (-28.32‰). The horizontal solid lines represent the interval of $-28.32 \pm 0.5\%$.

Temperature gradient mode

In temperature gradient mode, the background of each column increased steadily over the temperature ramp (see example in Figure 2.3). The $\delta^{13}\text{C}$ -value of successive CO_2 pulses was not affected by the background shift, with precision better than 0.14‰ and accuracy better than 0.18‰ compared with the standard value, as shown in Table 2.2. This observation is consistent with a GC/IRMS study where CO_2 pulses were analyzed over a smoothly rising background, and where a difference of 0.21‰ from the accepted value has been reported.^[34] However, the $\delta^{13}\text{C}$ -value of multiple injections of ethanol was impacted by the background shift when the used integration algorithm was ‘individual background’. This effect became significantly when the slope of the peak background was higher than approximate 2.0 mV s^{-1} . In Figure 2.5, this effect was presented clearly by the $\delta^{13}\text{C}$ -value of ethanol peaks (triangle) as the peaks successively distributed over the whole temperature program. The $\delta^{13}\text{C}$ -value of ethanol shifted by more than 0.5‰ in comparison with FIA result when the slope of increasing background was 2.60 and 3.70 mV s^{-1} on XBrige C_{18} and Acquity C_{18} column respectively (sixth peak ff.). The corresponding ramped temperature at that time was 145 and 160°C . The $\delta^{13}\text{C}$ -values shifted more strongly when the slope of the background was steeper. This $\delta^{13}\text{C}$ shift was due to the incorrect background subtraction. For the algorithm of ‘individual background’, the peak background is defined as the lowest running five-point average among the data preceding a peak start, and the peak area is calculated by summing the difference between baseline and signal for the region defined by the peak start and peak end.^[35] When the peak background increases, the peak end is higher than the peak start, meaning that the summed peak area is not correct due to the additional area from the background. Indeed, a higher peak area was observed when the slope of the peak background increased over the temperature ramp. However, this influence on $\delta^{13}\text{C}$ calculation depends on the peak height, the peak width, and the background change. In our study, for CO_2 pulses, the influence was not significant, and for ethanol peaks with a slope of background change lower than 2.0 mV s^{-1} , the influence was also insignificant.

Table 2.2 $\delta^{13}\text{C}$ of successive CO_2 pulses ($n = 21$) and multiple injections of 100 mg L^{-1} ethanol ($n = 8$) with each column under temperature-programmed conditions. The $|\Delta\delta_{\text{HTLC-FIA}}|_{\text{‰}}$ represents the difference of $\delta^{13}\text{C}$ obtained by temperature-programmed LC/IRMS and FIA/IRMS.

Column	XBridge C ₁₈		Acquity C ₁₈		Triart C ₁₈		Zirchrom PBD					
	CO ₂	Ethanol	CO ₂	Ethanol	CO ₂	Ethanol	CO ₂	Ethanol				
$\delta^{13}\text{C} \text{ ‰}$	-37.90	-28.51 ^a	-28.91 ^b	-37.87	-28.25 ^a	-29.03 ^b	-37.99	-28.49 ^a	-28.61 ^b	-37.95	-28.52 ^a	-28.55 ^b
SD	0.09	0.13	0.32	0.06	0.16	1.04	0.13	0.17	0.29	0.13	0.16	0.16
$ \Delta\delta_{\text{HTLC-FIA}} _{\text{‰}}$	0.09	0.19	0.59	0.07	0.07	0.61	0.18	0.17	0.29	0.14	0.20	0.23

For ^{a)} and ^{b)}, the algorithm of background subtraction was ‘dynamic background’ and ‘individual background’, respectively.

The different algorithms in Isodat 2.5 were used to integrate the peak with increased background, and the ‘dynamic background’ was observed to give correct peak areas and thus yield correct $\delta^{13}\text{C}$ -values. This algorithm uses a background function over the whole LC run, which can be used for a chromatogram with smoothly rising background. The correct threshold for the start slope of the analyte peak was very important for background subtraction when using ‘dynamic background’; it needed to be higher than the slope of peak background for correct definition of the background function. For XBridge C₁₈, Acquity C₁₈, Triart C₁₈, and Zirchrom PBD under temperature-programmed condition, the used start slope was 8.0, 8.0, 2.0, and 1.0 mV s^{-1} respectively (the end slope was 0.5 mV s^{-1} identical to that used for ‘individual background’). Under these conditions, the $\delta^{13}\text{C}$ -values of multiple injections of ethanol on each column were in agreement with the FIA result, lying within the interval of FIA result $\pm 0.5\text{‰}$ (See Figure 2.5). Furthermore, the $\delta^{13}\text{C}$ -values of each injected ethanol sample were highly reproducible with precision better than 0.17‰ (see Table 2.2).

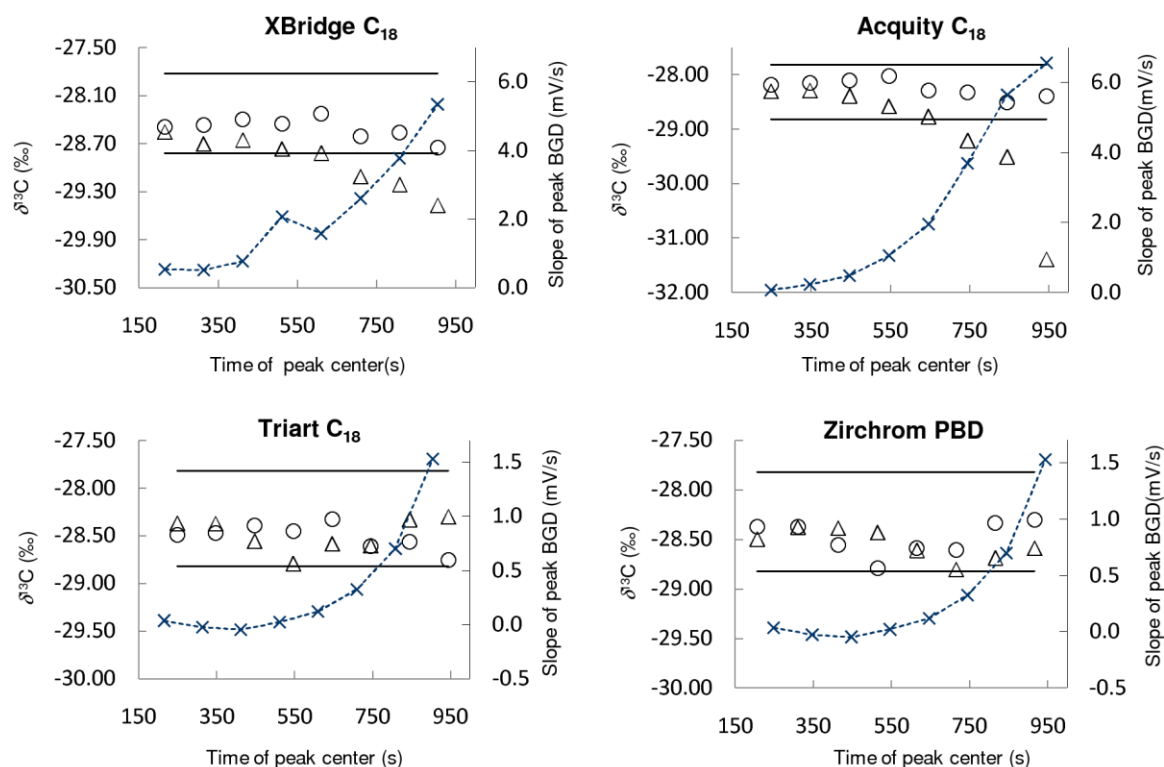


Figure 2.5 $\delta^{13}\text{C}$ -values of multiple injections of 100 mg L^{-1} ethanol calculated with algorithm of ‘individual background’ (triangle, left ordinate) and ‘dynamic background’ (circle, left ordinate) and the slopes of peak backgrounds on mass of 44 (cross, right ordinate) with four columns under temperature-programmed conditions. The x-axis represents the elution time of ethanol peak in temperature-programmed LC/IRMS chromatogram. The slope of peak background was calculated by the difference of backgrounds at the peak start and at the peak end divided by the peak width. The two horizontal solid lines represent the interval of FIA result $\pm 0.5\%$.

2.4.2 Effect of temperature on retention of caffeine

In order to illustrate that temperature can be a powerful parameter for chromatographic separation in LC/IRMS, the effect of temperature on the retention of caffeine was tested with two C_{18} columns. As the temperature increased, the retention time decreased dramatically and peak height increased markedly with a decrease of the peak width. For example, the retention time was reduced approximately by 3 times and the peak height increased approximately by 2 times on raising the temperature from 60 to 180°C (see Table 2.3). At room temperature, caffeine was not eluted in 40 min. It is well established that the temperature has a similar effect on retention time to an increase of the organic solvent during solvent gradient elution at room temperature.^[36-39] For example, a temperature increase of $4\text{-}5^\circ\text{C}$ has a similar effect on retention as a 1% increase in methanol content.^[38] The obtained shorter retention time was

attributed to the decreased polarity of water at high temperature, and the narrower peak was due to the smaller longitudinal diffusion at shorter retention time. At various temperatures, the peak area and $\delta^{13}\text{C}$ -values of caffeine were consistent. No compound degradation occurred on XBridge C_{18} up to 180°C , which could be a potential problem with the use of HTLC.^[22, 40] The consistent $\delta^{13}\text{C}$ -values measured by HT-RPLC/IRMS and by FIA/IRMS corroborated that there was no influence of column bleed on $\delta^{13}\text{C}$ -values during high temperature elution. Shorter retention times and narrower peaks of caffeine were also obtained on Acquity C_{18} with consistent peak area and $\delta^{13}\text{C}$ -values when the temperature increased from 100 to 200°C . CSIA could benefit from such shortened retention time and narrowed peak width at elevated temperature, for example by increasing sample throughput and reducing the detection limit for precise isotope analysis.

Table 2.3 IRMS results of 100 mg L^{-1} caffeine analyzed on XBridge C_{18} column at various temperatures.

T ($^\circ\text{C}$)	50	100	150	180
t_{R} of $^{44}\text{CO}_2$ (s)	1107	396.1	283.8	263.3
Peak height of $^{44}\text{CO}_2$ (mV)	735	1693	2112	2127
Peak area of $^{44}\text{CO}_2$ (Vs)	67.08	68.94	68.73	68.61
$\delta^{13}\text{C}$ ‰	-40.82	-40.86	-40.61	-40.96
$ \Delta\delta_{(\text{HTLC} - \text{FIA})} $ ‰	0.10	0.14	0.11	0.24

2.4.3 Detection limit of HT-RPLC/IRMS

In addition to $\delta^{13}\text{C}$ measurement, LC/IRMS could be used for compound quantification based on the fact that the carbon amount of injected analytes is proportional to the measured peak areas or amplitudes. In this work, the method detection limit (MDL) of HT-RPLC/IRMS was tested on XBridge C_{18} at 120°C and on Acquity C_{18} at 150°C by injection of caffeine at concentrations between 20 to 500 mg L^{-1} , following a previously described moving mean approach.^[41, 42] Within this concentration range the relationship between the peak area of $^{44}\text{CO}_2$ and concentration showed good linearity ($R \geq 0.99$). From 30 to 500 mg L^{-1} , the $\delta^{13}\text{C}$ -values were within the interval of mean value $\pm 0.5\text{‰}$, and SD was less than 0.5‰ for triplicate measurements, as shown in Figure 2.6. However, the triplicate measurements of caffeine at 20 mg L^{-1} had a low precision with SD higher than 0.70‰ . Therefore, 30 mg L^{-1} of caffeine (12.4 nmol carbon on-column) was defined as MDL, which is close to the MDL of

ethanol (8.7 nmol carbon on-column) measured by FIA/IRMS.^[41] The same concentration range of caffeine from 30 to 500 mg L⁻¹ (corresponding to 12.4 to 206.0 nmol carbon on-column) was also obtained for quantification measurement and $\delta^{13}\text{C}$ determination on Acquity C₁₈ at 150°C, yielding the same MDL (results not shown).

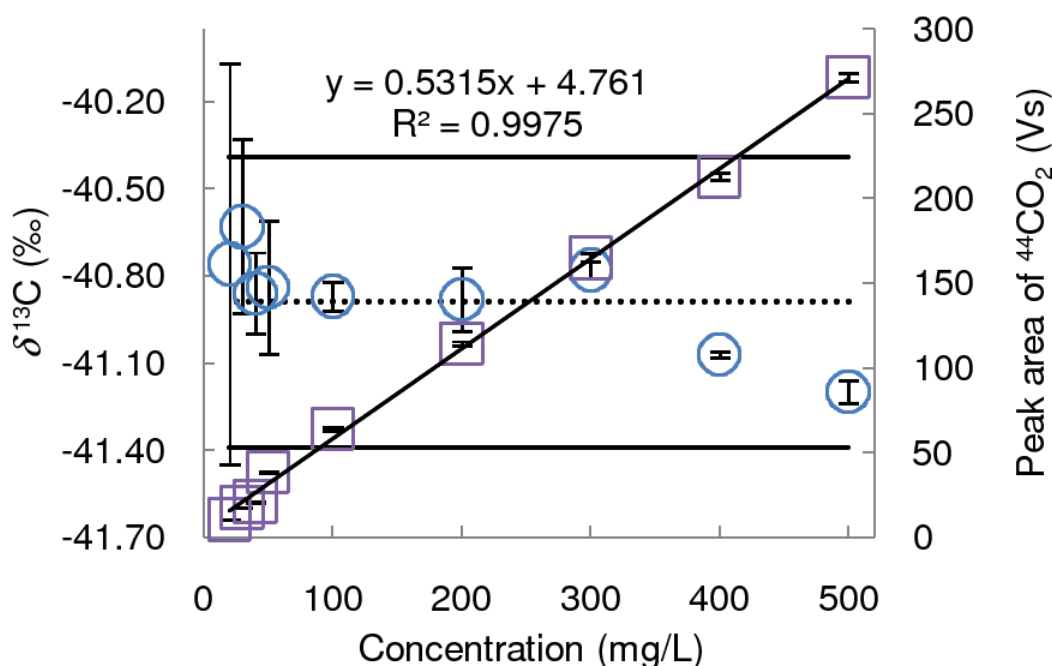


Figure 2.6 Determination of method detection limit for caffeine with XBridge C₁₈ at 120°C. The circles and squares represent the $\delta^{13}\text{C}$ and peak area of $^{44}\text{CO}_2$, respectively. The linear curve fit and the correlation coefficient for plotting peak area vs. concentration are shown in the graph. Error bars indicate the SD of triplicate measurements. The dotted line indicates the iteratively calculated mean value of $\delta^{13}\text{C}$. The horizontal solid lines represent the interval of mean value $\pm 0.5\%$.

2.4.4 Temperature-programmed LC/IRMS for CSIA

It is known that the temperature gradient elution can replace the organic solvent gradient elution to improve the chromatographic resolution.^[18, 21, 43] For precise LC/IRMS measurements, the baseline separation of the individual components is required. Therefore, the use of temperature-programmed elution has potential to push forward the application of LC/IRMS. A mixture of caffeine derivatives and a mixture of phenols as examples were completely separated by temperature-programmed elution on XBridge C₁₈ and Zirchrom PBD columns, respectively, as shown in Figure 2.6. The measured $\delta^{13}\text{C}$ -values were compared to the FIA results and the corrected $\delta^{13}\text{C}_{\text{EA/IRMS}}$ (converting the $\delta^{13}\text{C}$ -value measured by

EA/IRMS relative to the international standard VPDB using a spreadsheet evaluation). As shown in Table 2.4, each component was measured with high precision ($\leq 0.23\text{‰}$). There was no significant difference between $\delta^{13}\text{C}$ measured by temperature-programmed LC/IRMS and by FIA at room temperature. This is the first demonstration of successful separation by temperature-programmed LC for CSIA without column bleed having an effect on precision and accuracy of $\delta^{13}\text{C}$. However, compared with the corrected $\delta^{13}\text{C}_{\text{EA/IRMS}}$, the $\delta^{13}\text{C}$ measured by HTLC/IRMS and FIA had an offset. During the investigation of the effect of column bleed on $\delta^{13}\text{C}$ measurement, an offset for ethanol was also observed between the measured $\delta^{13}\text{C}$ and the standard $\delta^{13}\text{C}$. The fact that the $\delta^{13}\text{C}$ obtained by HT-RPLC/IRMS and by FIA/IRMS without column bleed agreed within error indicated that the offset of $\delta^{13}\text{C}$ resulted from the interface and not from the chromatography. Since the observed offset was dependent on the compound, it seems to result mainly from incomplete oxidation in the oxidation reactor. Other LC/IRMS studies on bentazone and small aliphatic alcohols also suggested that incomplete oxidation of analytes in LC-IsoLink interface was the main contribution to the offset for $\delta^{13}\text{C}$ measurements.^[44, 45] Since the $\delta^{13}\text{C}$ measured by HT-RPLC/IRMS was highly reproducible, the offset of $\delta^{13}\text{C}$ of each compound was stable. Hence, secondary working standards that are chemically identical to target analytes with known $\delta^{13}\text{C}$ -values can be used to correct measured $\delta^{13}\text{C}$ in order to obtain reliable $\delta^{13}\text{C}$. For example, Cabañero *et al.* has used commercial ethanol and glycerol as secondary working standards to correct $\delta^{13}\text{C}$ of wine ethanol and glycerol measured by LC/IRMS.^[46, 47]

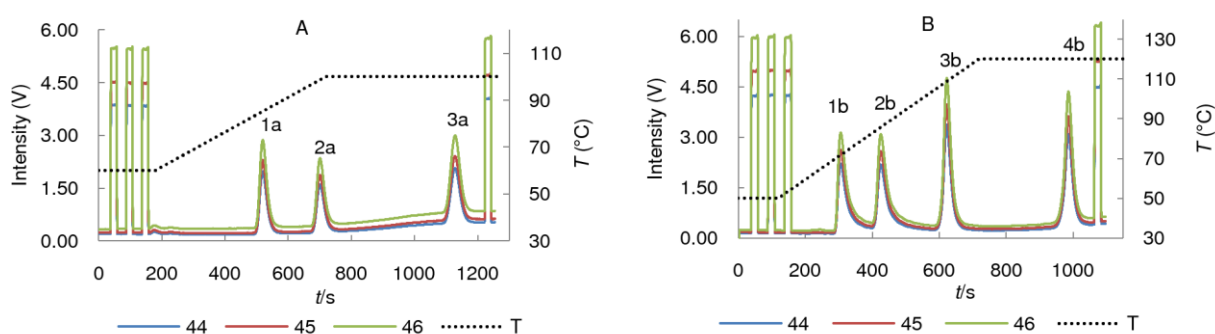


Figure 2.7 Temperature-programmed LC/IRMS chromatograms of caffeine derivatives and phenols using XBridge C_{18} (100 mm \times 30 mm, 3.5 μm , A) and Zirchrom PBD (150 mm \times 30 mm, 5 μm , B), respectively, with pure water at 500 $\mu\text{L min}^{-1}$. The compounds are (1a) theobromine; (2a) theophylline (3a) caffeine; (1b) phenol; (2b) 3-methylphenol; (3b) 2,6-dimethylphenol; (4b) 2,4,6-trimethylphenol in 100 $\mu\text{g L}^{-1}$.

Table 2.4 Comparison of $\delta^{13}\text{C}$ of caffeine derivatives and phenols measured by temperature-programmed LC/IRMS with the corrected $\delta^{13}\text{C}_{\text{EA/IRMS}}$ and the $\delta^{13}\text{C}$ -values measured by FIA/IRMS.

Components	HTLC/IRMS	FIA/IRMS	Corrected	$ \Delta\delta_{\text{HTLC-EA}} $	$ \Delta\delta_{\text{HTLC-FIA}} $
	$\delta^{13}\text{C} \pm \text{SD}$ (n = 3)	$\delta^{13}\text{C} \pm \text{SD}$ (n = 5)	$\delta^{13}\text{C}_{\text{EA/IRMS}} \pm \text{SD}$ (n = 3)		
Theobromine	-45.42 ± 0.16	-45.16 ± 0.11	-42.04 ± 0.03	3.38	0.26
Theophylline	-42.47 ± 0.23	-42.06 ± 0.10	-38.08 ± 0.03	4.39	0.41
Caffeine	-41.01 ± 0.12	-40.72 ± 0.06	-35.56 ± 0.02	5.45	0.29
Phenol	-28.56 ± 0.06	-28.13 ± 0.12	-27.04 ± 0.24	1.62	0.43
3-Methylphenol	-29.57 ± 0.16	-29.54 ± 0.06	-28.40 ± 0.11	1.17	0.03
2,6-Dimethylphenol	-32.73 ± 0.06	-32.28 ± 0.02	-31.52 ± 0.10	1.11	0.45
2,4,6-Trimethylphenol	-36.48 ± 0.08	-36.51 ± 0.09	-35.88 ± 0.05	0.60	0.03

The corrected $\delta^{13}\text{C}_{\text{EA/IRMS}}$ of compound was obtained by converting the $\delta^{13}\text{C}$ value measured by EA/IRMS relative to the international standard (VPDB) using a spreadsheet evaluation as recommended by Werner and Brand.^[30]

2.5 Conclusion

Under isothermal and temperature gradient conditions, the four investigated reversed-phase columns showed good capacity for compound-specific isotope analysis as the column bleed of XBridge C₁₈ (up to 180°C), Acquity C₁₈ (up to 200°C), Triart C₁₈ (up to 150°C), and Zirchrom PBD (up to 150°C) had no significant influence on precision and accuracy of $\delta^{13}\text{C}$ -values. Baseline separation of two mixtures showed that temperature-programmed LC/IRMS is a powerful tool for CSIA. According to the measurements described here, none of the columns showed an obvious deterioration and thus demonstrated good thermal stability with pure water elution. Future investigations in our laboratory will focus on isotopic composition measurements of specific compounds in food and pharmaceutical products by HT-RPLC/IRMS, and the long time stability of the column will be monitored during the real sample measurements.

2.6 Acknowledgements

We thank Thorsten Teutenberg and Steffen Wiese for their support in HT-RPLC. We acknowledge financial support from the German Federal Ministry of Economics and Technology within the agenda for the promotion of industrial cooperative research and development (IGF) based on a decision of the German Bundestag (IGF-Project No. 16120 N). We also acknowledge the financial support from the German Research Foundation.

2.7 References

- [1] Z. Muccio, G. P. Jackson. Isotope ratio mass spectrometry. *Analyst* **2009**, *134*, 213.
- [2] T. C. Schmidt, L. Zwank, M. Elsner, M. Berg, R. U. Meckenstock, S. B. Haderlein. Compound-specific stable isotope analysis of organic contaminants in natural environments: A critical review of the state of the art, prospects, and future challenges. *Anal. Bioanal. Chem.* **2004**, *378*, 283.
- [3] M. Elsner. Stable isotope fractionation to investigate natural transformation mechanisms of organic contaminants: Principles, prospects and limitations. *J. Environ. Monit.* **2010**, *12*, 2005.
- [4] M. Krummen, A. W. Hilkert, D. Juchelka, A. Duhr, H. J. Schlüter, R. Pesch. A new concept for isotope ratio monitoring liquid chromatography/mass spectrometry. *Rapid Commun. Mass Spectrom.* **2004**, *18*, 2260.
- [5] A. I. Cabañero, J. L. Recio, M. Rupérez. Liquid chromatography coupled to isotope ratio mass spectrometry: A new perspective on honey adulteration detection. *J. Agricul. Food Chem.* **2006**, *54*, 9719.
- [6] H. Schierbeek, T. C. W. Moerdijk-Poortvliet, C. H. P. van Den Akker, F. W. J. te Braake, H. T. S. Boschker, J. B. van Goudoever. Analysis of [U- $\delta^{13}\text{C}_6$]glucose in human plasma using liquid chromatography/isotope ratio mass spectrometry compared with two other mass spectrometry techniques. *Rapid Commun. Mass Spectrom.* **2009**, *23*, 3824.
- [7] J. P. Godin, J. Hau, L. B. Fay, G. Hopfgartner. Isotope ratio monitoring of small molecules and macromolecules by liquid chromatography coupled to isotope ratio mass spectrometry. *Rapid Commun. Mass Spectrom.* **2005**, *19*, 2689.
- [8] J. McCullagh, J. Gaye-Siessegger, U. Focken. Determination of underivatized amino acid $\delta^{13}\text{C}$ by liquid chromatography/isotope ratio mass spectrometry for nutritional studies: The effect of dietary non-essential amino acid profile on the isotopic signature of individual amino acids in fish. *Rapid Commun. Mass Spectrom.* **2008**, *22*, 1817.
- [9] J. S. O. McCullagh. Mixed-mode chromatography/isotope ratio mass spectrometry. *Rapid Commun. Mass Spectrom.* **2010**, *24*, 483.
- [10] J. S. O. McCullagh, D. Juchelka, R. E. M. Hedges. Analysis of amino acid $\delta^{13}\text{C}$ abundance from human and faunal bone collagen using liquid chromatography/isotope ratio mass spectrometry. *Rapid Commun. Mass Spectrom.* **2006**, *20*, 2761.
- [11] M. Raghavan, J. S. O. McCullagh, N. Lynnerup, R. E. M. Hedges. Amino acid $\delta^{13}\text{C}$ analysis of hair proteins and bone collagen using liquid chromatography/isotope ratio

- mass spectrometry: Paleodietary implications from intra-individual comparisons. *Rapid Commun. Mass Spectrom.* **2010**, *24*, 541.
- [12] H. Schierbeek, D. Rook, F. W. J. te Braake, K. Y. Dorst, G. Voortman, J. P. Godin, L. B. Fay, J. B. V. Goudoever. Simultaneous analysis of ^{13}C -glutathione as its dimeric form GSSG and its precursor [l - ^{13}C]glycine using liquid chromatography/isotope ratio mass spectrometry. *Rapid Commun. Mass Spectrom.* **2009**, *23*, 2897.
- [13] H. Schierbeek, F. te Braake, J. P. Godin, L. B. Fay, J. B. van Goudoever. Novel method for measurement of glutathione kinetics in neonates using liquid chromatography coupled to isotope ratio mass spectrometry. *Rapid Commun. Mass Spectrom.* **2007**, *21*, 2805.
- [14] D. J. Morrison, K. Taylor, T. Preston. Strong anion-exchange liquid chromatography coupled with isotope ratio mass spectrometry using a Liquiface interface. *Rapid Commun. Mass Spectrom.* **2010**, *24*, 1755.
- [15] L. Al-Khateeb, R. M. Smith. Superheated water chromatography on phenyl bonded hybrid stationary phases. *J. Chromatogr. A* **2008**, *1201*, 61.
- [16] O. Chienthavorn, R. M. Smith, S. Saha, I. D. Wilson, B. Wright, S. D. Taylor, E. M. Lenz. Superheated water chromatography-nuclear magnetic resonance spectroscopy and mass spectrometry of vitamins. *J. Pharm. Biomed. Anal.* **2004**, *36*, 477.
- [17] S. Heinisch, J. L. Rocca. Sense and nonsense of high-temperature liquid chromatography. *J. Chromatogr. A* **2009**, *1216*, 642.
- [18] R. M. Smith. Superheated water chromatography-A green technology for the future. *J. Chromatogr. A* **2008**, *1184*, 441.
- [19] R. Tajuddin, R. M. Smith. On-line coupled superheated water extraction (SWE) and superheated water chromatography (SWC). *Analyst* **2002**, *127*, 883.
- [20] T. Teutenberg, O. Lerch, H. J. Götze, P. Zinn. Separation of selected anticancer drugs using superheated water as the mobile phase. *Anal. Chem.* **2001**, *73*, 3896.
- [21] Y. Yang. Subcritical water chromatography: A green approach to high-temperature liquid chromatography. *J. Sep. Sci.* **2007**, *30*, 1131.
- [22] J. P. Godin, G. Hopfgartner, L. Fay. Temperature-programmed high-performance liquid chromatography coupled to isotope ratio mass spectrometry. *Anal. Chem.* **2008**, *80*, 7144.
- [23] T. Teutenberg, K. Hollebekkers, S. Wiese, A. Boergers. Temperature and pH-stability of commercial stationary phases. *J. Sep. Sci.* **2009**, *32*, 1262.

-
- [24] T. Teutenberg, J. Tuerk, M. Holzhauser, S. Giegold. Temperature stability of reversed phase and normal phase stationary phases under aqueous conditions. *J. Sep. Sci.* **2007**, *30*, 1101.
- [25] J. D. Thompson, J. S. Brown, P. W. Carr. Dependence of thermal mismatch broadening on column diameter in high-speed liquid chromatography at elevated temperatures. *Anal. Chem.* **2001**, *73*, 3340.
- [26] R. G. Wolcott, J. W. Dolan, L. R. Snyder, S. R. Bakalyar, M. A. Arnold, J. A. Nichols. Control of column temperature in reversed-phase liquid chromatography. *J. Chromatogr. A* **2000**, *869*, 211.
- [27] T. Teutenberg, H. J. Goetze, J. Tuerk, J. Ploeger, T. K. Kiffmeyer, K. G. Schmidt, W. g. Kohorst, T. Rohe, H. D. Jansen, H. Weber. Development and application of a specially designed heating system for temperature-programmed high-performance liquid chromatography using subcritical water as the mobile phase. *J. Chromatogr. A* **2006**, *1114*, 89.
- [28] J. P. Godin, L. B. Fay, G. Hopfgartner. Liquid chromatography combined with mass spectrometry for $\delta^{13}\text{C}$ isotopic analysis in life science research. *Mass Spectrom. Rev.* **2007**, *26*, 751.
- [29] Y. Yang, L. J. Lamm, P. He, T. Kondo. Temperature effect on peak width and column efficiency in subcritical water chromatography. *J. Chromatogr. Sci.* **2002**, *40*, 107.
- [30] R. A. Werner, W. A. Brand. Referencing strategies and techniques in stable isotope ratio analysis. *Rapid Commun. Mass Spectrom.* **2001**, *15*, 501.
- [31] T. B. Coplen, W. A. Brand, M. Gehre, M. Gröning, H. A. J. Meijer, B. Toman, R. M. Verkouteren. New guidelines for $\delta^{13}\text{C}$ measurements. *Anal. Chem.* **2006**, *78*, 2439.
- [32] T. Teutenberg, J. Tuerk, M. Holzhauser, T. K. Kiffmeyer. Evaluation of column bleed by using an ultraviolet and a charged aerosol detector coupled to a high-temperature liquid chromatographic system. *J. Chromatogr. A* **2006**, *1119*, 197.
- [33] S. Shen, H. Lee, J. McCaffrey, N. Yee, C. Senanayake, N. Grinberg, J. Clark. High temperature high performance liquid chromatography of substituted anilines using a C18 hybrid stationary phase. *J. Liq. Chromatogr. Relat. Tech.* **2006**, *29*, 2823.
- [34] D. A. Merritt, J. M. Hayes. Factors controlling precision and accuracy in isotope-ratio-monitoring mass spectrometry. *Anal. Chem.* **1994**, *66*, 2336.
- [35] K. J. Goodman, J. T. Brenna. Curve fitting for restoration of accuracy for overlapping peaks in gas chromatography/combustion isotope ratio mass spectrometry. *Anal. Chem.* **1994**, *66*, 1294.

-
- [36] S. D. Allmon, J. G. Dorsey. Retention mechanisms in subcritical water reversed-phase chromatography. *J. Chromatogr. A* **2009**, 1216, 5106.
- [37] J. W. Coym, J. G. Dorsey. Reversed-phase retention thermodynamics of pure-water mobile phases at ambient and elevated temperature. *J. Chromatogr. A* **2004**, 1035, 23.
- [38] A. Jones, Y. Yang. Separation of nonpolar analytes using methanol-water mixtures at elevated temperatures. *Anal. Chim. Acta* **2003**, 485, 51.
- [39] R. M. Smith, R. J. Burgess. Superheated water as an eluent for reversed-phase high-performance liquid chromatography. *J. Chromatogr. A* **1997**, 785, 49.
- [40] S. Giegold, M. Holzhauser, T. Kiffmeyer, J. Tuerk, T. Teutenberg, M. Rosenhagen, D. Hennies, T. Hoppe-Tichy, B. Wenclawiak. Influence of the stationary phase on the stability of thalidomide and comparison of different methods for the quantification of thalidomide in tablets using high-temperature liquid chromatography. *J. Pharm. Biomed. Anal.* **2008**, 46, 625.
- [41] M. A. Jochmann, D. Steinmann, S. Manuel, T. C. Schmidt. Flow injection analysis-isotope ratio mass spectrometry for bulk carbon stable isotope analysis of alcoholic beverages. *J. Agric. Food Chem.* **2009**, 57, 10489.
- [42] D. M. Kujawinski, M. Stephan, M. A. Jochmann, K. Krajenke, J. Haas, T. C. Schmidt. Stable carbon and hydrogen isotope analysis of methyl tert-butyl ether and tert-amyl methyl ether by purge and trap-gas chromatography-isotope ratio mass spectrometry: Method evaluation and application. *J. Environ. Monit.* **2010**, 12, 347.
- [43] L. A. Al-Khateeb, R. M. Smith. High-temperature liquid chromatography of steroids on a bonded hybrid column. *Anal. Bioanal. Chem.* **2009**, 394, 1255.
- [44] S. Reinnicke, A. Bernstein, M. Elsner. Small and reproducible isotope effects during methylation with trimethylsulfonium hydroxide (TMSH): A convenient derivatization method for isotope analysis of negatively charged molecules. *Anal. Chem.* **2010**, 82, 2013.
- [45] K. Tagami, S. Uchida. Online stable carbon isotope ratio measurement in formic acid, acetic acid, methanol and ethanol in water by high performance liquid chromatography-isotope ratio mass spectrometry. *Anal. Chim. Acta* **2008**, 614, 165.
- [46] A. I. Cabañero, J. L. Recio, M. Rupérez. Isotope ratio mass spectrometry coupled to liquid and gas chromatography for wine ethanol characterization. *Rapid Commun. Mass Spectrom.* **2008**, 22, 3111.

- [47] A. I. Cabañero, J. L. Recio, M. Rupérez. Simultaneous stable carbon isotopic analysis of wine glycerol and ethanol by liquid chromatography coupled to isotope ratio mass spectrometry. *J. Agric. Food Chem.* **2010**, 58, 722.

Chapter 3 Caffeine in your drink: natural or synthetic?

Redrafted from Lijun Zhang, Dorothea M. Kujawinski, Eugen Federherr, Torsten C. Schmidt, Maik A. Jochmann^{*}: Caffeine in your drink: Natural or synthetic? *Analytical Chemistry* 2012, 84, 2805-2810

3.1 Abstract

Owing to possible adulteration and health concerns, it is important to discriminate between natural and synthetic food ingredients. A new method for compound-specific isotope analysis (CSIA) by coupling high-temperature reversed-phase liquid chromatography to isotope ratio mass spectrometry (HT-RPLC/IRMS) was developed for discrimination of natural and synthetic caffeine contained in all types of drinks. The analytical parameters such as stationary phase, column inner diameter, and column temperature were optimized for the separation of caffeine directly from drinks (without extraction). On the basis of the carbon isotope analysis of 42 natural caffeine samples including coffee beans, tea leaves, guaraná powder, and maté leaves, and 20 synthetic caffeine samples from different sources by high temperature reversed-phase liquid chromatography coupled to isotope ratio mass spectrometry (HT-RPLC/IRMS), it is concluded that there are two distinguishable groups of $\delta^{13}\text{C}$ -values: one between -25 to -32‰ for natural caffeine, and the other between -33 to -38‰ for synthetic caffeine. Isotope analysis by HT-RPLC/IRMS has been applied to identify the caffeine source in 38 drinks. Four mislabelled products were detected due to added but non-labelled synthetic caffeine with $\delta^{13}\text{C}$ -values more negative than -33‰ . This work is the first application of HT-RPLC/IRMS to real-world food samples, which showed several advantages, simple sample preparation (only dilution), high throughput, long-term column stability, and high precision of $\delta^{13}\text{C}$ -value. Thus, HT-RPLC/IRMS can be a very promising tool in stable isotope analysis of non-volatile organic compounds.

3.2 Introduction

For manufacturers and customers, it is interesting to discriminate between natural and synthetic products, especially for widely consumed food products like caffeine-containing drinks. Caffeine-containing drinks are the most popular type of beverage in the world.^[1] Apart from natural drinks such as coffee, tea, guaraná, and maté, caffeine is also found in energy drinks and cola-type soft drinks that usually contain added synthetic caffeine. However, people prefer food products made of natural sources to those made of artificial chemicals. The food and drug administration (FDA) regulates that caffeine must be listed on the label of drinks when it has been added in the production, but not for drinks made from tea or coffee.^[2] In consideration of the growing demand for natural drinks on the one hand and the significant price differences between naturally occurring caffeine sources and synthetic caffeine chemicals on the other hand, there is a high risk of fraud by false declaration of caffeine origins. Moreover, the naturally caffeinated drinks are generally assumed to be healthier than energy drinks containing high levels of synthetic caffeine^[1, 3-5] that can lead to adverse effects, such as anxiety and insomnia.^[6, 7] Some energy drinks contain caffeine in excess of 400 mg, which is the maximum daily allowance of caffeine for a healthy adult.^[7, 8] Discrimination of natural and synthetic caffeine has received attention since energy drinks first appeared in Europe and Asia in 1960s when radiocarbon analysis of caffeine was used for identification as to its natural or synthetic origin.^[9, 10]

Stable isotope analysis has proved to be a powerful tool for detecting adulteration in food products.^[11-15] The stable carbon isotope ratio depends upon the origin of the material. For example, plants using the C₃-photosynthetic pathway have more negative $\delta^{13}\text{C}$ -values than those using the C₄ pathway. Commercial chemicals derived from petroleum and coal sources may have different $\delta^{13}\text{C}$ -value compared to those extracted from biogenic sources.^[16] Riching *et al.* reported that an elemental analyzer coupled to isotope ratio mass spectrometry (EA/IRMS) for $\delta^{13}\text{C}$ and $\delta^{18}\text{O}$ analysis has the potential to discriminate between natural and synthetic caffeine.^[17] However, both reported methods, radiocarbon analysis and EA/IRMS, need off-line extraction and purification of caffeine from the matrix, which is a labour-intensive and time-consuming process. Liquid chromatography coupled to isotope ratio mass spectrometry (LC/IRMS) has gained growing interest as it is able to measure stable carbon isotope ratios of single compounds directly from complex mixtures.^[18, 19] It has been applied successfully to authenticity control of ethanol in wine^[20, 21] and sugars in honey.^[20, 22] The recent introduction of high-temperature liquid chromatography coupled to isotope ratio mass

spectrometry (HTLC/IRMS) now enables the use of reversed-phase columns for compound-specific isotope analysis.^[23, 24]

In this work, HTLC/IRMS was developed for carbon isotope analysis of caffeine directly from drinks. The determined $\delta^{13}\text{C}$ -values can be used for discrimination of natural and synthetic caffeine based on two distinct ranges of caffeine isotope ratios as demonstrated by analyzing 42 natural caffeine samples including coffee, tea, guaraná, and maté, and 20 caffeine samples from various synthetic origins.

3.3 Experimental section

3.3.1 Chemicals

Ortho-phosphoric acid (99%) and sodium peroxodisulfate (99%) were purchased from Fluka (Buchs, Switzerland). Caffeine (99%) was purchased from Fluka (Steinheim, Germany). Theophylline monohydrate (99%) and theobromine (99%) were purchased from Alfa Aesar (Karlsruhe, Germany). Acetanilide (internal laboratory standard for elemental analysis) was purchased from Merck (Darmstadt, Germany). IAEA-600 caffeine with a $\delta^{13}\text{C}$ -value of $-27.77 \pm 0.04\text{‰}$ was purchased from International Atomic Energy Agency (Vienna, Austria).^[25] Deionised water was used for solution preparation and mobile phase. Water and solutions used in the interface were degassed in an ultrasonic bath (Bandelin Electronic, Berlin, and Germany) for 15 minutes under vacuum conditions. A MZ2D NT diaphragm pump (Vacuubrand, Wertheim, Germany) was used to generate the needed vacuum. After degassing, it was continuously purged with Helium 5.0 (Air Liquide, Oberhausen, Germany). The measured caffeine samples and preparation method for EA/IRMS and HT-RPLC/IRMS measurements are listed in Table 3.1. Prior to EA/IRMS measurement, the purity of isolated caffeine from coffee beans, tea leaves, and energy drinks was checked by a system 2000 Fourier transform infrared spectrometer (PerkinElmer, Rodgau, Germany) and by high performance liquid chromatography. In order to check for potential isotope fractionation in the sample preparation procedure of the EA/IRMS measurement, the synthetic caffeine sample with known $\delta^{13}\text{C}$ -value were subjected to the same sample procedure as coffee and tea samples and subsequently measured by EA/IRMS.^[26]

Table 3.1 The measured caffeine samples and preparation methods

Type	Sample	Total	EA/IRMS	LC/IRMS
Natural sources	Coffee beans (Arabic)	18	See reference ^[26]	Espresso was prepared using a espresso machine of Saeco Royal Coffee Bar (Essen, Germany), and then diluted 5 times and filtered through a 0.20 μm membrane filter ^[27]
	Tea leaves	21	See reference ^[28]	1g finely ground tea leaves in 100 g water was boiled for 20 minutes, then diluted 2 times and filtered through a 0.20 μm membrane filter
	Guaraná	1	NA	Same as tea leaves
	Maté	3	NA	Same as tea leaves
Synthetic caffeine	Commercial chemicals	2	Measured directly	100 m L^{-1}
	Energy drinks ^a	18	See reference ^[26]	Diluted 5 times and filtered through a 0.20 μm membrane filter
Tested drinks	Bottled or canned drinks	38	NA	Diluted (if necessary) ^b and filtered through a 0.20 μm membrane filter

Except two caffeine chemicals (Fluka, Steinheim Germany; Alfa Aesar, Karlsruhe, Germany), other samples were collected from local market. a) For energy drinks that contain synthetic caffeine, it is typical to see that an exact amount of caffeine is listed on the product label and no information about natural caffeine source is given. b) The sample with caffeine more than 200 mg L^{-1} was diluted in order to achieve a caffeine concentration of 100 mg L^{-1} approximately.

3.3.2 Instrumentation for HT-RPLC/IRMS

The eluent for liquid chromatography was delivered by a Rheos Allegro pump (Flux instruments AG, Basel, Switzerland). The injection was made into a 10 μL sample loop using a HTC PAL autosampler (CTC Analytics, Zwingen, Switzerland). An HT-HPLC 200 column oven (SIM, Oberhausen, Germany) was used for mobile phase preheating and column heating with two aluminium blocks. For isotope ratio measurement, a LC-IsoLink interface (Thermo Fisher Scientific, Bremen, Germany) connecting with the HT-HPLC oven with a Delta V Advantage isotope ratio mass spectrometer (Thermo Fisher Scientific) was used. The water flow rate was 0.5 mL min^{-1} . The flow rate of sodium peroxodisulfate (0.83 mol L^{-1}) and phosphoric acid (1.50 mol L^{-1}) was 50 $\mu\text{L min}^{-1}$. In order to avoid blockage in the system, an in-line filter with a pore size of 0.5 μm (Vici, Schenk, Switzerland) was placed in front of the oxidation reactor of the LC-IsoLink interface. The schematic setup is the same as shown

in Figure 1 of reference 23. Without the column, the setup may be used for flow injection analysis (FIA/IRMS).^[29]

For the separation of caffeine from drinks, an XBridge C₁₈ column (2.1 × 100 mm, 3.5 μm, Waters, Eschborn, Germany) with an XBridge C₁₈ guard column (2.1 × 10 mm, 3.5 μm) was used. Two other columns (XBridge C₁₈ (3.0 × 100 mm, 3.5 μm) and Zirchrom PBD (3.0 × 150 mm, 5 μm, Zirchrom, Anoka, USA)) were used for method development.

3.3.3 Isotopic calculation

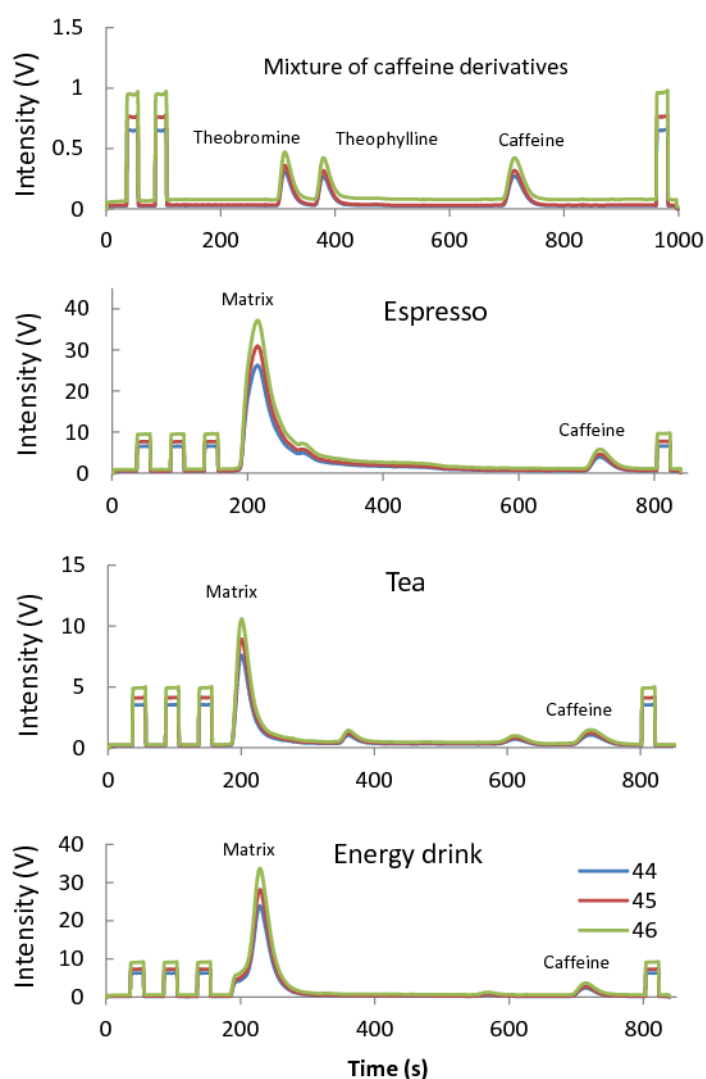


Figure 3.1 HT-RPLC/IRMS chromatograms of a mixture of caffeine derivatives (100 mg L⁻¹), espresso, tea, and energy drink sample. The temperature used was 80 °C and the column is XBridge C₁₈ (2.1 × 100 mm, 3.5 μm). The second reference gas peak was used for calibration of δ¹³C-values.

All reported isotope ratios are expressed as $\delta^{13}\text{C}$ -values relative to the international VPDB standard (Vienna Pee Dee Belemnite). $\delta^{13}\text{C}$ is defined as

$$\delta^{13}\text{C}_{s,VPDB} = \frac{R(^{13}\text{C}/^{12}\text{C})_S}{R(^{13}\text{C}/^{12}\text{C})_{VPDB}} - 1 \quad (3.1)$$

In the equation, $R(^{13}\text{C}/^{12}\text{C})_S$ and $R(^{13}\text{C}/^{12}\text{C})_{VPDB}$ (0.0111802)^[30] are the $^{13}\text{C}/^{12}\text{C}$ ratio in the sample and in the standard, respectively. At the beginning of each run, three pulses of a laboratory standard gas ($\delta^{13}\text{C} = -37.81\%$) were introduced. The second peak was used for $\delta^{13}\text{C}$ calibration. Furthermore, another pulse was set at the end of chromatographic run for controlling $\delta^{13}\text{C}$ consistency (see Figure 3.1). All data acquisition, processing, and evaluation were carried out using Isodat 2.5. The background subtraction was made automatically by Isodat 2.5; the background type used for peak integration was ‘individual background’ with identical start and end slopes of 0.5 mV s^{-1} .

According to the suggestion of Paul *et al.*,^[31] a two-point normalization was applied to correct the offset in $\delta^{13}\text{C}$ -values measured by HT-RPLC/IRMS. The method uses a linear regression of measured $\delta^{13}\text{C}$ -values ($\delta_{M, std1}; \delta_{M, std2}$) and true $\delta^{13}\text{C}$ -values ($\delta_{T, std1}; \delta_{T, std2}$) of two internal laboratory standards as shown in Figure 3.2. The $\delta^{13}\text{C}$ measured by HT-RPLC/IRMS ($\delta_{M, spl}$) was normalized by the following equation:^[31]

$$\delta_{T, spl} = \frac{\delta_{T, std1} - \delta_{T, std2}}{\delta_{M, std1} - \delta_{M, std2}} \times (\delta_{M, spl} - \delta_{M, std2}) + \delta_{T, std2} \quad (3.2)$$

On the basis of the identical treatment (IT) principle for referencing isotope analysis,^[30] two internal laboratory standards of caffeine chemicals at a concentration of 100 mg L^{-1} were measured along with the samples by HT-RPLC/IRMS, since they are chemically identical to the targeted compound and have $\delta^{13}\text{C}$ -values of -27.77 and -35.56% , which bracket the isotope ratio of most unknown samples.^[25]

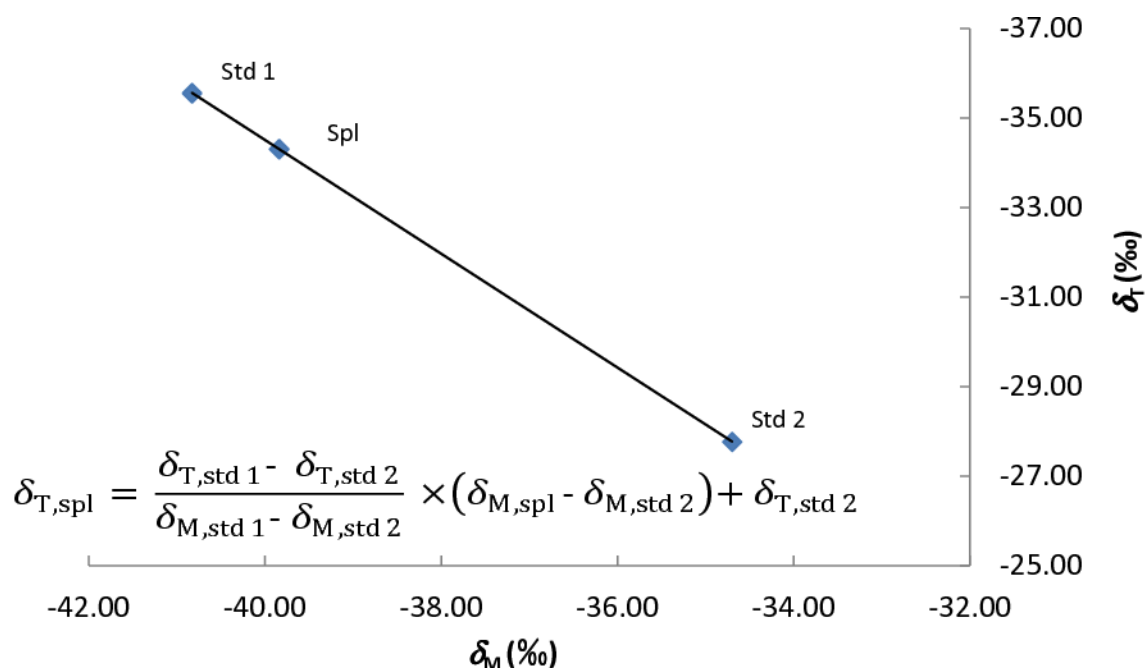


Figure 3.2 Illustration of the derivation of equation 3.2 used for two-point normalization of measured $\delta^{13}\text{C}$ by LC/IRMS. Two internal laboratory standards of caffeine samples (100 mg L^{-1}) with $\delta^{13}\text{C}$ of -27.77 ‰ ($\delta_{T, \text{std}1}$) and -35.56 ‰ ($\delta_{T, \text{std}2}$) were measured along with the samples by HT-HPLC/IRMS.

3.3.4 EA/IRMS measurement

$\delta^{13}\text{C}$ -values of pure compounds were measured with an EA 1110 Elemental Analyzer (CE instrument, Milan, Italy) coupled to a MAT 253 IRMS (Thermo Fisher Scientific) via a ConFlo IV interface (Thermo Fisher Scientific). In order to obtain the corrected $\delta^{13}\text{C}_{\text{EA/IRMS}}$ value of a compound, the $\delta^{13}\text{C}$ value measured by EA/IRMS was converted to the VPDB scale by using a spreadsheet evaluation as recommended by Werner and Brand.^[30] More detailed information can be found in the references.^[23, 30]

3.4 Results and discussion

3.4.1 Baseline separation of caffeine by HT-RPLC/IRMS

For compound-specific isotope analysis, baseline separation of target compounds from other components in the matrix is a key factor for obtaining precise and accurate $\delta^{13}\text{C}$. On the basis of a previous study, three different thermostable columns of two XBridge C_{18} columns and one Zirchrom PBD were selected to develop the method for the separation of caffeine from various mixtures including espresso, tea, and energy drink.^[23] At a temperature of 80 °C , the XBridge C_{18} column with inner diameter (i.d.) of 2.1 mm was able to fully separate caffeine

from the mixtures within 15 min (see Figure 3.1). The analytical method was fast and simple. None of samples required any pre-purification or pre-enrichment procedure. After dilution and filtration, they were directly injected. The background of the sample matrix did not affect the caffeine peak and no further coeluted peak was observed during separation. Moreover, the carryover from late-eluting residue from preceding samples did not affect subsequent measurements during sequence analysis. A guard column with the same stationary phase of C₁₈ was used for the separation. This can offer protection by trapping unwanted components that would otherwise be retained strongly on the analytical column. In one instance, carryover was observed during day-to-day measurements. In this case, the guard and analytical columns were cleaned by flushing with pure methanol and regenerated by purging with water at 80 °C. In order to check whether the generally coexisting caffeine derivatives in coffee and tea can affect the separation of caffeine, a mixture of theobromine, theophylline, and caffeine had been measured under the same conditions. As shown in Figure 3.1, theobromine and theophylline eluted much earlier than caffeine without coelution.

Another XBridge C₁₈ with an inner diameter of 3.5 mm was also able to baseline resolve caffeine from different mixtures mentioned above. However, the analysis time was 3 minutes longer than on the smaller column with an inner diameter of 2.1 mm while other separation parameters were the same. The optimum flow rate for the 2.1 mm i.d. column at a temperature of 80 °C was reported to be 0.5 ml min⁻¹ [24, 32]. This meets the requirement of the LC-IsoLink interface very well since the total flow of mobile phase, acid and oxidant reagent must be lower than 0.7 ml min⁻¹. A Zirchrom PBD column was also used for caffeine separation. However, this column was not able to baseline resolve caffeine in real-life samples. Therefore, the XBridge C₁₈ with 2.1 mm i.d. was chosen for the application of caffeine isotope analysis by HT-RPLC/IRMS.

Increasing the temperature can shorten analysis time of caffeine on the XBridge C₁₈ column due to the improved elution strength of water at elevated temperature. [23] However, using lower temperature can certainly prolong the life of the column by reducing the possibility of stationary phase degradation. Here we used a maximum temperature of 80 °C for XBridge C₁₈ column as recommended by the manufacturer. Under These conditions, the column has been used for approximately 800 injections in four months. After accomplishing all measurements in this work, it still had a good performance. Such a long-term stability renders the method usable for routine analysis. Furthermore, the long lifetime of the column in this application recommends also its use in high-temperature liquid chromatography with pure-water mobile phases.

3.4.2 Precision and accuracy of caffeine $\delta^{13}\text{C}$

For a reliable isotope analysis, $\delta^{13}\text{C}$ -values must be determined with high accuracy and precision. The precision of the developed method was tested in the concentration range of caffeine from 20 to 400 mg L^{-1} . At each concentration level, triplicates were measured. In the concentration range from 400 to 30 mg L^{-1} , the standard deviation (SD) for triple measurement at each concentration are less than 0.22‰ and the $\delta^{13}\text{C}$ -value at each concentration is within $\pm 0.5\text{‰}$ (See Figure 3.3). Furthermore, there is a good linear relationship between the total peak area and caffeine concentration ($R = 0.99999$). Therefore, not only precise $\delta^{13}\text{C}$ -values but also caffeine concentrations can be obtained in this concentration range. At a concentration of 20 mg L^{-1} , the $\delta^{13}\text{C}$ -value is outside $\pm 0.5\text{‰}$. Therefore, 30 mg L^{-1} is the detection limit of caffeine isotope analysis by HT-RPLC/IRMS according to the approach of defining the detection limit for compound-specific isotope analysis.^[33]

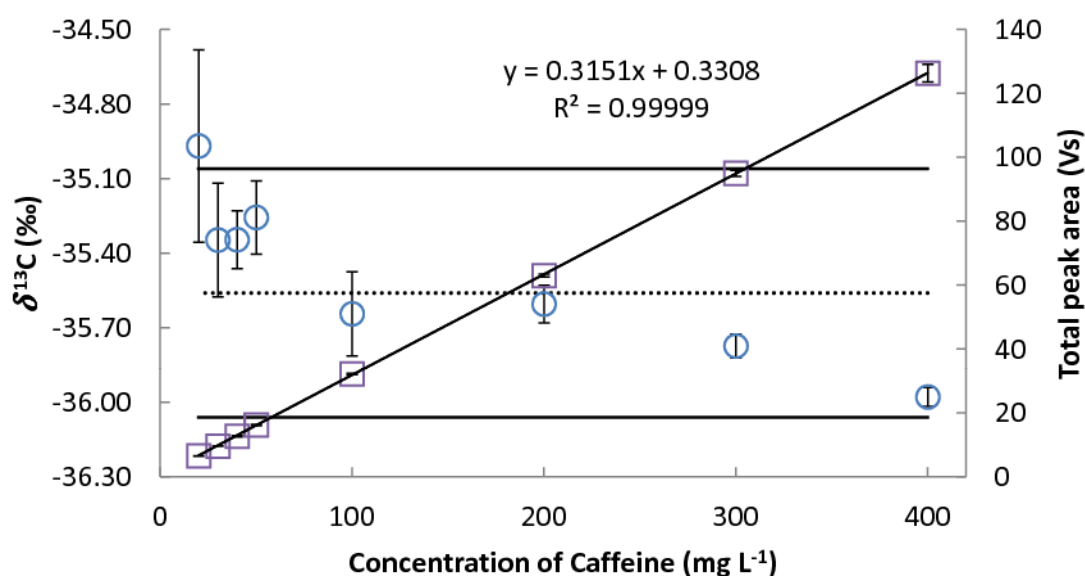


Figure 3.3 $\delta^{13}\text{C}$ -values of caffeine in the concentration range from 20 to 400 mg L^{-1} . The circles and squares represent the $\delta^{13}\text{C}$ and total peak area, respectively. The linear curve fit and the correlation coefficient for plotting peak area vs. concentration are shown in the graph. Error bars indicate the standard deviation of triplicate measurements. The dotted line indicates the iteratively calculated mean value of $\delta^{13}\text{C}$. The horizontal solid lines represent the interval of mean value $\pm 0.5\text{‰}$.^[33]

The accuracy of $\delta^{13}\text{C}$ -values obtained by the developed method was evaluated by comparison with $\delta^{13}\text{C}_{\text{EA/IRMS}}$ -values, which were obtained by EA/IRMS analysis of isolated pure caffeine samples from different sources. It is known that there is an offset between the $\delta^{13}\text{C}$ -values of caffeine measured by HT-RPLC/IRMS and true values (see Figure 3.1) due to the incomplete oxidation of caffeine in the LC-IsoLink interface.^[23] Therefore a procedure of two-point normalization was used to correct the $\delta^{13}\text{C}$ -values measured by HT-RPLC/IRMS ($\delta_{\text{M, spl}}$) as described in the experimental section. Via the correction, the obtained $\delta^{13}\text{C}$ -values ($\delta_{\text{T, spl}}$) are consistent with $\delta^{13}\text{C}_{\text{EA/IRMS}}$ -values proving acceptable accuracy (Table 3.2). The differences between $\delta_{\text{T, spl}}$ and $\delta^{13}\text{C}_{\text{EA/IRMS}}$ of caffeine in complex mixtures of espresso, tea, and energy drinks are lower than 0.43 ‰. The $\delta_{\text{T, spl}}$ of one pure caffeine chemical (-33.38 ± 0.18 ‰) are in good agreement with $\delta^{13}\text{C}_{\text{EA/IRMS}}$ results with a difference of 0.02‰. The insignificant differences between $\delta_{\text{T, spl}}$ and $\delta^{13}\text{C}_{\text{EA/IRMS}}$ results indicate that reliable $\delta^{13}\text{C}$ -values of caffeine have been achieved using the two-point normalization in this work. Two external standards, which possess the same chemical identity as the target compound and have $\delta^{13}\text{C}$ -values bracketing the $\delta^{13}\text{C}$ -values of most unknown samples, could be helpful for achieving reliable $\delta^{13}\text{C}$ for compound-specific isotope analysis according to the literature,^[25, 31] especially when no suitable internal standard is available.

Table 3.2 Comparison of corrected $\delta^{13}\text{C}$ -values of caffeine from various sources measured by HT-RPLC/IRMS ($\delta_{\text{T, spl}}$) with EA/IRMS analysis results.

Caffeine source	$\delta_{\text{T, spl}} \pm \text{SD}$ (n = 3)	$\delta^{13}\text{C}_{\text{EA/IRMS}} \pm \text{SD}$ (n = 3)	$ \delta_{\text{T, spl}} - \delta^{13}\text{C}_{\text{EA/IRMS}} $
Coffee beans 1	-28.19 ± 0.19	-28.23 ± 0.04	0.04
Coffee beans 2	-27.98 ± 0.27	-28.19 ± 0.07	0.21
Tea leaves 1	-31.27 ± 0.20	-30.92 ± 0.08	0.35
Tea leaves 2	-30.20 ± 0.18	-29.77 ± 0.08	0.43
Energy drink	-35.59 ± 0.06	-35.76 ± 0.03	0.17
Pure chemical	-33.38 ± 0.18	-33.36 ± 0.08	0.02

3.4.3 Distinguishable $\delta^{13}\text{C}$ ranges of natural and synthetic caffeine

Two distinguishable $\delta^{13}\text{C}$ ranges of natural and synthetic caffeine were found based on the measurements of 42 natural caffeine samples including espresso, tea, maté, and guaraná from various geographic origins, and measurements of 20 synthetic caffeine samples including energy drinks, cola-type drinks, and commercial chemicals (Figure 3.4). For drinks that contain synthetic caffeine, it is typical to see that an exact amount of caffeine is listed on the product label and no information about a natural caffeine source is given. Figure 3.4 shows that caffeine from natural sources of C_3 -plants has $\delta^{13}\text{C}$ -values between -25 and -32‰ , while synthetic caffeine has lower $\delta^{13}\text{C}$ -values between -33 and -38‰ .

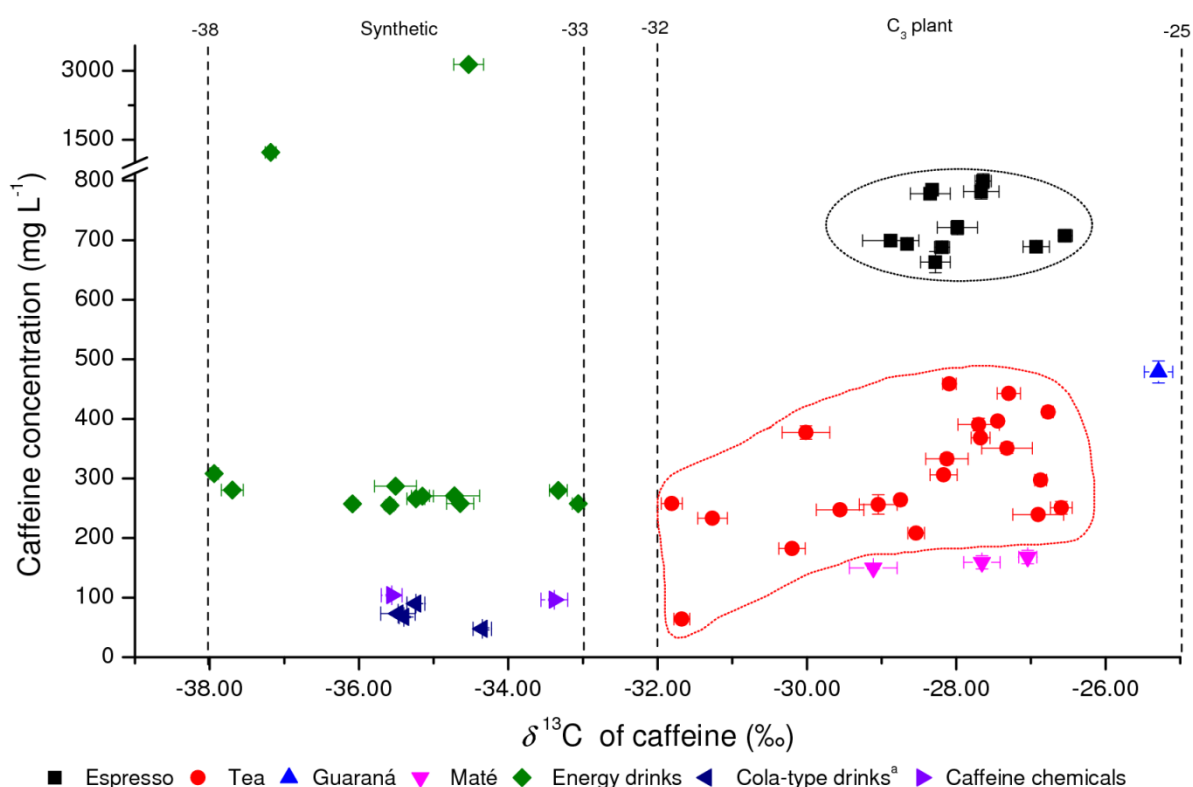


Figure 3.4 $\delta^{13}\text{C}$ -values and concentrations of caffeine from different sources. Error bars indicate the SD of triplicate measurements. Four dashed lines represent two different ranges of $\delta^{13}\text{C}$ -values, from -25 to -32‰ for natural caffeine in C_3 -plant and from -33 to -38‰ for synthetic caffeine. a) Cola-type drinks except for coca cola.

Among a variety of natural drinks, the $\delta^{13}\text{C}$ -value and content of caffeine in espresso ranges from -25.8 to -28.7‰ and from 663 to 950 mg L^{-1} (30 - 50 mg per cup in 52 mL), respectively (black squares in Figure 3.4). The espresso drinks were made from 18 coffee bean samples of different geographic origins distributed over east Africa, South America, Central America, and Oceania. According to several studies, caffeine $\delta^{13}\text{C}$ -values of various coffee beans (sample size: 50) measured by EA/IRMS are between -25.1 and -29.9‰ .^[26, 28, 34] Our $\delta^{13}\text{C}$ -values measured by HT-HPLC/IRMS are within the summarized range. The amounts of caffeine in various espresso drinks fit very well with the results (from 30 to 50 mg per cup) reported by the international food information council foundation.^[35] In tea drinks, the caffeine $\delta^{13}\text{C}$ -values and concentrations varied from -26.6 to -31.8‰ and from 64 to 459 mg L^{-1} , respectively. The collected 21 samples include four major types of tea: black, green, white, and Oolong. They originate from different countries including China, India, and Sri Lanka. The distribution of tea (red circles) and coffee caffeine (black squares) in Figure 3.4 indicates that ^{13}C of caffeine in some tea samples was more depleted than that in coffee samples, covering a wider isotopic range for tea samples. The same conclusion is true for other studies in the literature which report $\delta^{13}\text{C}$ -values of tea caffeine ranging between -27.2 and -32.4‰ (23 samples).^[28, 34] With these ranges it even becomes possible to differentiate between tea and coffee caffeine because tea caffeine but not coffee caffeine may have $\delta^{13}\text{C}$ -values more negative than -30‰ . Due to the difficulty in collecting maté leaves and guaraná seeds, only three maté and one guaraná samples were measured. Maté-caffeine $\delta^{13}\text{C}$ -values and concentrations vary from -27.7 to -29.1‰ and from 159 to 168 mg L^{-1} , respectively (rose triangles in Figure 3.4). The caffeine $\delta^{13}\text{C}$ -value of guaraná sample was -25.3‰ (blue triangles in Figure 3.4). $\delta^{13}\text{C}$ range for maté and guaraná caffeine reported in the literature cover a range from -25.9 to -32.3‰ (5 samples) and from -26.7 to -28.7‰ (32 samples), respectively.^[17] The variation of caffeine $\delta^{13}\text{C}$ -values in C_3 -plants can be explained by the different extent of isotopic fractionation during photosynthesis caused by secondary external factors, such as humidity, temperature, and sunlight availability.^[36, 37]

Compared with natural caffeine, synthetic caffeine used in energy drinks has a more negative carbon isotope ratio, falling in a distinct group between -33.1 to -37.9‰ . Most energy drinks contained caffeine with a concentration of approximately 300 mg L^{-1} , except for two brands ('quick energy'; 3136 mg L^{-1} and 'energy shot'; 1223 mg L^{-1}). The amount of caffeine found in various energy drinks is approximately the same as that declared on the label. The caffeine present in cola-type drinks, varied in concentration ranging from 48 to 90 mg L^{-1} , which is much lower than that found in energy drinks. Caffeine in different cola drinks was between

–34.4 and –35.5‰. Two commercial caffeine chemicals had $\delta^{13}\text{C}$ -values of –33.4 and –35.6‰. The few literature data also report more negative $\delta^{13}\text{C}$ -values for synthetic caffeine, ranging from –35.8 to –40‰ (7 samples).^[26, 28, 34] The variation in $\delta^{13}\text{C}$ of synthetic caffeine is probably due to different raw materials and synthesis pathways.

The results in this work corroborate the scarce information available in the literature and prove that $\delta^{13}\text{C}$ -values for natural and synthetic caffeine can be distinguished. They fall into two distinct groups without significant overlap: from –25 to –32‰ for natural caffeine, and from –33 and –40‰ for synthetic caffeine. This finding is based on a variety of natural caffeine samples with a large sample size (153 samples) and various synthetic caffeine samples (27 samples) that have been measured via two methodologies of LC/IRMS and EA/IRMS by different laboratories. If in the measurement of an unknown sample the observed $\delta^{13}\text{C}$ falls below the threshold of –32‰, it is assumed that the contained caffeine is synthetic, that is, not of natural provenience. The error probability for this assumption is $\alpha \approx 1\%$ (See the supporting information: setting a threshold for assigning an unknown caffeine sample to natural or synthetic provenience).

3.4.4 Authenticity control of caffeine-containing drinks

Identification of caffeine as either natural or synthetic is very important for authenticity control of caffeine-containing drinks. Naturally caffeinated drinks such as bottled or canned tea and instant coffee have expanded around the world. Some energy drinks use guaraná extracts to meet the customer's preference for natural products. According to the descriptions on the labels, all 38 drinks in this study were supposed to contain natural caffeine. Sample preparation was very simple for all drinks; after dilution (if necessary) and filtration, it was directly injected and measured by HT-HPLC/IRMS. Subsequently, the obtained $\delta^{13}\text{C}$ -values were used for identification of natural or synthetic origin based on the respective isotope ratio range.

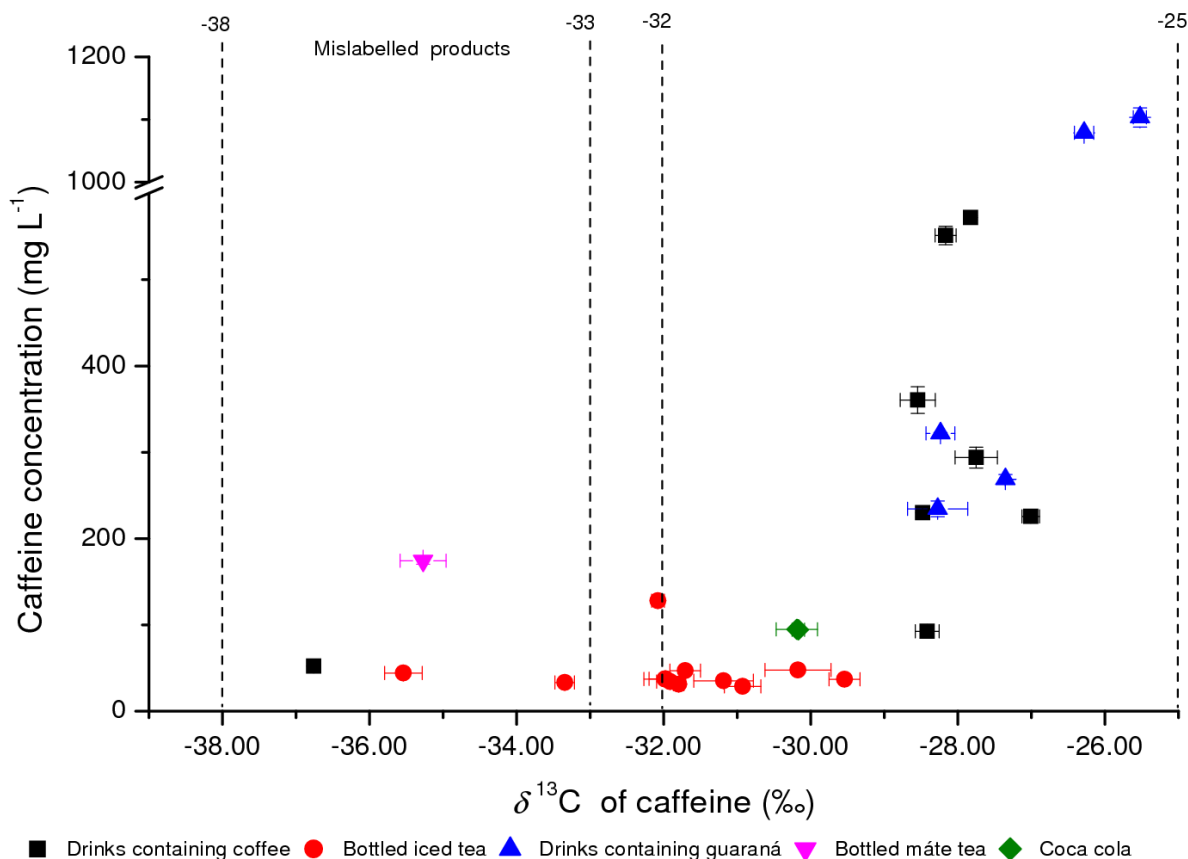


Figure 3.5 $\delta^{13}\text{C}$ -values and concentrations of caffeine in various drinks that were supposed to contain natural caffeine sources according to the labels. Four products were found to be mislabelled. Error bars indicate the SD of triplicate measurements. Four dashed lines represent two different ranges of $\delta^{13}\text{C}$ -values, from -25 to -32‰ for natural caffeine in C3-plant and from -33 to -38‰ for synthetic caffeine.

As seen in Figure 3.5, four out of the 38 tested drinks contain caffeine with $\delta^{13}\text{C}$ -values lower than -33‰ , falling into the group of synthetic caffeine. These four probably mislabelled drinks are one instant drink mix, two bottled iced tea drinks, and one maté drink. For six different instant coffee samples, the caffeine $\delta^{13}\text{C}$ -values vary from -27.0 to -28.8‰ lying within the range found in coffee beans (from -25.1 to -29.9‰), and the caffeine concentrations are from 229 to 571 mg L^{-1} . One natural cola drink, which according to product description contained a coffee bean extract, has caffeine $\delta^{13}\text{C}$ -value of -28.4‰ , confirming a natural origin. However, one instant coffee had a $\delta^{13}\text{C}$ -value of -36.8‰ , indicating a synthetic origin. Twelve drinks of bottled tea contain caffeine with concentrations and $\delta^{13}\text{C}$ -values ranging from 30 to 128 mg L^{-1} and from -29.6 to 31.9‰ , respectively. The $\delta^{13}\text{C}$ -values fall into the group for tea samples, suggesting a natural origin. In contrast, the $\delta^{13}\text{C}$ -values of the other two tea drinks (-33.3 and -35.5‰) fall into the group of synthetic

caffeine indicating a synthetic origin. For the ready-to-drink products containing guaraná extract, the $\delta^{13}\text{C}$ -values are between -26.3 and -28.3% , lying within the range for guaraná seeds (-25.3 to -28.7%). No mislabelled guaraná drinks were found in this study. However, one maté drink was found to be probably mislabelled since the caffeine $\delta^{13}\text{C}$ -value was -35.3% . It is interesting to note that two different coca cola products show identical $\delta^{13}\text{C}$ -values of -30.2% , indicating a natural source of the kola nut extract. Among these 38 drinks, 6 tea drinks and 2 guaraná drinks were found to contain caffeine lower than 30 mg L^{-1} . The latter results are not included in Figure 3.5 because the concentration below the detection limit of HT-RPLC/IRMS.

3.5 Conclusions

Compound-specific isotope analysis by HT-RPLC/IRMS has been applied to the measurement of caffeine in various drinks, allowing us to differentiate between natural and synthetic caffeine. Two separate ranges of $\delta^{13}\text{C}$ -values for natural and synthetic caffeine have been identified based on the results in this work and in the literature: one from -25 to -32% and the other from -33 and -40% . The method has been applied to control the stated natural caffeine sources in 38 drinks, out of which four products were found to be mislabelled due to added synthetic caffeine. The advantages of the presented method include simple sample preparation, short analysis time, long-term column stability, high precision of $\delta^{13}\text{C}$ -values. It has the potential to become a routine method for authenticity control of caffeine-containing drinks.

3.6 Acknowledgements

We thank Thorsten Teutenberg and Steffen Wiese for their support in HT-RPLC. We thank Prof. Karl Molt for calculation of the threshold for assigning an unknown caffeine sample to natural or synthetic provenience. We acknowledge financial support from the German Federal Ministry of Economics and Technology within the agenda for the promotion of industrial cooperative research and development (IGF) based on a decision of the German Bundestag (IGF-Project No. 16120 N). We also appreciate financial support from the German Research Foundation (DFG).

3.7 Appendix: Setting a threshold for assigning an unknown caffeine sample to natural or synthetic provenience

Figure 3.6 gives a plot of the $\delta^{13}\text{C}$ -values shown in Figure 3.4 of the article for the samples containing natural and synthetic caffeine. One-sided prediction intervals around the means were calculated for both groups. The lower and the upper limit of these confidence intervals are given by:

$$\delta_{nat,lower} = \bar{\delta}_{nat} - t_{\alpha,df} \cdot s_{nat} \cdot \sqrt{1 + \frac{1}{n_{nat}}} \quad (3.3)$$

$$\delta_{synth,upper} = \bar{\delta}_{synth} - t_{\alpha,df} \cdot s_{synth} \cdot \sqrt{1 + \frac{1}{n_{synth}}} \quad (3.4)$$

With

$\bar{\delta}_{nat}$ mean $\delta^{13}\text{C}$ -values for samples of natural provenience

$\bar{\delta}_{synth}$ mean $\delta^{13}\text{C}$ -values for samples of synthetic provenience

n_{nat} number of “natural” samples

n_{synth} number of “synthetic” samples

s_{nat} standard deviation of $\delta^{13}\text{C}$ -values for “natural” samples

s_{synth} standard deviation of $\delta^{13}\text{C}$ -values for “synthetic” samples

$t_{\alpha,df}$ t value for a given confidence level $1 - \alpha$ and $n - 1$ degrees of freedom

Setting $\alpha = 0.01$ one gets the following results:

	$\bar{\delta}$	s	n	df	$t_{\alpha,df}$	Limit of confidence level
“Natural” samples	-28.1	1.422	42	41	2.420803	-31.6
“Synthetic” samples	-35.3	1.299	20	19	2.539483	-31.9

The threshold for discriminating between natural and synthetic provenience of caffeine is set to $\delta_{thr} = -32\%$. If in the measurement of an unknown sample the observed $\delta^{13}\text{C}$ -values falls below this threshold, it is assumed that the contained caffeine is synthetic, i.e. not of natural provenience. The error probability for this assumption is $\alpha \approx 1\%$.

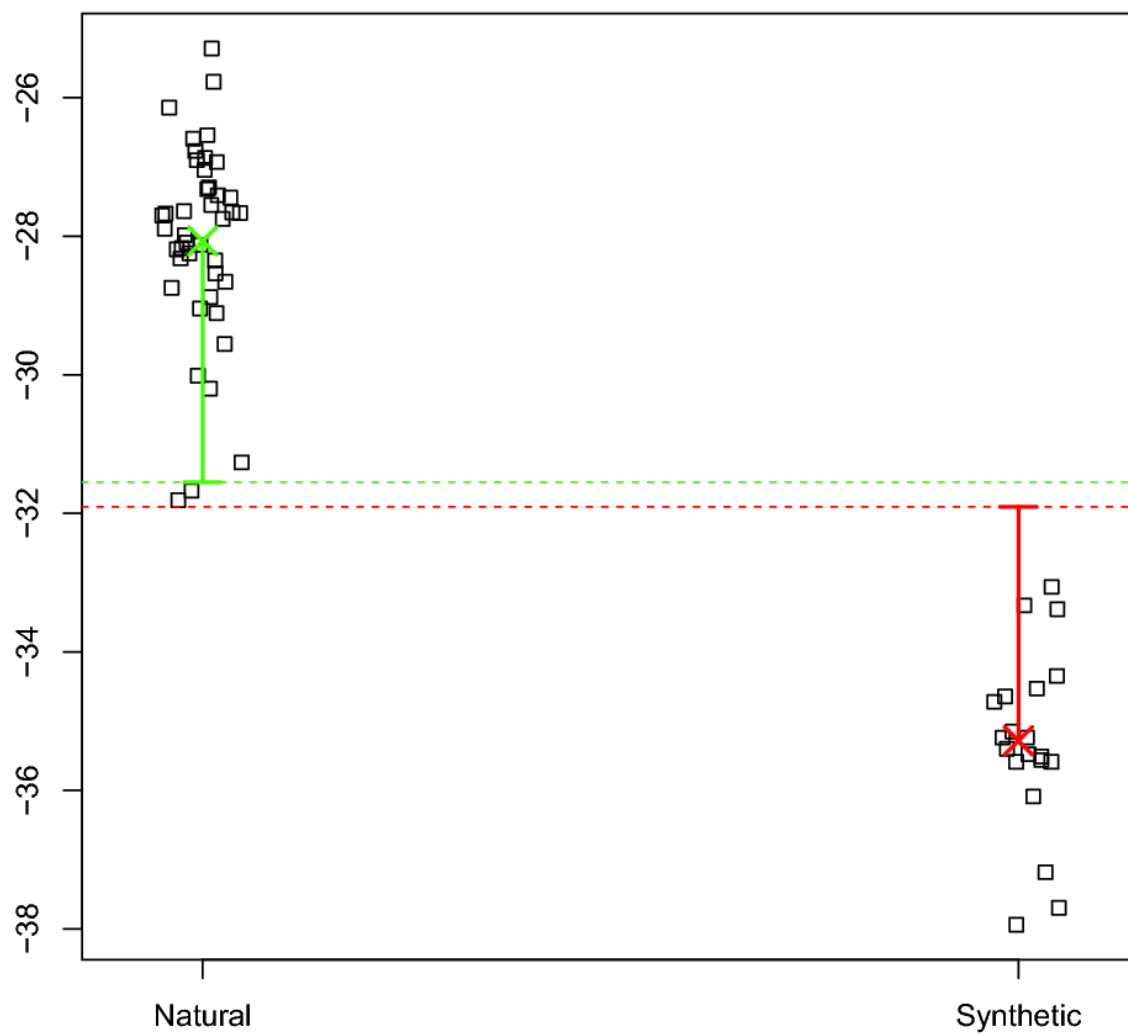


Figure 3.6 A plot of the $\delta^{13}\text{C}$ -values shown in Figure 3.4 of the article for the samples containing natural and synthetic caffeine. One-sided prediction intervals around the means were calculated for both groups.

3.8 References

- [1] Y. Wang, C. T. Ho. Polyphenols chemistry of tea and coffee: A century of progress. *J. Agric. Food Chem.* **2009**, *57*, 8109.
- [2] G. Bank. Caffeine in your supplement: is it natural or synthetic? *Nutraceuticals World* **2005**, *July/August*.
- [3] D. L. McKay, J. B. Blumberg. The role of tea in human health: An update. *J. Am. Coll. Nutr.* **2002**, *21*, 1.
- [4] H. M. Rawel, S. E. Kulling. Nutritional contribution of coffee, cacao and tea phenolics to human health. *Journal für Verbraucherschutz und Lebensmittelsicherheit* **2007**, *2*, 399.
- [5] C. S. Yang, J. M. Landau. Effects of tea consumption nutrition health. *J. Nutr.* **2000**, *130*, 2409.
- [6] A. A. Modi, J. J. Feld, Y. Park, D. E. Kleiner, J. E. Everhart, T. J. Liang, J. H. Hoofnagle. Increased caffeine consumption is associated with reduced hepatic fibrosis. *Hepatology* **2010**, *51*, 201.
- [7] P. Nawrot, S. Jordan, J. Eastwood, J. Rotstein, A. Hugenholtz, M. Feeley. Effects of caffeine on human health. *Food Addit. Contam.* **2003**, *20*, 1.
- [8] C. J. Reissig, E. C. Strain, R. R. Griffiths. Caffeinated energy drinks-A growing problem. *Drug Alcohol Depend.* **2009**, *99*, 1.
- [9] A. B. Allen. Caffeine identification: Differentiation of synthetic and natural caffeine. *J. Agric. Food Chem.* **1961**, *9*, 294.
- [10] O. J. Weinkauff, R. W. Radue, R. E. Keller, H. R. Crane. Identification of caffeine as natural or synthetic. *J. Agric. Food Chem.* **1961**, *9*, 397.
- [11] T. C. Schmidt, L. Zwank, M. Elsner, M. Berg, R. U. Meckenstock, S. B. Haderlein. Compound-specific stable isotope analysis of organic contaminants in natural environments: A critical review of the state of the art, prospects, and future challenges. *Anal. Bioanal. Chem.* **2004**, *378*, 283.
- [12] Z. Muccio, G. P. Jackson. Isotope ratio mass spectrometry. *Analyst* **2009**, *134*, 213.
- [13] C. Cordella, I. Moussa, A. C. Martel, N. Sbirrazzouli, L. Lizzani-Cuvelier. Recent developments in food characterization and adulteration detection: Technique-oriented perspectives. *J. Agric. Food Chem.* **2002**, *50*, 1751.
- [14] F. Hülsemann, U. Flenker, M. Parr, H. Geyer, W. Schänzer. Authenticity control and identification of origin of synthetic creatine-monohydrate by isotope ratio mass spectrometry. *Food Chem.* **2010**.

-
- [15] H. Kroll, J. Friedrich, M. Menzel, P. Schreier. Carbon and hydrogen stable isotope ratios of carotenoids and β -carotene-based dietary supplements. *J. Agric. Food Chem.* **2008**, *56*, 4198.
- [16] A. M. Gioacchini, A. Roda, A. Cipolla, M. Parenti, M. Baraldini. Differentiation between natural and synthetic taurine using the $^{13}\text{C}/^{12}\text{C}$ isotope ratio. *Rapid Commun. Mass Spectrom.* **1995**, *9*, 1106.
- [17] E. Richling, C. Höhn, B. Weckerle, F. Heckel, P. Schreier. Authentication analysis of caffeine-containing foods via elemental analysis combustion/pyrolysis isotope ratio mass spectrometry (EA-C/P-IRMS). *Eur. Food Res. Technol.* **2003**, *216*, 544.
- [18] J.-P. Godin, J. S. O. McCullagh. Review: Current applications and challenges for liquid chromatography coupled to isotope ratio mass spectrometry (LC/IRMS). *Rapid Commun. Mass Spectrom.* **2011**, *25*, 3019.
- [19] M. Krummen, A. W. Hilker, D. Juchelka, A. Duhr, H. J. Schlüter, R. Pesch. A new concept for isotope ratio monitoring liquid chromatography/mass spectrometry. *Rapid Commun. Mass Spectrom.* **2004**, *18*, 2260.
- [20] A. I. Cabañero, J. L. Recio, M. Rupérez. Liquid chromatography coupled to isotope ratio mass spectrometry: A new perspective on honey adulteration detection. *J. Agric. Food Chem.* **2006**, *54*, 9719.
- [21] A. I. Cabañero, J. L. Recio, M. Rupérez. Simultaneous stable carbon isotopic analysis of wine glycerol and ethanol by liquid chromatography coupled to isotope ratio mass spectrometry. *J. Agric. Food Chem.* **2010**, *58*, 722.
- [22] L. Elflein, K. P. Ræzke. Improved detection of honey adulteration by measuring differences between $^{13}\text{C}/^{12}\text{C}$ stable carbon isotope ratios of protein and sugar compounds with a combination of elemental analyzer-Isotope ratio mass spectrometry and liquid chromatography-Isotope ratio mass spectrometry ($\delta^{13}\text{C}$ -EA/LC-IRMS). *Apidologie* **2008**, *39*, 574.
- [23] L. Zhang, D. M. Kujawinski, M. A. Jochmann, T. C. Schmidt. High-temperature reversed-phase liquid chromatography coupled to isotope ratio mass spectrometry. *Rapid Commun. Mass Spectrom.* **2011**, *25*, 2971.
- [24] J. P. Godin, G. Hopfgartner, L. Fay. Temperature-programmed high-performance liquid chromatography coupled to isotope ratio mass spectrometry. *Anal. Chem.* **2008**, *80*, 7144.
- [25] T. B. Coplen, W. A. Brand, M. Gehre, M. Gröning, H. A. J. Meijer, B. Toman, R. M. Verkouteren. New guidelines for $\delta^{13}\text{C}$ measurements. *Anal. Chem.* **2006**, *78*, 2439.

-
- [26] B. Weckerle, E. Richling, S. Heinrich, P. Schreier. Origin assessment of green coffee (*Coffea arabica*) by multi-element stable isotope analysis of caffeine. *Anal. Bioanal. Chem.* **2002**, 374, 886.
- [27] M. C. Gennaro, C. Abrigo. Caffeine and theobromine in coffee, tea and cola-beverages - Simultaneous determination by reversed-phase ion-interaction HPLC. *Fresenius' J. Anal. Chem.* **1992**, 343, 523.
- [28] J. Dunbar, A. T. Wilson. Determination of geographic origin of caffeine by stable isotope analysis [4]. *Anal. Chem.* **1982**, 54, 590.
- [29] M. A. Jochmann, D. Steinmann, S. Manuel, T. C. Schmidt. Flow injection analysis-isotope ratio mass spectrometry for bulk carbon stable isotope analysis of alcoholic beverages. *J. Agric. Food Chem.* **2009**, 57, 10489.
- [30] R. A. Werner, W. A. Brand. Referencing strategies and techniques in stable isotope ratio analysis. *Rapid Commun. Mass Spectrom.* **2001**, 15, 501.
- [31] D. Paul, G. Skrzypek, I. Fórizs. Normalization of measured stable isotopic compositions to isotope reference scales-A review. *Rapid Commun. Mass Spectrom.* **2007**, 21, 3006.
- [32] F. Lestremau, A. de Villiers, F. Lynen, A. Cooper, R. Szucs, P. Sandra. High efficiency liquid chromatography on conventional columns and instrumentation by using temperature as a variable. Kinetic plots and experimental verification. *J. Chromatogr. A* **2007**, 1138, 120.
- [33] M. A. Jochmann, M. Blessing, S. B. Haderlein, T. C. Schmidt. A new approach to determine method detection limits for compound-specific isotope analysis of volatile organic compounds. *Rapid Commun. Mass Spectrom.* **2006**, 20, 3639.
- [34] E. Richling, C. Höhn, B. Weckerle, F. Heckel, P. Schreier. Authentication analysis of caffeine-containing foods via elemental analysis combustion/pyrolysis isotope ratio mass spectrometry (EA-C/P-IRMS). *Eur. Food Res. Technol.* **2003**, 216, 544.
- [35] www.ific.org, International food information council foundation review, **2008**.
- [36] A. Gessler, M. Lw, C. Heerd, M. O. D. Beeck, J. Schumacher, T. E. E. Grams, G. Bahnweg, R. Ceulemans, H. Werner, R. Matyssek, H. Rennenberg, K. Haberer. Within-canopy and ozone fumigation effects on $\delta^{13}\text{C}$ and $\delta^{18}\text{O}$ in adult beech (*Fagus sylvatica*) trees: Relation to meteorological and gas exchange parameters. *Tree Physiol.* **2009**, 29, 1349.

- [37] C. I. Rodrigues, R. Maia, M. Miranda, M. Ribeirinho, J. M. F. Nogueira, C. Máguas. Stable isotope analysis for green coffee bean: A possible method for geographic origin discrimination. *J. Food Compos. Anal.* **2009**, 22, 463.

Chapter 4 Derivatization-free carbon isotope ratio analysis of steroids by hyphenation with high temperature liquid chromatography

4.1 Abstract

Generally, compound-specific isotope analysis of steroids is carried out by the hyphenation of gas chromatography with isotope ratio mass spectrometry. Thus, a derivatization of the steroids prior to the measurement is compelling and a correction of the isotopic data is necessary. To overcome this limitation, we present a new approach of high-temperature liquid chromatography coupled to photodiode array detector and isotope ratio mass spectrometry (HTLC/PDA/IRMS) for the carbon isotope ratio analysis of underivatized steroids. A steroid mixture containing 19-norandrosterone (19NA), testosterone (T), epitestosterone (EpiT), androsterone (A), 5 β -pregnane-3 α ,17 α ,20 α -triol (PT) was fully separated on a C₄ column under high-temperature elution with water. The detection limits for precise and accurate isotope analysis were around 20 $\mu\text{g g}^{-1}$ for testosterone, epitestosterone (79 ng steroid on column), and 30 $\mu\text{g g}^{-1}$ for 19-norandrosterone, androsterone and 5 β -pregnane-3 α ,17 α ,20 α -triol (119 ng steroid on column). A linear relationship was obtained between the concentration and peak area from PDA and IRMS, and the additional quantitative measurement by PDA can be used to check peak purity of the IRMS chromatogram. The applicability of the method was tested by measuring a pharmaceutical gel containing testosterone. Additionally, with this work, the scope of LC/IRMS applications has been extended to non-polar organic compounds.

4.2 Introduction

Compound-specific isotope analysis (CSIA) of steroids is nowadays an important tool in food analysis^[1-4] and steroid abuse detection in sports^[5]. Steroids such as testosterone can be legally prescribed in various dosage forms to treat conditions associated with steroid hormone deficiency.^[6] Therefore, the origin and authenticity of pharmaceutical products containing steroids is an increasing task in connection with consumer protection due to product fakes.

CSIA of steroids nowadays relies on gas chromatography coupled to isotope ratio mass spectrometry (GC/IRMS), which requires a derivatization of the involved steroids.^[7-11] However, derivatization is a laborious step during sample preparation and is prone to alter isotopic signatures of the target analytes. Additionally, a correction of the measured isotopic signatures is necessary.^[12] However, a derivatization step can be avoided by employing liquid chromatography hyphenated with isotope ratio mass spectrometry (LC/IRMS). LC/IRMS was introduced and described in detail in 2004 by Krummen *et al.*^[13] For a measurement of carbon isotope ratios, the analytes were converted to carbon dioxide and water by online chemical oxidation with sodium peroxodisulfate (conc. Na₂S₂O₈) under acidic conditions (conc. H₃PO₄) in a heated capillary.^[13] In the following step CO₂ permeates from the aqueous phase into a Helium carrier gas stream via a membrane, and is transported to the IRMS inlet after drying.

The main difficulty of using LC/IRMS for steroid analysis is the method inherent need of a carbon-free eluent for separation,^[13] because organic buffer or solvent in the eluent can result in a severe decrease of sensitivity by saturation, or even wrong carbon isotope ratios.^[14] An ordinary reversed-phase separation using organic solvent as eluent and modifier is therefore not possible to elute the relatively non-polar steroids. Additionally, the low water solubility of the steroids requires an organic solvent as solution mediator.

Recently, Godin *et al.* and Zhang *et al.* demonstrated the applicability of high-temperature liquid chromatography (HTLC) in LC/IRMS.^[15, 16] HTLC/IRMS has been reported for carbon isotope analysis of polar and medium polar organic compounds (fatty acids¹⁴, caffeine¹⁷ and sulfonamides¹⁴), but so far not for non-polar organic compounds such as steroids. At elevated temperatures, the elution strength of water increases since its static permittivity decreases. Hence, the polarity of water can be changed towards that of organic solvents by applying temperature gradients.^[17] Thus, organic solvents and modifiers, which are necessary in reversed-phase separation, are not necessary.^[18]

In the following we show that a derivatization-free measurement of the steroid isotopic signature is possible even with the use of a solvent mediator (methanol). A new approach of

high-temperature liquid chromatography coupled to photodiode array detector and isotope ratio mass spectrometry (HTLC/PDA/IRMS) for carbon isotope analysis of free steroids is presented. Therefore a mixture of free steroids containing 19-norandrosterone (19NA), testosterone (T), epitestosterone (EpiT), androsterone (A), 5 β -pregnane-3 α ,17 α ,20 α -triol (PT) was separated. Additionally, a real pharmaceutical gel containing testosterone was measured to demonstrate applicability of the new method to real samples.

4.3 Experimental

4.3.1 Materials

Analytical standards of 19-nortestosterone (>99%), testosterone, epitestosterone, androsterone (all >99%), and 5 β -pregnane-3 α , 17 α , 20 α -triol (>99%) were purchased from Sigma-Aldrich GmbH (Steinheim, Germany). Methanol (GC grade) and sodium dihydrogen phosphate (99%) were from Merck (Darmstadt, Germany). Ortho-phosphoric acid (99%) and sodium peroxodisulfate (99%) were from Fluka (Buchs, Switzerland). Two certified isotope standards of IAEA-600 caffeine ($\delta^{13}\text{C} = -27.77 \pm 0.04 \text{ ‰}$)^[19] and IAEA-CH-6 sucrose ($\delta^{13}\text{C} = -10.449 \pm 0.033 \text{ ‰}$) were supplied by International Atomic Energy Agency (Vienna, Austria).

Five stock solutions, each of which contains one steroid standard in methanol at a concentration of 1000 $\mu\text{g g}^{-1}$, were prepared prior to analysis and were stored at 4°C in the refrigerator for two weeks. The test mixtures were prepared by mixing and diluting the stock solutions in methanol with the required amount. A pharmaceutical sample of Testogel (Laboratoires Besins International, Paris, France) was used to demonstrate applicability of the method to real samples. Testogel is a hydroalcoholic gel containing 1% testosterone (25 mg in 2.5 g), ethanol (96%), isopropyl myristate and poly (acrylic acid) (Carbomer 980), which is used to control the release of the active ingredient to the human skin. The gel was homogenized and dissolved in 5 mL of methanol, and then filtered through a 0.20 μm membrane filter. In the end, it was diluted 50 times by methanol and theoretically contained approximately 77.4 $\mu\text{g g}^{-1}$ testosterone.

4.3.2 Instrumentation for HTLC/PDA/IRMS

A Rheos Allegro pump (Flux instruments AG, Basel, Switzerland) was used to deliver the chromatographic eluent. Five microliter of sample was injected by a HTC PAL autosampler (CTC Analytics, Zwingen, Switzerland). An HT-HPLC 200 column oven (SIM, Oberhausen, Germany) was used for eluent preheating, column heating, and eluent cooling with three

aluminium blocks. An Accela PDA 80 detector (Thermo Fisher Scientific, Bremen, Germany) was connected between the column oven and LC-IsoLink interface (Thermo Fisher Scientific). The scan wavelength of PDA detector was from 190 to 800 nm. A Delta V Advantage isotope ratio mass spectrometer (Thermo Fisher Scientific, Bremen, Germany) was used for carbon isotope analysis. In the LC-IsoLink interface, the flow of sodium peroxodisulfate (0.83 M) and phosphoric acid (1.50 M) was 30 and 50 $\mu\text{L min}^{-1}$, respectively. In order to avoid blockage in the system, two in-line filters with a pore size of 0.5 μm (Vici, Schenkon, Switzerland) were placed before the tubing of the preheating unit and after the cooling unit.

An XBridge BEH300 C₄ column (2.1 \times 50 mm, 3.5 μm , Waters, Eschborn, Germany) was used for steroid separation at elevated temperatures. The eluent was 10 mM phosphate buffer at pH 3.0 with a flow of 0.5 mL min^{-1} . The used temperature program started at 80 $^{\circ}\text{C}$ and ramped to 160 $^{\circ}\text{C}$ at 3 $^{\circ}\text{C min}^{-1}$, where it was held for 11 min.

4.3.3 EA/IRMS measurement

$\delta^{13}\text{C}$ values of pure compounds were measured with an EA 1110 Elemental Analyzer (CE instrument, Milan, Italy) coupled to a MAT 253 IRMS (Thermo Fisher Scientific) via a ConFlo IV interface (Thermo Fisher Scientific). The reported $\delta^{13}\text{C}_{\text{EA/IRMS}}$ values of steroids were corrected by a two-point normalization method with two certified standards of IAEA-600 caffeine and IAEA-CH-6.

4.3.4 Data acquisition and handling

All reported $\delta^{13}\text{C}$ values were normalized to the VPDB scale (Vienna Pee Dee Belemnite). The open split was out from 100 to 500 s in order not to introduce methanol into the ion source (see Figure 4.1). Four pulses of reference gas were injected at 30, 900, 950, and 2250 s, and the second reference peak was used for $\delta^{13}\text{C}$ ionization correction. At 180 s, the sample was injected and the autosampler sent a start signal to the PDA detector for data collection and to the HT-HPLC oven for temperature programming. The acquisition and processing of IRMS data was performed by Isodat 2.5. The background type used for peak integration was 'individual background' with start slope of 0.7 mV s^{-1} and end slope of 0.5 mV s^{-1} . A standard mixture of five steroids at 100 $\mu\text{g g}^{-1}$ with known $\delta^{13}\text{C}$ values was measured along with samples by HTLC/IRMS for compound-specific offset correction. Offsets of steroids are listed in Table 4.1.

Table 4.1 $\delta^{13}\text{C}$ values measured by EA/IRMS and HTLC/IRMS of steroids at $100 \mu\text{g g}^{-1}$ and $\delta^{13}\text{C}$ -value differences between the two methods ($\Delta\delta^{13}\text{C} = \delta^{13}\text{C}_{\text{EA/IRMS}} - \delta^{13}\text{C}_{\text{HTLC/IRMS}}$).

No.	Name	Structure	$\delta^{13}\text{C}_{\text{EA/IRMS}} \pm \text{SD}$ (n = 4)	$\delta^{13}\text{C}_{\text{HTLC/IRMS}} \pm \text{SD}$ (n = 3)	$\Delta\delta^{13}\text{C}$	Remark
1	19-Nortestosterone (19NA)		-28.69 ± 0.03	-30.31 ± 0.06	1.62 ± 0.07	Exogenous AAS ^[20]
2	Testosterone (T)		-29.42 ± 0.02	-31.20 ± 0.13	1.78 ± 0.13	Endogenous AAS ^[20]
3	Epitestosterone (EpiT)		-31.56 ± 0.02	-33.14 ± 0.12	1.58 ± 0.12	Masking agent for testosterone use ^[20, 21]
4	Androsterone (A)		-31.18 ± 0.02	-32.82 ± 0.29	1.64 ± 0.29	One of main metabolites of testosterone ^[9, 20]
5	5 β -pregnane-3 α , 17 α , 20 α -triol (PG)		-29.56 ± 0.05	-30.80 ± 0.11	1.24 ± 0.12	Endogenous reference compound (ERC) ^[20]

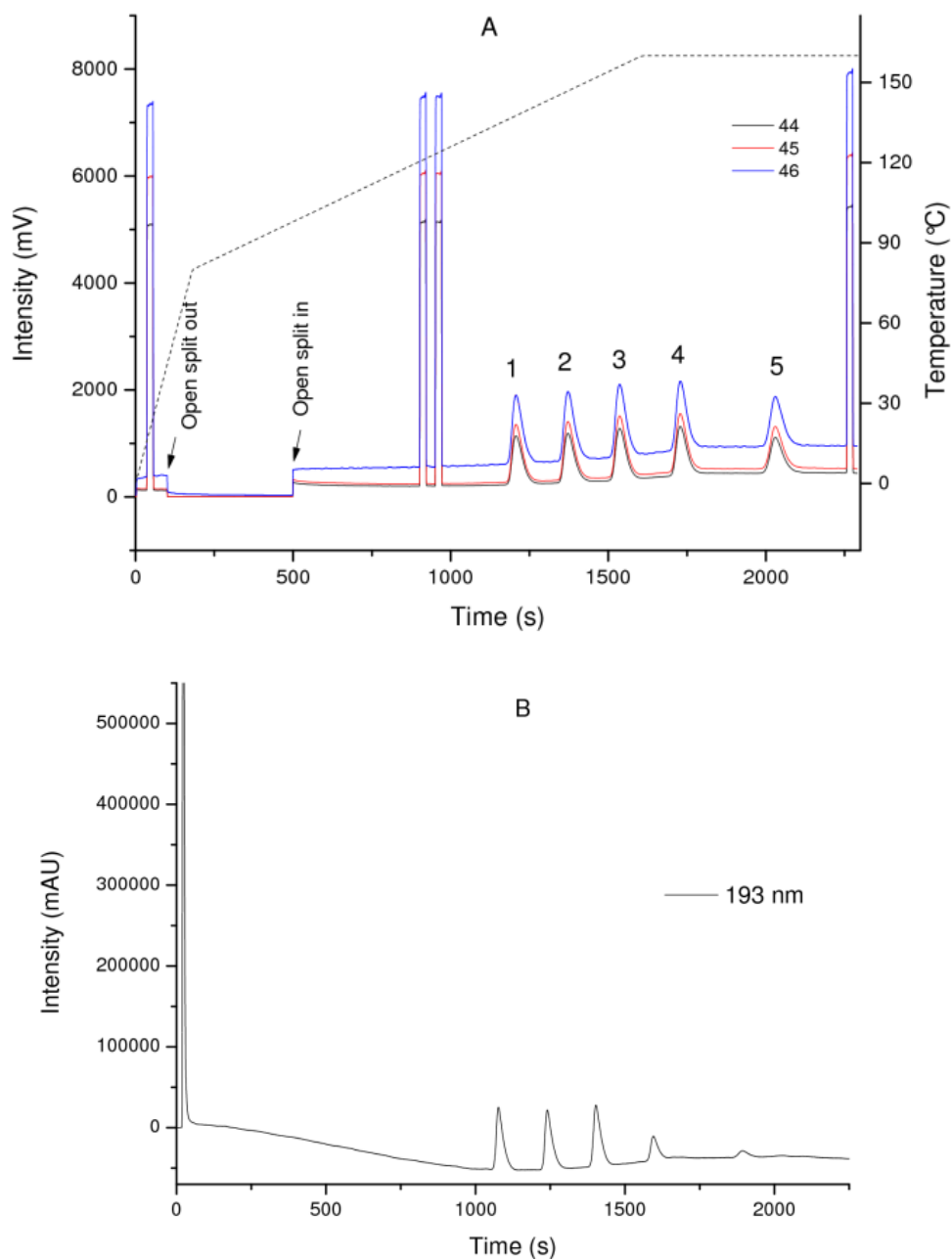


Figure 4.1 Chromatogram obtained by HTLCL/PDA/IRMS of a steroid mixture (A: m/z of 44, 45, 46; B: Absorption at 193 nm). The sample contains five steroids in methanol, at a concentration of $100 \mu\text{g g}^{-1}$ (listed in Table 4.1). The used temperature program is indicated by the dashed line in A. The open split was set in “out” position (back-flush mode) from 100 to 500 s in order to prevent methanol entering into the ion source. The sample was injected at 180s.

4.4 Results and discussion

4.4.1 Chromatographic separation of steroid mixture

Pure free steroids are practically insoluble in pure water but soluble in organic solvents such as alcohols. Thus, methanol was used as solvent mediator to dissolve the steroid standards in water. In general, methanol within the aqueous solvent would lead to an elevated carbon background in LC/IRMS. By applying a steep temperature gradient from room temperature to 80°C within the first 3.3 minutes it was possible to elute the methanol as solvent peak. During sample injection at 180 s, the open split was out from 100 to 500 s in order not to introduce the solvent of pure methanol into the ion source (back-flush mode, see also Figure 4.1A). After the open-split was set 'in', the background was stable and a raised background from methanol was not observed. This indicates that methanol was fully separated from the steroids and eluted before 500 s because of the low retention on the C₄ column at 80°C. The possible influence of methanol was investigated by four CO₂ reference gas pulses. These pulses showed consistent isotope ratios with standard deviations lower than 0.18 ‰ and five steroids were measured with standard deviation better than 0.29 ‰ (see Table 4.1). Thus, the methanol used for dissolving steroids had obviously no influence on the steroid isotope analysis.

As shown in Figure 4.1A, a mixture of the free steroids was fully separated by a C₄ column under temperature-programmed elution. The chromatographic resolution of neighbouring steroid peaks was higher than 2.15, so that no isotopic signature alteration by overlapping peaks can occur. The slope of peak background of five steroids (background at peak start and peak end divided by peak width) is lower than 0.67 mV s⁻¹, which suggest a negligible column bleed and a stable background during separation. Under this condition, the integration algorithm of 'individual background' with start slope of 0.7 mV s⁻¹ can be used for background subtraction without precision loss. This was in accordance to our previous investigation of column bleed effect on isotope analysis under high temperature.^[16] The low background at high temperature up to 160 °C proved again that HPLC columns packed with ethyl-bridged hybrid particles have an excellent thermal stability.^[16, 22] Compared with the normalized $\delta^{13}\text{C}_{\text{EA/IRMS}}$ -values of steroids, the $\delta^{13}\text{C}$ -values directly measured by HTLC/IRMS had an offset. This offset in LC/IRMS has also been observed for other compounds.^[14, 16, 23, 24] It originates from the incomplete oxidation of analytes in the LC-IsoLink interface.^[14] Since the $\delta^{13}\text{C}$ values measured by LC/IRMS were highly reproducible and the offset was stable, accurate $\delta^{13}\text{C}$ values of steroids can still be obtained by correction.^[16] In this work, a

standard mixture containing compounds of interest with known $\delta^{13}\text{C}$ values was measured along with samples for the compound-specific offset correction. The offsets varied little within these five steroids as seen in Table 4.1 (from 1.24 to 1.78‰).

The maximum UV absorption wavelength of 19-nortestosterone, testosterone, epitestosterone, androsterone, 5 β -pregnane-3 α , 17 α , 20 α -triol was 247, 248, 248, 193, 193 nm, respectively, according to the absorbance spectra (from 190 to 800 nm) at the peak centre. The chromatogram at 193 nm (see Figure 4.1B) shows that the use of pure water as eluent allows us to monitor UV absorption with a wavelength shorter than 195 nm, which is especially useful for steroids not having a conjugated π -electron system like androsterone and 5 β -pregnane-3 α ,17 α ,20 α -triol. Lowering the feasible UV detection wavelength is one advantage of high-temperature liquid chromatography with water as eluent, because organic solvents that absorb in these spectral region will not disturb.^[25]

4.4.2 Method detection limit

The detection limit of steroids was tested in the concentration range from 20 to 200 $\mu\text{g g}^{-1}$. The precision of triple measurements at each concentration down to 20 $\mu\text{g g}^{-1}$ is better than 0.42‰ for T, EpiT, (Table 4.2), and the difference to $\delta^{13}\text{C}_{\text{EA/IRMS}}$ value is within ± 0.5 ‰ after the correction by adding the individual offset to the measured $\delta^{13}\text{C}_{\text{HTLC/IRMS}}$ values (see an example of T in Figure 4.2A). It shows that the offset of steroids in HTLC/IRMS system was constant within the range of 20 to 200 $\mu\text{g g}^{-1}$. For 19NA, A and PT, the precision is better than 0.32 ‰ down to 30 $\mu\text{g g}^{-1}$, and the offset corrected $\delta^{13}\text{C}$ -values are also within the interval of $\delta^{13}\text{C}_{\text{EA/IRMS}} \pm 0.5$ ‰ (see an example of PG in Figure 4.2B). At 20 $\mu\text{g g}^{-1}$, the precision for 19NA, A and PT became higher than 0.5 ‰, which is the commonly acceptable precision for compound-specific isotope analysis.^[16, 26] Therefore, precise and accurate $\delta^{13}\text{C}$ -values can be obtained for T, and EpiT down to 20 $\mu\text{g g}^{-1}$ (corresponding to approximately 79 ng steroid or 61 ng carbon on-column) and for 19NA, A and PT down to 30 $\mu\text{g g}^{-1}$ (corresponding to approximately 118 ng steroid or 92 ng carbon on-column). The obtained detection limit is relatively low in comparison to previously reported detection limits of LC/IRMS analysis.^[27, 28]

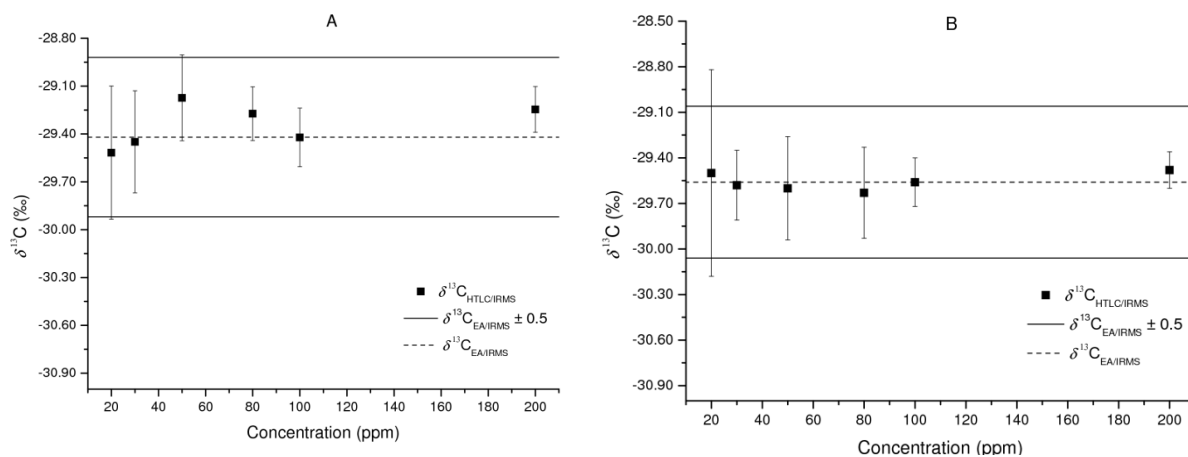


Figure 4.2 Offset corrected $\delta^{13}\text{C}$ values of testosterone (A) and 5β -pregnane- 3α , 17α , 20α -triol (B) at different concentrations from 200 to $20 \mu\text{g g}^{-1}$. The error bars indicate the standard deviations of triplicate measurements. The dashed lines show the $\delta^{13}\text{C}_{\text{EA/IRMS}}$ -values of the two steroids. The solid lines represent the interval of $\delta^{13}\text{C}_{\text{EA/IRMS}} \pm 0.5$ ‰.

Table 4.2 $\delta^{13}\text{C}$ values of steroids at different concentrations ($n = 3$) measured by HTLC/IRMS and corrected by adding the offset to $\delta^{13}\text{C}_{\text{EA/IRMS}}$ -values.

Con. ($\mu\text{g g}^{-1}$)	19NA	T	EpiT	A	PT
200	-28.44 ± 0.13	-29.25 ± 0.14	-31.46 ± 0.15	-31.11 ± 0.35	-29.54 ± 0.12
100	-28.69 ± 0.09	-29.42 ± 0.18	-31.56 ± 0.17	-31.18 ± 0.41	-29.56 ± 0.16
80	-28.67 ± 0.17	-29.27 ± 0.17	-31.39 ± 0.24	-31.22 ± 0.34	-29.67 ± 0.30
50	-28.88 ± 0.31	-29.17 ± 0.27	-31.70 ± 0.13	-31.27 ± 0.30	-29.60 ± 0.34
30	-28.84 ± 0.30	-29.45 ± 0.32	-31.48 ± 0.30	-31.53 ± 0.36	-29.68 ± 0.23
20	-29.81 ± 0.68	-29.52 ± 0.42	-32.06 ± 0.22	-30.79 ± 0.51	-29.92 ± 0.68

Table 4.3 Linear relationships between concentration and peak areas from IRMS (for all steroids from 20 to $200 \mu\text{g g}^{-1}$) and UV detection at 193 nm (for 19NA, T, EpiT from 20 to $200 \mu\text{g g}^{-1}$ and for A and PT from 30 to $200 \mu\text{g g}^{-1}$)

	19NA	T	EpiT	A	PT
IRMS	$y = 0.350x + 1.604$ $R^2 = 0.998$	$y = 0.366x + 1.856$ $R^2 = 0.998$	$y = 0.384x + 2.147$ $R^2 = 0.998$	$y = 0.358x + 3.144$ $R^2 = 0.997$	$y = 0.310x + 1.281$ $R^2 = 0.998$
UV	$y = 21761x + 175484$ $R^2 = 0.999$	$y = 21687x + 89923$ $R^2 = 0.998$	$y = 22598x + 80053$ $R^2 = 0.999$	$y = 8642x - 54482$ $R^2 = 0.999$	$y = 3456x - 1272$ $R^2 = 0.992$

Furthermore, there are good linear relationships between the concentrations and peak areas from IRMS and PDA detector (Table 4.3). It has to be noted that the peak area is not reproducible for A and PT at $20 \mu\text{g g}^{-1}$ because of their weak UV absorption. Therefore, the linear relationship for them is shown in the range of 30 to $200 \mu\text{g g}^{-1}$. The obtained additional concentration from the in-line PDA detector can be used to confirm the chromatographic peak purity in IRMS, as they give different information: carbon amount from IRMS and UV absorption behaviour of analytes from PDA.

4.4.3 Testogel sample

The developed method was applied to a Testogel pharmaceutical sample (Figure 4.3). Knowing $\delta^{13}\text{C}$ -values of pharmaceutical steroids is interesting for authenticity control of pharmaceutical products based on their different $\delta^{13}\text{C}$ -values. A Testogel sample was measured by HTLC/PDA/IRMS after a simple sample preparation that included methanol extraction, filtration and 50 times dilution. As shown in Figure 4.3, the ethanol and isopropyl myristate present in the matrix of Testogel were eluted before entering the IRMS ion source, giving clean and stable background for isotope analysis of testosterone. The $\delta^{13}\text{C}$ -value of testosterone in Testogel is -29.35 ‰ , which is in the reported range of exogenous pharmaceutical testosterone (-26.18 and -30.04 ‰).^[29] The precision of isotope analysis is as high as 0.13 ‰ . The obtained concentrations from two detectors are consistent, confirming the peak purity of testosterone in IRMS. The detected level matches very well the theoretical concentration of $77 \mu\text{g g}^{-1}$.

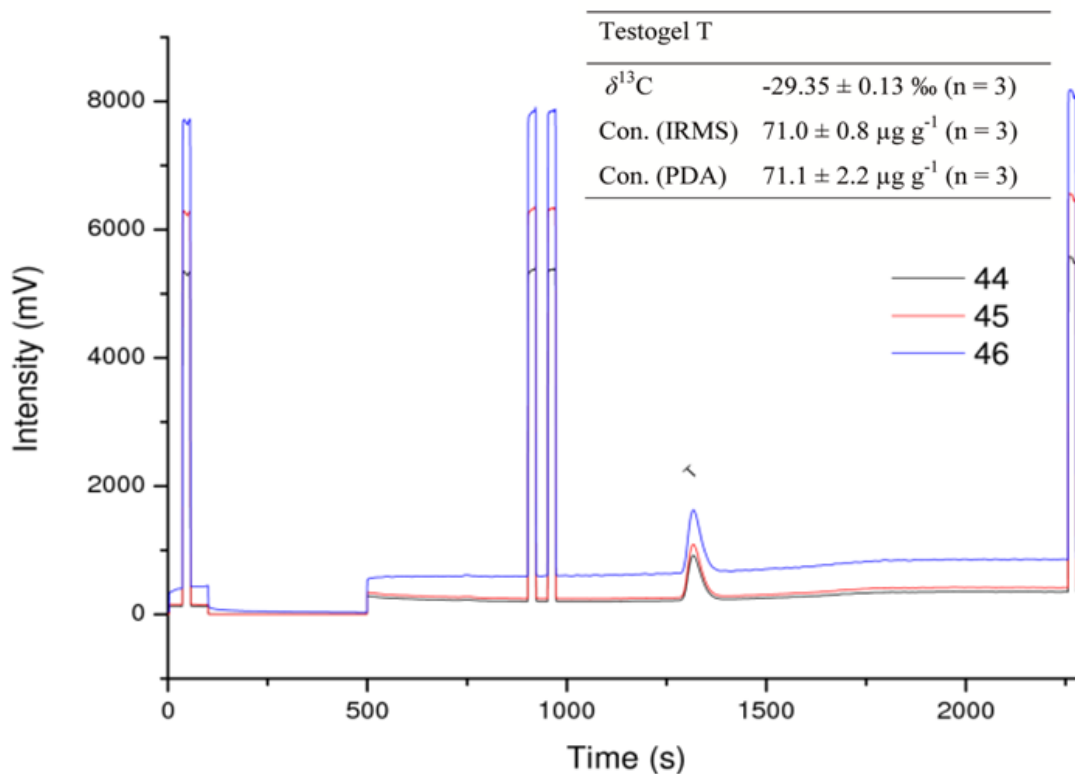


Figure 4.3 Chromatogram of a Testogel sample. $\delta^{13}\text{C}$ -value of testosterone in a Testogel sample (n = 3), which was corrected by adding the offset; and calculated concentrations ($\mu\text{g g}^{-1}$) from the peak areas of IRMS and PDA detector at 193 nm based on the linear relationships in Table 4.3.

4.5 Conclusion

A new HTLC/PDA/IRMS was developed for carbon isotope ratio analysis of non-polar free steroids. Five steroids of 19NA, T, EpiT, A, and PT were fully separated on a C_4 column by high-temperature elution with water as eluent. The achieved detection limit for precise and accurate isotope analysis shows that the developed method is feasible to measure steroids in pharmaceutical products. Polar organic compounds like solvent and the main additives of pharmaceutical samples have no influence on isotope analysis of steroids. The developed method aimed at isotope analysis of free steroids without derivatization and avoids potential isotope fractionation so that no correction of the isotopic data is necessary. The good separation of five steroids with high similarity in molecular structure indicates that the developed method can be adopted for isotope analysis of other non-polar organic compounds.

4.6 Reference

- [1] P. M. Mason, S. E. Hall, I. Gilmour, E. Houghton, C. Pillinger, M. A. Seymour. The use of stable carbon isotope analysis to detect the abuse of testosterone in cattle. *Analyst* **1998**, *123*, 2405.
- [2] M. Hebestreit, U. Flenker, C. Buisson, F. Andre, B. Le Bizec, H. Fry, M. Lang, A. P. Weigert, K. Heinrich, S. Hird, W. Schanzer. Application of stable carbon isotope analysis to the detection of testosterone administration to cattle. *Journal of Agricultural and Food Chemistry* **2006**, *54*, 2850.
- [3] E. Bichon, F. Kieken, N. Cesbron, F. Monteau, S. Prevost, F. Andre, B. Le Bizec. Development and application of stable carbon isotope analysis to the detection of cortisol administration in cattle. *Rapid Communications in Mass Spectrometry* **2007**, *21*, 2613.
- [4] G. Janssens, D. Courtheyn, S. Mangelinckx, S. Prevost, E. Bichon, F. Monteau, G. De Poorter, N. De Kimpe, B. Le Bizec. Use of isotope ratio mass spectrometry to differentiate between endogenous steroids and synthetic homologues in cattle: A review. *Analytica Chimica Acta* **2013**, *772*, 1.
- [5] A. T. Cawley, U. Flenker. The application of carbon isotope ratio mass spectrometry to doping control. *J. Mass Spectrom.* **2008**, *43*, 854.
- [6] in *Drug facts: anabolic steroids, Vol. July 2012*, National institute on drug abuse, <http://www.drugabuse.gov/publications/drugfacts/anabolic-steroids>, **2012**.
- [7] R. Aguilera, T. E. Chapman, B. Starcevic, C. K. Hatton, D. H. Catlin. Performance characteristics of a carbon isotope ratio method for detecting doping with testosterone based on urine diols: Controls and athletes with elevated testosterone/epitestosterone ratios. *Clin. Chem.* **2001**, *47*, 292.
- [8] M. K. Kioussi, Y. S. Angelis, A. T. Cawley, M. Koupparis, R. Kazlauskas, J. T. Brenna, C. G. Georgakopoulos. External calibration in Gas Chromatography-Combustion-Isotope Ratio Mass Spectrometry measurements of endogenous androgenic anabolic steroids in sports doping control. *J. Chromatogr. A* **2011**, *1218*, 5675.
- [9] T. Piper, U. Mareck, H. Geyer, U. Flenker, M. Thevis, P. Platen, W. Schänzer. Determination of $^{13}\text{C}/^{12}\text{C}$ ratios of endogenous urinary steroids: Method validation, reference population and application to doping control purposes. *Rapid Commun. Mass Spectrom.* **2008**, *22*, 2161.

-
- [10] M. Polet, W. Van Gansbeke, K. Deventer, P. Van Eenoo. Development of a sensitive GC-C-IRMS method for the analysis of androgens. *Biomedical Chromatography* **2012**.
- [11] Y. Zhang, H. J. Tobias, J. T. Brenna. Steroid isotopic standards for gas chromatography-combustion isotope ratio mass spectrometry (GCC-IRMS). *Steroids* **2009**, *74*, 369.
- [12] G. Rieley. Derivatization of organic compounds prior to gas chromatographic-combustion-isotope ratio mass spectrometric analysis: Identification of isotope fractionation processes. *Analyst* **1994**, *119*, 915.
- [13] M. Krummen, A. W. Hilker, D. Juchelka, A. Duhr, H. J. Schlüter, R. Pesch. A new concept for isotope ratio monitoring liquid chromatography/mass spectrometry. *Rapid Commun. Mass Spectrom.* **2004**, *18*, 2260.
- [14] D. M. Kujawinski, L. Zhang, T. C. Schmidt, M. A. Jochmann. When other separation techniques fail: Compound-specific carbon isotope ratio analysis of sulfonamide containing pharmaceuticals by high-temperature- liquid chromatography-isotope ratio mass spectrometry. *Anal. Chem.* **2012**, *84*, 7656.
- [15] J. P. Godin, G. Hopfgartner, L. Fay. Temperature-programmed high-performance liquid chromatography coupled to isotope ratio mass spectrometry. *Anal. Chem.* **2008**, *80*, 7144.
- [16] L. Zhang, D. M. Kujawinski, M. A. Jochmann, T. C. Schmidt. High-temperature reversed-phase liquid chromatography coupled to isotope ratio mass spectrometry. *Rapid Commun. Mass Spectrom.* **2011**, *25*, 2971.
- [17] Y. Yang. Subcritical water chromatography: A green approach to high-temperature liquid chromatography. *J. Sep. Sci.* **2007**, *30*, 1131.
- [18] T. Teutenberg, J. Tuerk, M. Holzhauser, S. Giegold. Temperature stability of reversed phase and normal phase stationary phases under aqueous conditions. *J. Sep. Sci.* **2007**, *30*, 1101.
- [19] T. B. Coplen, W. A. Brand, M. Gehre, M. Gröning, H. A. J. Meijer, B. Toman, R. M. Verkouteren. New guidelines for $\delta^{13}\text{C}$ measurements. *Anal. Chem.* **2006**, *78*, 2439.
- [20] World anti-doping agency, Technical document, <http://www.wada-ama.org/en/Science-Medicine/Anti-Doping-Laboratories/Technical-Documents/>, **2004**.
- [21] R. Aguilera, C. K. Hatton, D. H. Catlin. Detection of epitestosterone doping by isotope ratio mass spectrometry. *Clin. Chem.* **2002**, *48*, 629.

-
- [22] T. Teutenberg, K. Hollebekkers, S. Wiese, A. Boergers. Temperature and pH-stability of commercial stationary phases. *J. Sep. Sci.* **2009**, *32*, 1262.
- [23] K. Tagami, S. Uchida. Online stable carbon isotope ratio measurement in formic acid, acetic acid, methanol and ethanol in water by high performance liquid chromatography-isotope ratio mass spectrometry. *Anal. Chim. Acta* **2008**, *614*, 165.
- [24] S. Reinnicke, A. Bernstein, M. Elsner. Small and reproducible isotope effects during methylation with trimethylsulfonium hydroxide (TMSH): A convenient derivatization method for isotope analysis of negatively charged molecules. *Anal. Chem.* **2010**, *82*, 2013.
- [25] T. Yarita, R. Nakajima, K. Shimada, S. Kinugasa, M. Shibukawa. Superheated water chromatography of low molecular weight polyethylene glycols with ultraviolet detection. *Anal. Sci.* **2005**, *21*, 1001.
- [26] M. A. Jochmann, M. Blessing, S. B. Haderlein, T. C. Schmidt. A new approach to determine method detection limits for compound-specific isotope analysis of volatile organic compounds. *Rapid Commun. Mass Spectrom.* **2006**, *20*, 3639.
- [27] D. J. Morrison, K. Taylor, T. Preston. Strong anion-exchange liquid chromatography coupled with isotope ratio mass spectrometry using a Liquiface interface. *Rapid Commun. Mass Spectrom.* **2010**, *24*, 1755.
- [28] C. I. Smith, B. T. Fuller, K. Choy, M. P. Richards. A three-phase liquid chromatographic method for $\delta^{13}\text{C}$ analysis of amino acids from biological protein hydrolysates using liquid chromatography-isotope ratio mass spectrometry. *Anal. Biochem.* **2009**, *390*, 165.
- [29] X. De la Torre, J. C. González, S. Pichini, J. A. Pascual, J. Segura. $^{13}\text{C}/^{12}\text{C}$ isotope ratio MS analysis of testosterone, in chemicals and pharmaceutical preparations. *J. Pharm. Biomed. Anal.* **2001**, *24*, 645.

Chapter 5 Carbon isotope analysis of AICAR by liquid chromatography coupled to PDA and isotope ratio mass spectrometry

5.1 Abstract

Gene doping is an emerging potential threat to the integrity of sport and the health of athletes. 5-Aminoimidazole-4-carboxamide ribonucleotide (AICAR) is one of the first gene doping drugs prohibited by the World Anti-Doping Agency. Conventional quantitative determination of excreted AICAR is not adequate to prove an additional exogenous administration due to its endogenous production. Carbon isotope analysis has proven to be a useful tool in discrimination between endogenous and exogenous doping drugs. In this context, liquid chromatography coupled to photodiode array detector and isotope ratio mass spectrometry (LC/PDA/IRMS) was developed for compound-specific isotope analysis of AICAR. Suitable chromatographic conditions and prepurification procedure of urinary samples were investigated for precise carbon isotope analysis. It has been shown that endogenous AICAR in a urine sample and synthetic AICAR from two sources have significantly different carbon isotope values. This shows potential application of carbon isotope analysis to the detection of AICAR abuse in sport.

5.2 Introduction

Doping control plays a key role in ensuring a fair competition for all athletes. Gene doping is a new threat for international sporting events.^[1] 5-Aminoimidazole-4-carboxamide ribonucleotide (AICAR), an analog of adenosine monophosphate (AMP), is a gene doping drug (see the chemical structure in Figure 5.1). It can be used as an activator of AMP-activated protein kinase, which regulates the response of the cell to energy change.^[2] It has been observed that four weeks of AICAR treatment increased running endurance of untrained mice by 44%.^[3] AICAR has been banned in sport by the World Anti-doping Agency (WADA) since 2009.^[4]

Fighting against AICAR abuse is a challenging work. AICAR is a naturally occurring intermediate of the biosynthetic pathway of purines and the variation of its concentration is dependent on health and nutrition condition of athlete.^[5] Recently, Thomas *et al.* have measured the levels of AICAR in 499 urinary samples from elite athletes with liquid chromatography coupled with mass spectrometry and reported a reference value of AICAR concentration in urine, $2186 \pm 1655 \text{ ng mL}^{-1}$.^[6] This wide variation shows that only quantitative measurement of excreted AICAR is not enough to confirm the AICAR administration. As a potential additional analytical tool, stable isotope analysis has already been widely used to differentiate endogenous and exogenous steroids based on different isotope ratio values.^[7-9] The naturally occurring AICAR of human beings is derived from the diet, a mixture of C₃ and C₄ plants. The synthetic AICAR might have different carbon isotope ratio, which is produced industrially from the fermentation broth of glucose.^[10] To our best knowledge, compound-specific isotope analysis of AICAR has not been reported yet. There are two methodologies for compound-specific isotope analysis: gas chromatography coupled with isotope ratio mass spectrometry (GC/IRMS) and liquid chromatography coupled with isotope ratio mass spectrometry (LC/IRMS). AICAR is a very polar organic compound and has a boiling point of 726 °C. It needs to be derivatized for GC/IRMS analysis, which is a labour intensive and time-consuming step. Therefore, LC/IRMS was chosen for AICAR isotope analysis.

In this context, a new method of liquid chromatography coupled to photodiode array detector and isotope ratio mass spectrometry (LC/PDA/IRMS) was developed for AICAR isotope analysis. The possibility of applying the developed method to the detection of AICAR abuse was discussed.

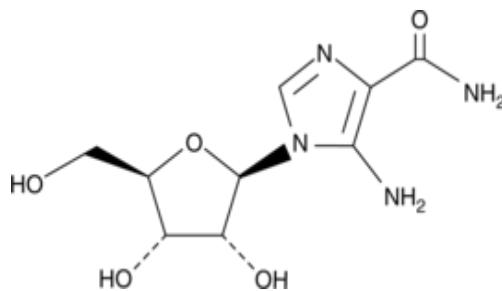


Figure 5.1 Chemical structure of AICAR

5.3 Materials and Methods

5.3.1 Chemicals and reagents

Ortho-phosphoric acid (99%) and sodium peroxodisulfate (99%) were bought from Fluka (Buchs, Switzerland). Monosodium dihydrogen phosphate (99.5%) and disodium hydrogen phosphate (99.5%) were from Merck (Darmstadt, Germany). The AICAR standard ($\geq 98\%$) was purchased from Sigma Aldrich (Steinheim, Germany). Two isotope reference materials, NBS 22 oil with a $\delta^{13}\text{C}$ -value of $-30.03 \pm 0.04\text{‰}$ and IAEA-CH-6 with a $\delta^{13}\text{C}$ -value of $-10.45 \pm 0.03\text{‰}$, were purchased from the International Atomic Energy Agency (IAEA, Vienna, Austria).

5.3.2 Prepurification of human urine samples

Three urine samples were pre-purified with three different procedures by the institute of biochemistry in the German Sport University Cologne.

The first procedure

200 mL of urine was mixed with 50 mL of dichloromethane, whereby the organic phase was discarded. 0.2 M NaOH was added to the urine adjusting pH to 12 and was washed with dichloromethane. The organic phase was also discarded. Acetic acid was added to the urine adjusting pH to 3. The urine was extracted again with dichloromethane and the organic phase was discarded. NaOH was added to the aqueous phase adjusting pH to 7 and was evaporated to dryness in a rotary evaporator. The residue was dissolved in a hot 1:1 mixture of ethanol and chloroform. The insoluble matter was filtered by a short silica gel column (4 cm) and washed out by a 1:1 mixture of ethanol/chloroform. The eluent was evaporated to dryness and then dissolved in 10 mL of water adjusted to pH 8.5-9.0 by ammonia. The solution was mixed 1:1 with 0.2 M ammonium acetate at pH 8.8.

The HPLC purification system was an Agilent 1100 series HPLC system coupled with an AB SCIEX 4000 QTrap mass spectrometry. Electrospray ionization in positive mode and multiple-reaction monitoring mode were used. A chromatographic column for HPLC purification was packed with 0.6g polymer-bounded 3-aminophenylboronacid gel (Sigma Aldrich, Steinheim, Germany) and washed by ammonium acetate buffer. Afterwards, it was conditioned by 5 mL of ammonium acetate buffer. The sample of 20 mL was filled in and washed by 5 mL of ammonium acetate buffer. The eluent was 0.1 M of formic acid and the aliquot was 1 mL of eluent. The aliquots were directly measured by a LC-ESI-MS/MS. The fractions 1-3 were collected. Approximately 13 μ g of AICAR was extracted. The collected fractions were evaporated to dryness in a vacuum centrifuge.

The second procedure

200 mL of urine was evaporated in a rotary evaporator to approximately 50 mL. The residue was filtered and mixed 1:1 with ammonium acetate buffer. A column for purification was packed with 0.6 g of polymer-bounded 3-aminophenylboronacid gel (Sigma Aldrich, Steinheim, Germany), washed and reconditioned by ammonium acetate buffer. The fractions 1-3 were collected and concentrated.

The HPLC purification system has been mentioned in the first procedure. The separation column was Phenomenex C₆-Phenyl (10 x 250 mm, 3 μ m). The eluent of solution A is NH₄OAc 5 mM + 0.1% HOAc, at pH 3.5. Solvent B is acetonitrile. The gradient: 100% A (1 min) > 30% A (7 min) > 0% A (1 min) > 100% A (6 min).

The flow of 3 mL min⁻¹ was splitted by a T-piece and approximately 2% of eluent was introduced to the MS. The pre-concentrated sample was dissolved in 300 μ L of 2% HOAc + 10% MeOH and 100 μ L of solution was injected. AICAR had a retention time of 8.5 min. The fractions from 8.0 to 9.0 min were collected and concentrated under vacuum. The collected fractions were evaporated to dryness in a vacuum centrifuge. Approximately 3 μ g of AICAR was extracted.

The third procedure

500 mL of human urine was concentrated under reduced pressure at 50 °C and the obtained viscous residue was extracted with hot ethanol (3 x 50 mL). The organic solvent was evaporated under reduced pressure and the residue was extracted by 5 mL of methanol. A silica gel column was used for purification using CHCl₃/MeOH with composition from 3:1 to 1:1. The fractions 19-24, which contained AICAR according to the detection of LC/MS, were collected. Afterwards, the fractions were evaporated to dryness and dissolved in 10 mL of water. Ammonia was added to the solution adjusting pH to 8.5, which was mixed with 10 mL

of NH_4OAc buffer at pH 8.8. A boronic acid gel column with eluent of 0.1 mol L^{-1} formic acid was used for purification. The fractions 2-4 were combined and concentrated. The residue was dissolved in $250 \text{ }\mu\text{L}$ of water and finally purified by a HPLC (column: Phenomenex C_6 -Phenyl, $10 \times 250 \text{ mm}$; eluent: $\text{H}_2\text{O}/\text{ACN}$) cleanup with online MS using multiple injections of $50\text{-}75 \text{ }\mu\text{L}$. The fraction 4 from 8.2-8.6 min containing AICAR were collected and concentrated.

5.3.3 Sample preparation for LC/IRMS

The spiked synthetic urine sample is a mixture of synthetic urine and $200 \text{ }\mu\text{g mL}^{-1}$ of AICAR in volume of 50:50. The synthetic urine contains 25 g L^{-1} of urea and 2 g L^{-1} of creatinine. The spiked urine sample is a mixture of filtered morning urine and $200 \text{ }\mu\text{g mL}^{-1}$ of AICAR in volume of 50:50.

Dry residues, obtained from the last step of the first, the second, and the third prepurification procedures, were dissolved in $200 \text{ }\mu\text{L}$, $60 \text{ }\mu\text{L}$, and $100 \text{ }\mu\text{L}$ of phosphate buffer (5 mM , pH 6.0), respectively; and the solutions were centrifuged for 4 min at 10000 rpm. The supernatant was transferred into a $300 \text{ }\mu\text{L}$ insert of autosampler vial.

5.3.4 LC/PDA/IRMS

A Rheos Allegro pump (Flux instruments AG, Basel, Switzerland) was used to pump chromatographic mobile phase. Samples of $10 \text{ }\mu\text{L}$ were injected by a HTC PAL autosampler (CTC Analytics, Zwingen, Switzerland). An Accela PDA 80 detector (Thermo Fisher Scientific, Bremen, Germany) was connected between the column and LC-IsoLink interface (Thermo Fisher Scientific). The scan wavelength of PDA detector was from 200 to 400 nm. A Delta V Advantage isotope ratio mass spectrometer (Thermo Fisher Scientific) was used for carbon isotope analysis. In the LC-IsoLink interface, the flow of sodium peroxodisulfate (0.83 M) and phosphoric acid (1.50 M) was $50 \text{ }\mu\text{L min}^{-1}$. In order to avoid blockage in the system, two in-line filters with a pore size of $0.5 \text{ }\mu\text{m}$ (Vici, Schenk, Switzerland) were placed before and after the column. The temperature of the oxidation reactor was set to $99.9 \text{ }^\circ\text{C}$. The used columns and mobile phase compositions are listed in Table 5.1. The concentration of phosphate was 10 mmol L^{-1} . The column temperature was $25 \text{ }^\circ\text{C}$.

Table 5.1 Chromatographic columns and compositions of eluent used in LC/IRMS for AICAR separation.

Supplier	Name	Stationary phase	Size (mm)	Particle size	Mobile phase	Retention time
Waters	XBridge C ₁₈	C ₁₈ bonded to ethyl-bridged hybrid substance	50 x 3.0	2.5	Phosphate buffer pH 6.0	270 s
					Pure water	270 s
Zirchrom	Zirchrom PBD	Polybutadiene-coated zirconia material	150 x 3.0	5	Phosphate buffer pH 6.0	320 s
					Pure water	325 s
Hamilton	PRP-X400	Polymer styrene-divinylbenzene bonded with sulfonate	150 x 4.0	7	Phosphate buffer pH 6.0 5mM H ₂ SO ₄ + 0.1/0.2/0.5 M Na ₂ SO ₄	Not eluted Not eluted
Thermo	Hypercarb	Porous graphitic carbon	30 x 3.0	3	Phosphate buffer pH 6.0	220 s
					Pure water	275 s
Agilent	Zorbax Bonus-RP	Polar amide embedded in a long alkyl chain	30 x 1.0	3.5	Phosphate buffer pH 6.0	523 s

5.3.5 EA/IRMS measurement

$\delta^{13}\text{C}$ -values of pure compounds were measured with an EA 1110 Elemental Analyzer (CE instrument, Milan, Italy) coupled to a MAT 253 IRMS (Thermo Fisher Scientific) via a ConFlo IV interface (Thermo Fisher Scientific). The temperature of the oxidation oven was 1050 °C. The GC oven temperature was 65 °C. The carrier gas was 65 mL min⁻¹. The reported $\delta^{13}\text{C}_{\text{EA/IRMS}}$ values of AICAR were corrected by a two-point normalization method with two certified standards of IAEA-600 caffeine and IAEA-CH-6. More detailed information of the normalization can be found in reference.^[11]

5.3.6 Data acquisition and handling

All reported $\delta^{13}\text{C}$ -values are normalized to the VPDB scale (Vienna Pee Dee Belemnite). Four pulses of reference gas were injected at 30, 80, 130, and 1050 s, and the second reference peak was used for $\delta^{13}\text{C}$ calibration. At 240 s, the sample was injected and the autosampler sent a start signal to the PDA detector for data collection. The acquisition and processing of

IRMS data was performed by Isodat 2.5. The background type used for peak integration was 'individual background' with start slope and end slope of 0.5 mV s^{-1} .

5.4 Results and discussion

5.4.1 Suitable chromatographic column

Five columns with different stationary phases combined with different mobile phases were used for investigation of suitable chromatographic conditions. The chosen columns include C_{18} , polybutadiene-coated, porous graphitic carbon, and amide-embedded reversed-phase column, and sulfonate-functionalized cation exchange column. Due to the design of the LC-IsoLink interface, organic modifiers cannot be used for the chromatographic separation. The mobile phase used for reversed-phase chromatographic elution was an aqueous phosphate buffer at pH 6.0. At this condition, 98.6 % of AICAR is present as a neutral species for the singly protonated AICAR at nitrogen atom of imidazole has a pK_a of 4.51. On XBridge C_{18} , Zirchrom PBD, and Hypercarb, the retention time of AICAR is approximately 270, 325, 275 s, respectively, which is close to ethanol retention time (270 s). It indicates that the hydrophobic interaction between AICAR and the stationary phase of these columns is very weak. AICAR was not eluted from the cation exchange column of PRP-X400 with a mobile phase of 5 mmol L^{-1} of H_2SO_4 aqueous solution. In order to achieve the elution of AICAR, different amount of salt was added to the mobile phase for increasing the ionic strength (0.1, 0.2, or 0.5 mol L^{-1} of Na_2SO_4) and the eluting buffer was changed to 10 mmol L^{-1} phosphate buffer for increasing the buffer pH to 6. However, AICAR was still not eluted and no peak of AICAR was observed. It suggests that the electrostatic interaction between the stationary phase of bonded sulfonate and AICAR could be very strong.

A suitable chromatographic condition was achieved for AICAR retention with Zorbax Bonus-RP column. Retention time was 523 s with an eluent of phosphate buffer at pH 6. The retention mechanism is probably the hydrogen bonding interaction between AICAR and the embedded polar amide group in the long alkyl chain.

5.4.2 Detection limit for precise and accurate isotope analysis

It is important to achieve the lowest method detection limit for precise and accurate isotope analysis of AICAR, since it defines the required amount of initial urine sample and the enrichment factor for doping control analysis. For determination of the detection limit, AICAR solutions in the concentration range from 10 to $200 \mu\text{g mL}^{-1}$ were measured and

$\delta^{13}\text{C}$ -values measured by LC/IRMS were compared with that measured by elemental analyzer coupled to isotope ratio mass spectrometry (EA/IRMS). From 20 to 200 $\mu\text{g mL}^{-1}$, the standard deviations for triplicate measurement are better than 0.21 ‰ and $\delta^{13}\text{C}$ -values at different concentration lie in the interval of $\delta^{13}\text{C}_{\text{EA/IRMS}} \pm 0.5\text{‰}$. At the concentration of 10 $\mu\text{g mL}^{-1}$, the standard deviation is 1.42‰, which is significantly higher than 0.5‰, the commonly acceptable precision for compound-specific isotope analysis.^[12, 13] Therefore, the lowest detection limit for AICAR isotope analysis is 20 $\mu\text{g mL}^{-1}$, corresponding to 83.6 ng of carbon on-column. There is a good linear relationship between concentration and peak area as shown in Figure 5.2. It indicates that LC/IRMS can provide both the $\delta^{13}\text{C}$ -values and concentrations of AICAR.

Additionally, AICAR can absorb UV light due to the conjugated π -system. The in-line combined PDA detector can be used for quantitative analysis too. The wavelength of maximum absorption of AICAR is 265 nm. The linear relationship between the absorption intensity and the concentration was shown in Figure 5.3. This simultaneous measurement by PDA can be used to check the peak purity of AICAR in IRMS chromatogram, since the PDA detector gives us information about the UV absorbance behaviour of compounds.

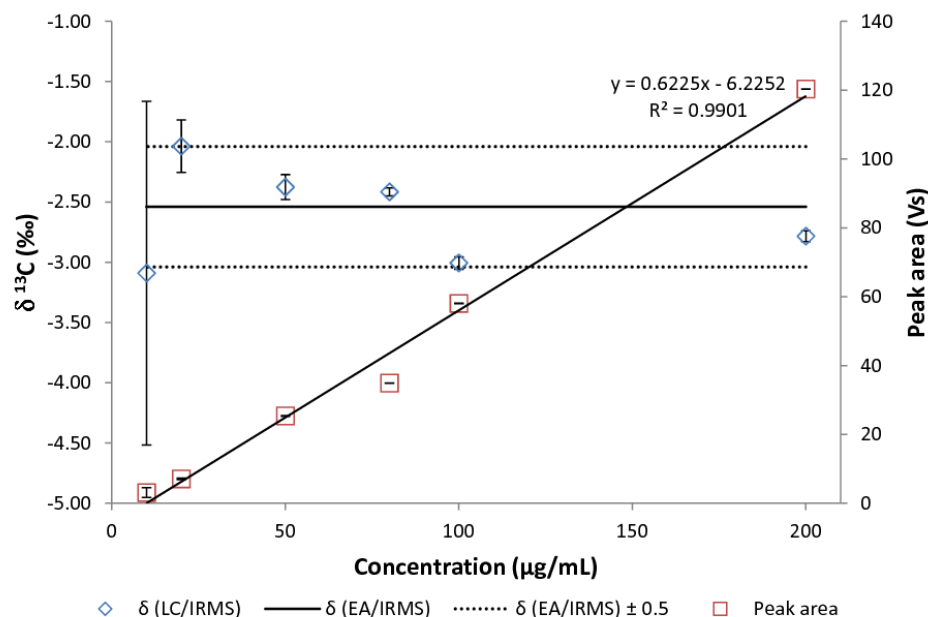


Figure 5.2 $\delta^{13}\text{C}$ -value (diamond) and peak area (square) of AICAR at different concentrations from 200 to 10 $\mu\text{g mL}^{-1}$. The equation and R-squared value of linear regression of peak area to concentration are displayed on the chart. The error bars indicate the standard deviations of triple measurements. The dashed lines show the $\delta^{13}\text{C}_{\text{EA/IRMS}}$ -values of AICAR (-2.54‰). The solid lines represent the interval of $\delta^{13}\text{C}_{\text{EA/IRMS}} \pm 0.5\text{‰}$.

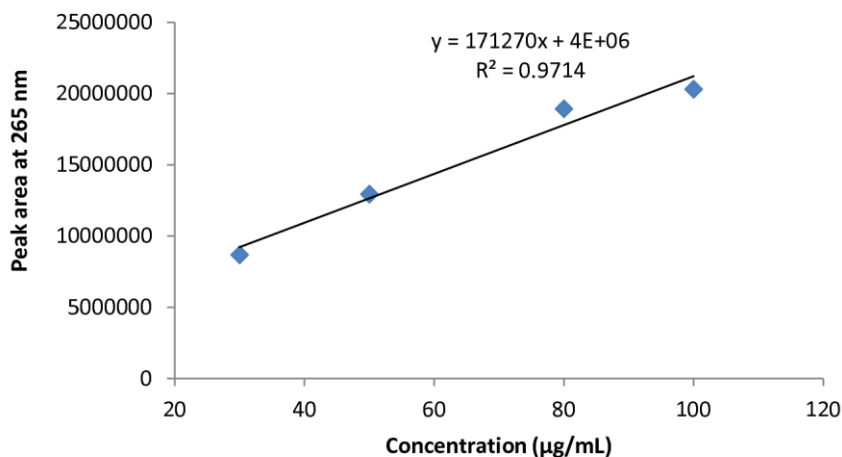


Figure 5.3 the linear relationship between the peak area of UV absorption at 265 nm and concentration of AICAR.

5.4.3 Spiked urine sample

In order to evaluate the possibility of applying the developed method for urinary AICAR analysis, two spiked urine samples were measured. The spiked synthetic urine sample is a mixture of synthetic urine and $200 \mu\text{g mL}^{-1}$ of AICAR in volume of 50:50. The contained two components of urea and creatinine in synthetic urine were separated from AICAR as shown in Figure 5.4a. $\delta^{13}\text{C}$ -value of AICAR is precise and accurate compared with $\delta^{13}\text{C}_{\text{EA/IRMS}}$ -values. The spiked urine sample is a mixture of filtered morning urine and $200 \mu\text{g mL}^{-1}$ of AICAR in volume of 50:50. The matrix of urine contributed to an increased background as seen in Figure 5.4b. Some unknown components were coeluted with AICAR as the obtained concentration of $141 \mu\text{g mL}^{-1}$ is higher than the theoretical concentration ($100 \mu\text{g mL}^{-1}$). The $\delta^{13}\text{C}$ of AICAR is $-4.93 \text{‰} \pm 10.89\text{‰}$. The relatively high standard deviation was caused by coeluted unknown components and the unstable background from the urine matrix. It indicates that real urine samples need prepurification for precise isotope analysis of LC/IRMS.

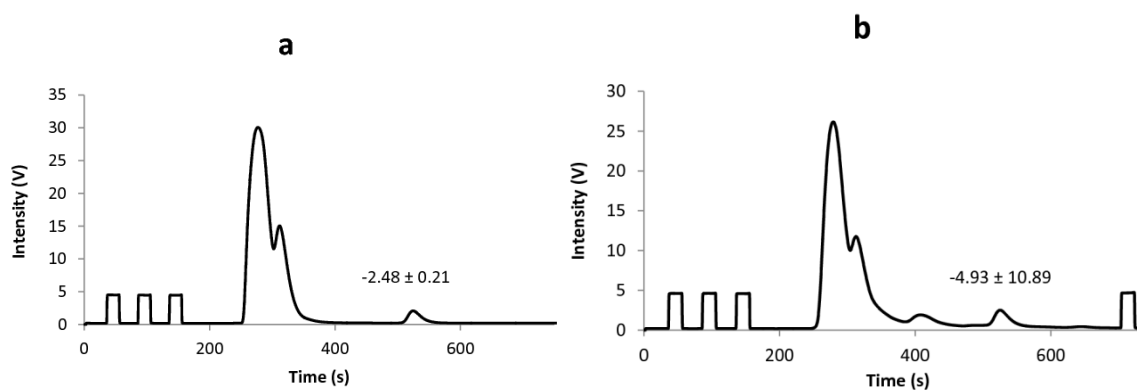


Figure 5.4 Chromatograms of spiked synthetic urine sample (a) and spiked urine sample (b). The $\delta^{13}\text{C}$ -value and standard deviation of AICAR are given in the figure panels ($n = 3$). The spiked urine sample is a mixture of filtered morning urine and $200 \mu\text{g mL}^{-1}$ of AICAR in volume of 50:50 and the spiked synthetic urine sample is a mixture of synthetic urine and $200 \mu\text{g mL}^{-1}$ of AICAR in volume of 50:50.

5.4.4 Endogenous AICAR in urine

Three procedures were used to enrich and purify AICAR from urine. The IRMS chromatograms of three purified urine samples are shown in Figure 5.5. The matrix components were not separated from AICAR and high background was observed in the urine sample prepurified by the first procedure (Figure 5.5a). It resulted from carbon-containing components in the purified residue. In the step of HPLC purification of the first procedure, ammonium acetate buffer was used for preparing sample solution and conditioning the column. The last step is that the collected fraction was evaporated to dryness in a vacuum centrifuge. Under this condition, it is difficult to remove all ammonium acetate from the residue. Therefore, carbon-containing compounds resulting in the high background include some impurities from the urinary matrix and the used buffer of ammonium acetate. In the second procedure, ammonium acetate was added to buffer the sample solution and the eluent for chromatographic purification. The chromatogram of the second urine sample also has high background and AICAR was not separated from the matrix. In LC/IRMS, target compounds have to be baseline separated for precise isotope analysis.^[14, 15] Therefore, the given $\delta^{13}\text{C}$ values of endogenous AICAR in the first and second urine samples cannot represent the real value.

The third procedure was developed for AICAR purification containing three steps of HPLC purification. In the last HPLC purification step, the sample solvent was pure water and the eluent was a mixture of $\text{H}_2\text{O}/\text{ACN}$, which can be removed easily in a vacuum centrifugal

evaporator. No ammonium acetate was used in the last purification step of the third procedure. As shown in Figure 5.5c, the third urine sample is very clean after this intensive clean-up. AICAR was baseline separated from the matrix. $\delta^{13}\text{C}$ -value was obtained with high precision of 0.40‰. The calculated concentration is $76 \mu\text{g mL}^{-1}$ based on the linear relationship between concentration and peak area.

According to another quantitative analysis by combined PDA detector, the urine sample contained $70 \mu\text{g mL}^{-1}$ of AICAR. The three-dimensional views of PDA data of the standard mixture ($100 \mu\text{g mL}^{-1}$ of AICAR) and the third urine sample are shown in Figure 5.6. The spectral similarity between the detected AICAR peak in the urine sample and that in the standard mixture is 99.99 %. The results from the UV absorbance indicate that the detected peak in the IRMS chromatogram is indeed rather pure AICAR.

The endogenous AICAR in the urine sample has a $\delta^{13}\text{C}$ -value of -25.54‰ . It is significantly different to the value of synthetic AICAR (-2.54‰). Another synthetic AICAR from black market was also measured having a $\delta^{13}\text{C}$ -value of $-4.06 \pm 0.10\text{‰}$. It indicates that synthetic and endogenous AICAR probably have different and distinguishable carbon isotope ratios. The $\delta^{13}\text{C}$ -values of AICAR from limited samples were reported in this work for the first time. More synthetic samples and endogenous urinary AICAR need be measured to establish a reference range of endogenous and exogenous AICAR for doping control purposes.

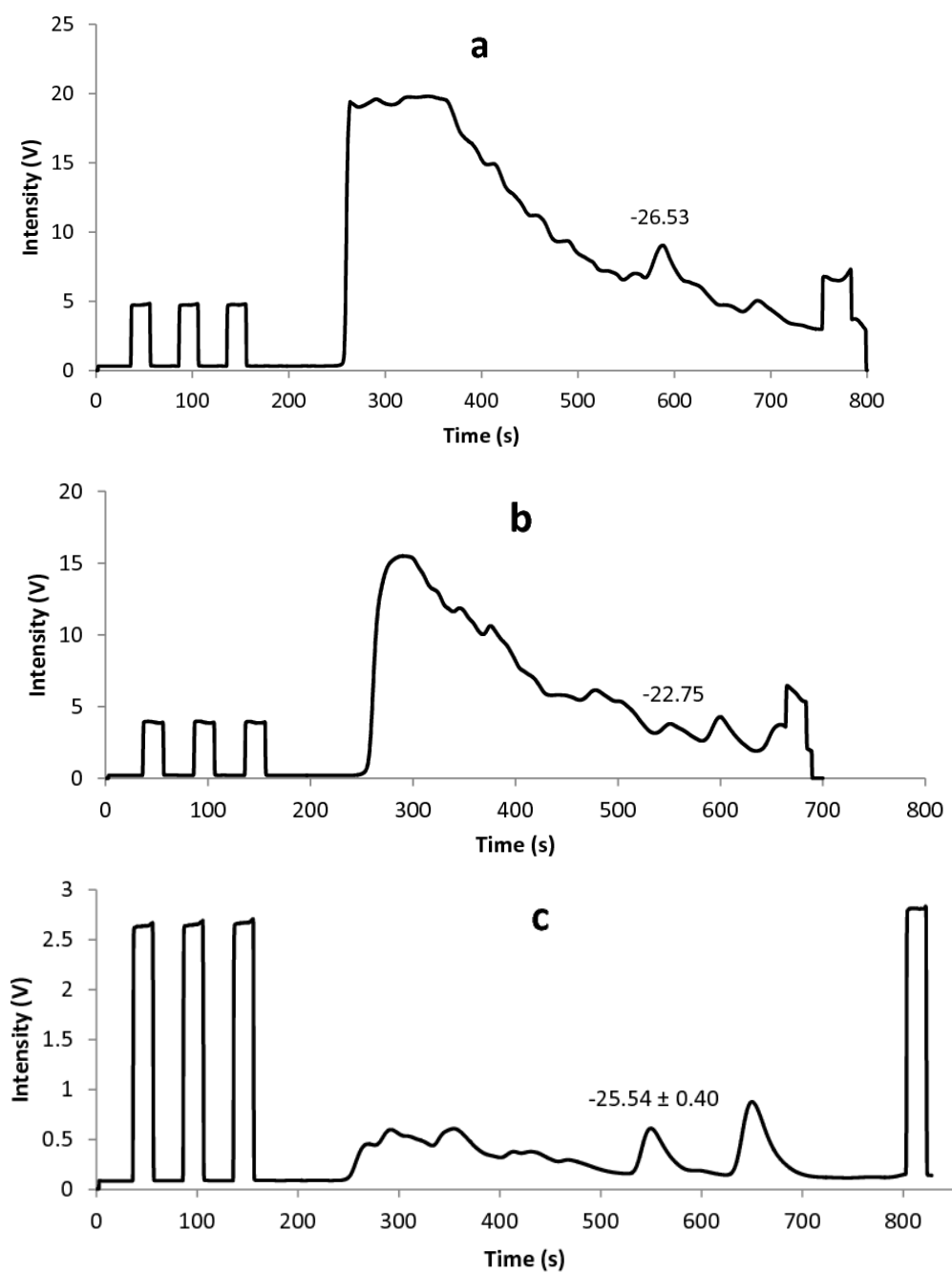


Figure 5.5 Chromatograms of three urinary samples prepurified by the first (a), the second (b), and the third (c) procedure. The $\delta^{13}\text{C}$ -values of AICAR are represented above the peak. The standard deviation of triple measurement is given for the last sample.

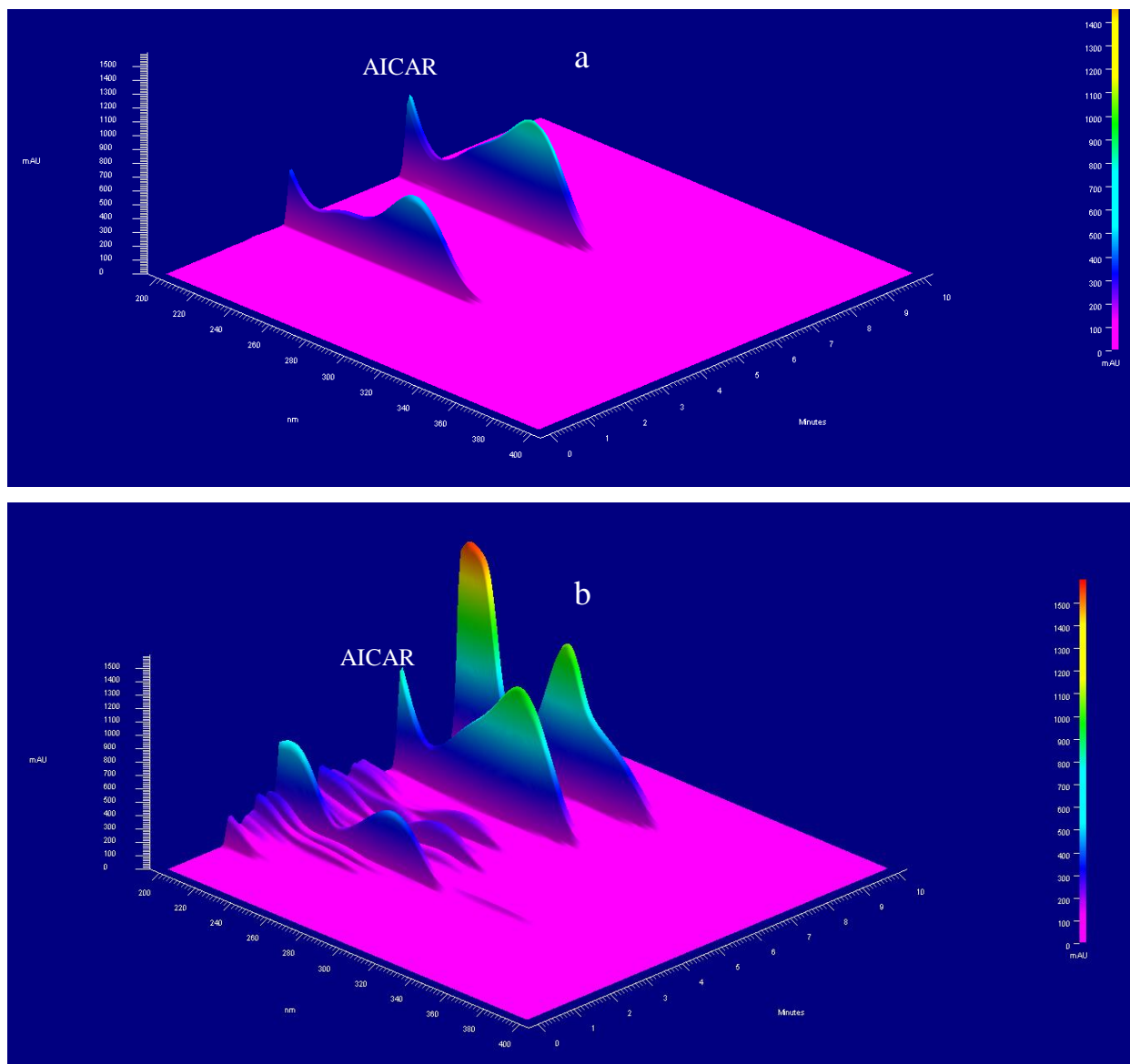


Figure 5.6 3-dimensional views of PDA data of the standard mixture of 100 µg mL⁻¹ AICAR (a) and the urine sample prepurified with the third procedure (b). The wavelength range is from 200 to 400 nm.

5.5 Conclusion

A new method of liquid chromatography simultaneously coupled to photodiode array detector and isotope ratio mass spectrometry (LC/PDA/IRMS) was developed for stable carbon isotope analysis and quantitative determination of AICAR. A suitable clean-up procedure for urine samples was established for precise isotope analysis of endogenous urinary AICAR. The $\delta^{13}\text{C}$ -values of synthetic AICAR from two sources and endogenous AICAR from a urine sample were distinctly different. This preliminary work shows that carbon isotope analysis of LC/IRMS can be potentially used to discriminate between exogenous and endogenous AICAR in doping control.

5.6 Acknowledgements

The author thanks Prof. Thevis, Dr. Piper and Mr. Beuck for their cooperation and thanks Susanne Brüggem for her assistance.

5.7 References

- [1] T. van der Gronde, O. de Hon, H. J. Haisma, T. Pieters. Gene doping: An overview and current implications for athletes. *Br. J. Sports Med.* **2013**.
- [2] S. Theodoropoulou, P. E. Kolovou, Y. Morizane, M. Kayama, F. Nicolaou, J. W. Miller, E. Gragoudas, B. R. Ksander, D. G. Vavvas. Retinoblastoma cells are inhibited by aminoimidazole carboxamide ribonucleotide (AICAR) partially through activation of AMP-dependent kinase. *FASEB J.* **2010**, *24*, 2620.
- [3] V. A. Narkar, M. Downes, R. T. Yu, E. Embler, Y. X. Wang, E. Banayo, M. M. Mihaylova, M. C. Nelson, Y. Zou, H. Juguilon, H. Kang, R. J. Shaw, R. M. Evans. AMPK and PPAR δ Agonists Are Exercise Mimetics (DOI:10.1016/j.cell.2008.06.051). *Cell* **2008**, *135*, 189.
- [4] World anti-doping agency, The 2012 Prohibited List International Standard, <http://www.wada-ama.org/en/World-Anti-Doping-Program/Sports-and-Anti-Doping-Organizations/International-Standards/Prohibited-List/>, **2012**.
- [5] L. Sweetman, W. L. Nyhan. Detailed comparison of the urinary excretion of purines in a patient with the Lesch-Nyhan syndrome and a control subject. *Biochem. Med.* **1970**, *4*, 121.
- [6] A. Thomas, S. Beuck, J. C. Eickhoff, S. Guddat, O. Krug, M. Kamber, W. Schänzer, M. Thevis. Quantification of urinary AICAR concentrations as a matter of doping controls. *Anal. Bioanal. Chem.* **2010**, *396*, 2899.
- [7] C. Ayotte, in *Handbook of experimental pharmacology*, Vol. 195 (Eds.: Detlef, Hemmersbach), **2010**, pp. 77.
- [8] C. Saudan, N. Baume, N. Robinson, L. Avois, P. Mangin, M. Saugy. Testosterone and doping control. *Br. J. Sports Med.* **2006**, *40*, i21.
- [9] E. Strahm, C. Emery, M. Saugy, J. Dvorak, C. Saudan. Detection of testosterone administration based on the carbon isotope ratio profiling of endogenous steroids: International reference populations of professional soccer players. *Br. J. Sports Med.* **2009**, *43*, 1041.
- [10] N. Kohyama, Y. Yamamoto. A Facile Synthesis of AICAR from Inosine. *Synthesis* **2003**, 2639.
- [11] T. B. Coplen, W. A. Brand, M. Gehre, M. Gröning, H. A. J. Meijer, B. Toman, R. M. Verkouteren. New guidelines for $\delta^{13}\text{C}$ measurements. *Anal. Chem.* **2006**, *78*, 2439.

-
- [12] L. Zhang, D. M. Kujawinski, M. A. Jochmann, T. C. Schmidt. High-temperature reversed-phase liquid chromatography coupled to isotope ratio mass spectrometry. *Rapid Commun. Mass Spectrom.* **2011**, *25*, 2971.
- [13] M. A. Jochmann, M. Blessing, S. B. Haderlein, T. C. Schmidt. A new approach to determine method detection limits for compound-specific isotope analysis of volatile organic compounds. *Rapid Commun. Mass Spectrom.* **2006**, *20*, 3639.
- [14] M. Krummen, A. W. Hilker, D. Juchelka, A. Duhr, H. J. Schlüter, R. Pesch. A new concept for isotope ratio monitoring liquid chromatography/mass spectrometry. *Rapid Commun. Mass Spectrom.* **2004**, *18*, 2260.
- [15] J. P. Godin, G. Hopfgartner, L. Fay. Temperature-programmed high-performance liquid chromatography coupled to isotope ratio mass spectrometry. *Anal. Chem.* **2008**, *80*, 7144.

Chapter 6 General conclusions and future work

High temperature liquid chromatography coupled to isotope ratio mass spectrometry (HTLC/IRMS) has been well-established for compound-specific isotope analysis in this thesis. The measured compounds by HTLC/IRMS have covered medium polar and non-polar organic compounds. The application scope of LC/IRMS has been extended to pharmaceutical analysis.

First, a suite of reversed-phase columns with different stationary phases has proven to be suitable for the use of HTLC/IRMS in the isothermal and temperature-gradient modes. Increasing the column temperature of LC/IRMS can shorten analysis time and improve the peak shape of analytes, for example, narrow peak widths. Second, HTLC/IRMS has been applied to caffeine in different drinks. Two distinguishable ranges of $\delta^{13}\text{C}$ -values between natural and synthetic caffeine have been established, -25 to -32‰ for natural caffeine and -33 and -40‰ for synthetic caffeine. The method has been applied to identify the caffeine source in 38 drinks. Four products were suspected to be mislabelled due to added but non-labelled synthetic caffeine. It has been shown that isotope analysis of caffeine by HTLC/IRMS can be used for routine authenticity control of caffeine-containing drinks. Sample preparation is very simple and only requires dilution of products before injection. Third, temperature-programmed liquid chromatography coupled to isotope ratio mass spectrometry was used to measure isotope ratios of five underivatized steroids in a mixture, which are non-polar organic compounds with highly similar molecular structure. It was demonstrated that HTLC/IRMS can be a powerful tool in compound-specific isotope analysis. It is the first time for LC/IRMS to be applied for isotope analysis of hardly water-soluble organic compounds. The solvent mediator methanol has no influence on isotope analysis of steroids because of full separation from the target compounds. Forth, a new method of LC/IRMS was developed for compound specific isotope analysis of AICAR, a gene doping drug. It was applied to measure the isotope ratio of endogenous AICAR in urine. The endogenous and synthetic AICAR were observed to have significantly different isotope ratios, showing the potential in doping control. In this framework, the used different reversed-phase columns packed with ethyl-bridged hybrid particles had a good thermal stability. Such columns can be also used for other applications of high temperature liquid chromatography. The detection limit obtained for precise isotope analysis was around $30 \mu\text{g g}^{-1}$ by the use of HTLC/IRMS, corresponding to approximately 100 ng carbon on-column. However, it should

be noted that there is an offset in $\delta^{13}\text{C}$ -values between LC/IRMS and EA/IRMS, dependent on the measured compound. Therefore, care must be taken for the $\delta^{13}\text{C}$ -value correction. Since compound-specific offset correction is recommended for obtaining accurate isotope ratios, a standard mixture containing compounds of interest with known $\delta^{13}\text{C}$ -values needs to be measured along with samples.

The research carried out in the frame of this dissertation has highlighted the potential of high-temperature liquid chromatography coupled to isotope ratio mass spectrometry. However, there is still plenty of room for improvement. One area of promising future work is the use of HTLC/IRMS for the detection of steroid abuse in sports. A protocol of sample preparation needs to be developed for urinary steroid enrichment and purification prior to HTLC/IRMS analysis. Isotope analysis of AICAR by LC/IRMS is also interesting for doping control. More measurements of endogenous AICAR in urine samples are recommended for establishing the reference range of endogenous and exogenous AICAR. The investigation of $\delta^{13}\text{C}$ and content variation in administrated and excreted urine AICAR at natural abundance or at low enrichment level can provide more details for the detection of AICAR abuse. Additionally, the $\delta^{13}\text{C}$ -values of synthetic AICAR are exceptionally high (-2 to -4.06‰) compared with $\delta^{13}\text{C}$ -values of other compounds reported. Investigation of ^{13}C -enrichment in AICAR and isotopic fractionation during the synthesis of AICAR could be helpful for the better understanding of the fundamentals of stable isotope enrichment.

LC/IRMS could become a method of choice for tracer studies in complex aqueous mixtures. The measuring of isotope enrichment using LC/IRMS can be applied to biological and hydrological systems. For example, Tracer labelled with ^{13}C can be initiated at the source area and monitored to investigate where the contaminants would be expected to distribute. Additionally, the flow injection mode of LC/IRMS is a sensitive method for bulk isotope analysis and total carbon detection, especially for high volume injection. It could be useful in some aspects of carbon cycling, for example, carbon isotope analysis of dissolved organic and inorganic carbon in soils.

Supplement

List of figures

- Figure 1.1 Schematic of isotope ratio mass spectrometry for stable carbon isotope analysis. 10
- Figure 1.2 Schematic of an EA/IRMS for nitrogen and carbon isotope analysis (Flash Elemental Analyzer coupled with IRMS, Thermo Fisher Scientific, Bremen). It consists of an autosampler, an oxidation reactor, a reduction reactor, a water trap, a gas chromatographic column, a thermal conductivity detector, open split, and an IRMS system. 12
- Figure 1.3 Schematic of gas chromatography coupled to isotope ratio mass spectrometry for carbon and nitrogen isotope analysis. 13
- Figure 1.4 The schematic of liquid chromatography coupled to isotope ratio mass spectrometry using an interface of LC-IsoLink for compound-specific isotope analysis. The system can be used for bulk isotope analysis without a column, known as flow injection analysis mode (FIA). 16
- Figure 2.1 The HTLC/IRMS setup. 40
- Figure 2.2 HTLC/IRMS chromatograms of CO₂ pulses (A) and multiple injections of 100 mg L⁻¹ ethanol (B) obtained on XBridge C₁₈ column at 100°C. The second reference gas peak was used for calibration of $\delta^{13}\text{C}$ -values. 41
- Figure 2.3 Temperature-programmed LC/IRMS chromatograms of successive CO₂ pulses (A) and multiple injections of 100 mg L⁻¹ ethanol (B) obtained on XBridge C₁₈ column. The temperature program was 1 min at 60°C, and then ramped at 20°C min⁻¹ to 120°C where it was held for 1 min, then at 5 °C min⁻¹ to 180°C where it was held for 1 min..... 41
- Figure 2.4 (A) $\delta^{13}\text{C}$ of CO₂ gas pulses (circles, left ordinate) and background of ⁴⁴CO₂ (squares, right ordinate) were determined with XBridge C₁₈ (1), Acquity C₁₈ (2), Triart C₁₈ (3), and Zirchrom PBD (4) at various temperatures. Error bars indicate the SD (n = 9). The dotted lines represent the standard value of CO₂ gas (-37.81‰). The horizontal solid lines represent the interval of standard value $\pm 0.5\%$. (B) $\delta^{13}\text{C}$ of multiple injections of 100 mg L⁻¹ ethanol determined with corresponding column at various temperatures. Error bars indicate

the SD ($n = 3$). The dotted lines represent the FIA result (-28.32%). The horizontal solid lines represent the interval of $-28.32 \pm 0.5\%$ 45

Figure 2.5 $\delta^{13}\text{C}$ -values of multiple injections of 100 mg L^{-1} ethanol calculated with algorithm of ‘individual background’ (triangle, left ordinate) and ‘dynamic background’ (circle, left ordinate) and the slopes of peak backgrounds on mass of 44 (cross, right ordinate) with four columns under temperature-programmed conditions. The x-axis represents the elution time of ethanol peak in temperature-programmed LC/IRMS chromatogram. The slope of peak background was calculated by the difference of backgrounds at the peak start and at the peak end divided by the peak width. The two horizontal solid lines represent the interval of FIA result $\pm 0.5\%$ 48

Figure 2.6 Determination of method detection limit for caffeine with XBridge C_{18} at 120°C . The circles and squares represent the $\delta^{13}\text{C}$ and peak area of $^{44}\text{CO}_2$, respectively. The linear curve fit and the correlation coefficient for plotting peak area vs. concentration are shown in the graph. Error bars indicate the SD of triplicate measurements. The dotted line indicates the iteratively calculated mean value of $\delta^{13}\text{C}$. The horizontal solid lines represent the interval of mean value $\pm 0.5\%$ 50

Figure 2.7 Temperature-programmed LC/IRMS chromatograms of caffeine derivatives and phenols using XBridge C_{18} ($100 \text{ mm} \times 30 \text{ mm}$, $3.5 \mu\text{m}$, A) and Zirchrom PBD ($150 \text{ mm} \times 30 \text{ mm}$, $5 \mu\text{m}$, B), respectively, with pure water at $500 \mu\text{L min}^{-1}$. The compounds are (1a) theobromine; (2a) theophylline (3a) caffeine; (1b) phenol; (2b) 3-methylphenol; (3b) 2,6-dimethylphenol; (4b) 2,4,6-trimethylphenol in $100 \mu\text{g L}^{-1}$ 51

Figure 3.1 HT-RPLC/IRMS chromatograms of a mixture of caffeine derivatives (100 mg L^{-1}), espresso, tea, and energy drink sample. The temperature used was 80°C and the column is XBridge C_{18} ($2.1 \times 100 \text{ mm}$, $3.5 \mu\text{m}$). The second reference gas peak was used for calibration of $\delta^{13}\text{C}$ -values..... 63

Figure 3.2 Illustration of the derivation of equation 3.2 used for two-point normalization of measured $\delta^{13}\text{C}$ by LC/IRMS. Two internal laboratory standards of caffeine samples (100 mg L^{-1}) with $\delta^{13}\text{C}$ of -27.77 ‰ ($\delta_{\text{T, std1}}$) and -35.56 ‰ ($\delta_{\text{T, std2}}$) were measured along with the samples by HT-HPLC/IRMS. 65

Figure 3.3 $\delta^{13}\text{C}$ -values of caffeine in the concentration range from 20 to 400 mg L⁻¹. The circles and squares represent the $\delta^{13}\text{C}$ and total peak area, respectively. The linear curve fit and the correlation coefficient for plotting peak area vs. concentration are shown in the graph. Error bars indicate the standard deviation of triplicate measurements. The dotted line indicates the iteratively calculated mean value of $\delta^{13}\text{C}$. The horizontal solid lines represent the interval of mean value $\pm 0.5\%$.^[33] 67

Figure 3.4 $\delta^{13}\text{C}$ -values and concentrations of caffeine from different sources. Error bars indicate the SD of triplicate measurements. Four dashed lines represent two different ranges of $\delta^{13}\text{C}$ -values, from -25 to -32‰ for natural caffeine in C₃-plant and from -33 to -38‰ for synthetic caffeine. a) Cola-type drinks except for coca cola..... 69

Figure 3.5 $\delta^{13}\text{C}$ -values and concentrations of caffeine in various drinks that were supposed to contain natural caffeine sources according to the labels. Four products were found to be mislabelled. Error bars indicate the SD of triplicate measurements. Four dashed lines represent two different ranges of $\delta^{13}\text{C}$ -values, from -25 to -32‰ for natural caffeine in C₃ plant and from -33 to -38‰ for synthetic caffeine. 72

Figure 3.6 A plot of the $\delta^{13}\text{C}$ -values shown in Figure 3.4 of the article for the samples containing natural and synthetic caffeine. One-sided prediction intervals around the means were calculated for both groups. 75

Figure 4.1 Chromatogram obtained by HTLC/PDA/IRMS of a steroid mixture (A: m/z of 44, 45, 46; B: Absorption at 193 nm). The sample contains five steroids in methanol, at a concentration of 100 µg g⁻¹ (listed in Table 4.1). The used temperature program is indicated by the dashed line in A. The open split was set in “out” position (back-flush mode) from 100 to 500 s in order to prevent methanol entering into the ion source. The sample was injected at 180s. 86

Figure 4.2 Offset corrected $\delta^{13}\text{C}$ values of testosterone (A) and 5β-pregnane-3α, 17α, 20α-triol (B) at different concentrations from 200 to 20 µg g⁻¹. The error bars indicate the standard deviations of triplicate measurements. The dashed lines show the $\delta^{13}\text{C}_{\text{EA/IRMS}}$ -values of the two steroids. The solid lines represent the interval of $\delta^{13}\text{C}_{\text{EA/IRMS}} \pm 0.5\%$ 89

Figure 4.3 Chromatogram of a Testogel sample. $\delta^{13}\text{C}$ -value of testosterone in a Testogel sample ($n = 3$), which was corrected by adding the offset; and calculated concentrations ($\mu\text{g g}^{-1}$) from the peak areas of IRMS and PDA detector at 193 nm based on the linear relationships in Table 4.3.	91
Figure 5.1 Chemical structure of AICAR	98
Figure 5.2 $\delta^{13}\text{C}$ -value (diamond) and peak area (square) of AICAR at different concentrations from 200 to 10 $\mu\text{g mL}^{-1}$. The equation and R-squared value of linear regression of peak area to concentration are displayed on the chart. The error bars indicate the standard deviations of triple measurements. The dashed lines show the $\delta^{13}\text{C}_{\text{EA/IRMS}}$ -values of AICAR (-2.54%). The solid lines represent the interval of $\delta^{13}\text{C}_{\text{EA/IRMS}} \pm 0.5\%$	103
Figure 5.3 the linear relationship between the peak area of UV absorption at 265 nm and concentration of AICAR.	104
Figure 5.4 Chromatograms of spiked synthetic urine sample (a) and spiked urine sample (b). The $\delta^{13}\text{C}$ -value and standard deviation of AICAR are given in the figure panels ($n = 3$). The spiked urine sample is a mixture of filtered morning urine and 200 $\mu\text{g mL}^{-1}$ of AICAR in volume of 50:50 and the spiked synthetic urine sample is a mixture of synthetic urine and 200 $\mu\text{g mL}^{-1}$ of AICAR in volume of 50:50.	105
Figure 5.5 Chromatograms of three urinary samples prepurified by the first (a), the second (b), and the third (c) procedure. The $\delta^{13}\text{C}$ -values of AICAR are represented above the peak. The standard deviation of triple measurement is given for the last sample.	107
Figure 5.6 3-dimensional views of PDA data of the standard mixture of 100 $\mu\text{g mL}^{-1}$ AICAR (a) and the urine sample prepurified with the third procedure (b). The wavelength range is from 200 to 400 nm.	108

List of tables

Table 1.1 Isotopic abundances of hydrogen, carbon, nitrogen, oxygen and sulfur ^[9]	9
Table 1.2 Chromatographic methods based on ion interaction in LC/IRMS: column, mobile phase composition, and analytes. Anion exchange columns (type 1), cation exchange columns (type 2), ligand exchange columns (type 3), and ion exclusion columns (type 4).....	18
Table 1.3 Mixed-mode columns used in LC/IRMS, mobile phase compositions, and analytes. Primesep A (blue cells) and Primesep100 (red cells)	20
Table 1.4 Reversed-phase columns, mobile phase composition, and analytes in LC/IRMS...	21
Table 2.1 Overview of evaluated columns	40
Table 2.2 $\delta^{13}\text{C}$ of successive CO_2 pulses ($n = 21$) and multiple injections of 100 mg L^{-1} ethanol ($n = 8$) with each column under temperature-programmed conditions. The $ \Delta\delta_{(\text{HTLC} - \text{FIA})} \text{‰}$ represents the difference of $\delta^{13}\text{C}$ obtained by temperature-programmed LC/IRMS and FIA/IRMS.....	47
Table 2.3 IRMS results of 100 mg L^{-1} caffeine analyzed on XBridge C_{18} column at various temperatures.	49
Table 2.4 Comparison of $\delta^{13}\text{C}$ of caffeine derivatives and phenols measured by temperature-programmed LC/IRMS with the corrected $\delta^{13}\text{C}_{\text{EA/IRMS}}$ and the $\delta^{13}\text{C}$ -values measured by FIA/IRMS.....	52
Table 3.1 The measured caffeine samples and preparation methods	62
Table 3.2 Comparison of corrected $\delta^{13}\text{C}$ -values of caffeine from various sources measured by HT-RPLC/IRMS ($\delta_{\text{T,sp1}}$) with EA/IRMS analysis results.	68
Table 4.1 $\delta^{13}\text{C}$ values measured by EA/IRMS and HTLC/IRMS of steroids at $100 \mu\text{g g}^{-1}$ and $\delta^{13}\text{C}$ -value differences between the two methods ($\Delta\delta^{13}\text{C} = \delta^{13}\text{C}_{\text{EA/IRMS}} - \delta^{13}\text{C}_{\text{HTLC/IRMS}}$).	85

Table 4.2 $\delta^{13}\text{C}$ values of steroids at different concentrations ($n = 3$) measured by HTLC/IRMS and corrected by adding the offset to $\delta^{13}\text{C}_{\text{EA/IRMS}}$ -values..... 89

Table 4.3 Linear relationships between concentration and peak areas from IRMS (for all steroids from 20 to 200 $\mu\text{g g}^{-1}$) and UV detection at 193 nm (for 19NA, T, EpiT from 20 to 200 $\mu\text{g g}^{-1}$ and for A and PT from 30 to 200 $\mu\text{g g}^{-1}$)..... 89

Table 5.1 Chromatographic columns and compositions of eluent used in LC/IRMS for AICAR separation. 101

List of abbreviations

A	Androsterone
AAS	Anabolic androgenic steroid
AICAR	5-Aminoimidazole-4-carboxamide ribonucleotide
AMP	Adenosine monophosphate
CSIA	Compound-specific isotope analysis
EA/IRMS	Elemental analyzer coupled to isotope ratio mass spectrometry
FIA/IRMS	Flow injection analysis coupled to isotope ratio mass spectrometry
FDA	Food and drug administration
EpiT	Epitestosterone
GC/IRMS	Gas chromatography coupled to isotope ratio mass spectrometry
HTLC/IRMS	High-temperature liquid chromatography coupled to isotope ratio mass spectrometry
HTLC/PDA/IRMS	High-temperature liquid chromatography coupled to photodiode array detector and isotope ratio mass spectrometry
HT-RPLC/IRMS	High temperature reversed-phase liquid chromatography coupled to isotope ratio mass spectrometry
LC/IRMS	Liquid chromatography coupled to isotope ratio mass spectrometry
MDL	Method detection limit
19NA	19-nortestosterone
PBD	Polybutadiene
PDA	Photodiode array detector
PG	5 β -pregnane-3 α ,17 α ,20 α -triol
PS-DVB	Polystyrene divinylbenzene
RPLC/IRMS	Reversed-phase liquid chromatography coupled to isotope ratio mass spectrometry

SD	Standard deviation
T	Testosterone
VPDB	Vinna Pee De Belemnite
WADA	World Anti-Doping Agency

List of publications

A. Peer-reviewed international journals

1. Lijun Zhang, Mario Thevis, Maik A. Jochmann, Thomas Piper, Torsten C. Schmidt: Derivatization-free carbon isotope ratio analysis of steroids by hyphenation with high temperature liquid chromatography. (Submitted to Analytical Chemistry)
2. Lijun Zhang, Dorothea M. Kujawinski, Eugen Federherr, Torsten C. Schmidt, Maik A. Jochmann: Caffeine in your drink: natural or synthetic? Analytical Chemistry 2012, 84, 2805-2810.
3. Lijun Zhang, Dorothea M. Kujawinski, Maik A. Jochmann, Torsten C. Schmidt: High temperature reversed-phase liquid chromatography coupled to isotope ratio mass spectrometry, Rapid Communications in Mass Spectrometry 2011, 25, 2971-2980
4. Lijun Zhang, Qinji Xie, Shouzuo Yao: EQCM study on the potential oscillations during galvanostatic oxidation of glucose, galactose and ethanol, Acta Physico-Chimica Sinica, 2005, 21(9), 977-982.
5. Dorothea M. Kujawinski, Lijun Zhang, Maik A. Jochmann, Torsten C. Schmidt: When Other Separation Techniques Fail: Compound-Specific Carbon Isotope Ratio Analysis of Sulfonamide Containing Pharmaceuticals by High-Temperature-Liquid Chromatography-Isotope Ratio Mass Spectrometry. Anal. Chem. 2012, 84, 7656-7663.
6. Dorothea M. Kujawinski, Benjamin J. Wolbert, Lijun Zhang, Maik A. Jochmann, David Widory, Nicole Baran, Torsten C. Schmidt: Carbon isotope ratio measurements of glyphosate and AMPA by liquid chromatography coupled to isotope ratio mass spectrometry, Analytical and Bioanalytical Chemistry. 2013, 405, 2869–2878

B. Other published papers

1. T. Teutenberg, S. Wiese, M.A. Jochmann, D.M. Kujawinski, L. Zhang, T.C. Schmidt, B. Fischer, H. Bettermann: Kopplungsverfahren zur Authentizitätskontrolle: Neuartige Kombination innovativer Detektionstechniken auf Basis der Isotopenmassenspektrometrie und Ramanspektroskopie, GIT Labor-Fachzeitschrift 2010, S. 182-185

Oral presentations

1. Lijun Zhang, Dorothea M. Kujawinski, Maik A. Jochmann, Torsten C. Schmidt, High temperature reversed-phase liquid chromatography coupled to isotope ratio mass spectrometry Brugge, Belgium, Benelux Association for Stable Isotope Scientists-Annual Meeting, 17-18 March 2011
2. Lijun Zhang, Dorothea M. Kujawinski, Maik A. Jochmann, Torsten C. Schmidt, Compound-specific isotope analysis by high temperature liquid chromatography coupled to isotope ratio mass spectrometry, Bonn, Germany, the fourth annual workshop of GCCCD-NRW, 28 May 2011
3. Lijun Zhang, Dorothea M. Kujawinski, Maik A. Jochmann, Torsten C. Schmidt, A new hyphenation of high temperature liquid chromatography coupled to isotope ratio mass spectrometry 22. Doktorandenseminar des Arbeitskreises Separation Science, 08-10 January 2012
4. Lijun Zhang, Challenges and opportunities of food safety in China, Bonn Rhein academic forum, 14 April 2012
5. Lijun Zhang, Mario Thevis, Maik A. Jochmann, Torsten C. Schmidt New possibility of steroid analysis for anti-doping: HTLC/PDA/IRMS, ANAKON, 04-07 March 2013

Poster Presentations

1. Lijun Zhang, Dorothea M. Kujawinski, Maik A. Jochmann, Torsten C. Schmidt, Evaluation of stationary phases for high temperature liquid chromatography-isotope ratio mass spectrometry, Munich, Analytica 2010, 23 – 26 March 2010
2. Lijun Zhang, Dorothea M. Kujawinski, Maik A. Jochmann, Torsten C. Schmidt, Evaluation of stationary phases for high temperature liquid chromatography-isotope ratio mass spectrometry, Arnhem, Benelux Association for Stable Isotope Scientists-Annual Meeting, 15 – 16 April 2010
3. Lijun Zhang, Dorothea M. Kujawinski, Maik A. Jochmann, Torsten C. Schmidt, High temperature liquid chromatography coupled to isotope ratio mass spectrometry, Amsterdam, Fifth International Symposium on Isotopomers (ISI 2010), 21 – 25 June 2010
4. Lijun Zhang, Dorothea M. Kujawinski, Maik A. Jochmann, Torsten C. Schmidt, High temperature reversed-phase liquid chromatography coupled to isotope ratio mass spectrometry, Oxford University, LC-IRMS User's Meeting, 24-25 November 2010
5. Lijun Zhang, Eugen Federherr, Dorothea M. Kujawinski, Maik A. Jochmann, Torsten C. Schmidt, Caffeine in your drink: natural or synthetic? Munich, Analytica 201, 17-20 April 2012
6. Lijun Zhang, Mario Thevis, Maik A. Jochmann, Torsten C. Schmidt, New possibility of steroids analysis for anti-doping: HTLC/PDA/IRMS, Leipzig, Jesium 2012, 2-7 September 2012

Erklärung

Hiermit versichere ich, dass ich die vorliegende Arbeit mit dem Titel

„Development and application of liquid chromatography coupled to isotope ratio mass spectrometry (LC/IRMS)”

selbst verfasst und keine außer den angegebenen Hilfsmitteln und Quellen benutzt habe, und dass die Arbeit in dieser oder ähnlicher Form noch bei keiner anderen Universität eingereicht wurde.

Essen, 10 Oktober 2013

UNTERSCHRIFT

Lijun Zhang

Acknowledgments

I would like to express my sincere gratitude to Prof. Dr. Torsten C. Schmidt and Dr. Maik Jochmann for their invaluable guidance, warm encouragement, helpful suggestion and discussion during the past four and half years.

I would like to thank Prof. Dr. Molt, PD. Dr. Telgheder, Mrs. Ullrich, Mr. Knierim, Mr. Fischer, Miss Kujawinsk, Mr. Laaks, Mr.Schulte, Mr, Wolbert, Mr. Michalski, Mr. Federherr, and all other staffs from the department of instrumental analytical chemistry at University of Duisburg-Essen for their help and support.

I appreciate the cooperation from Dr. Teutenberg (the institute of energy and environmental technology), Dr. Wiese (the institute of energy and environmental technology), Prof. Bettermann (Heinrich Heine University Düsseldorf), and Dr. Fischer (Heinrich Heine University Düsseldorf). I thank Prof. Thevis, Dr. Piper and Mr. Beuck from the institute of biochemistry at the German Sport University Cologne for their cooperation.

Furthermore, I acknowledge financial support from the German Federal Ministry of Economics and Technology within the agenda for the promotion of industrial cooperative research and development (IGF) based on a decision of the German Bundestag (IGF-Project No. 16120 N).

Last but not least, I want to thank my husband, my daughter, and my parents for their love and continuous support.